Timing and low temperature behavior of SiPM

G.Bisogni[1], G.Collazuol[1], A.Del Guerra[1,2], C.Piemonte[3]
[1] INFN sezione di Pisa, [2]Dipartimento di fisica Universita` di Pisa, [3]FKB-IRST Trento

Overview
- Introduction
- Experimental methods (low T)
- Measurements and discussion (low T)
- Summary about Timing measurements
- Conclusions

Introduction

Main contributions to SiPM characterization:

(A) intrinsic timing – measurements since 2007 (VCI 2007 conference)
Characterization of intrinsic timing resolution of different kind of SiPM devices with ultra-fast laser pulses and waveform analysis with optimum timing filtering

(B) cryogenic behavior – very recent studies (VCI 2010 conference)
Characterization of FBK SIPM in the range 50K<T<320K
1) junction forward and reverse (breakdown) characteristics
2) gain, dark current, after-pulses, cross-talk
3) photon detection efficiency (PDE)

Improved SiPM performances at low temperature (w/ respect to T_{room})

1) lower dark noise by orders of magnitude
2) lower after-pulsing probability (down to ~100K)
3) higher PDE (down to ~100K, depending on λ)
4) better timing resolution
5) better $V_{breakdown}$ stability (w.r.t. to variations of T)

→ SiPM is an excellent alternative to PMT at low T
even more than at room temperature !!!

Experimental Setup

Vacuum vessel (P~10^{-3} mbar)

Alogen Lamp

Monocromator (200-900nm)

Quartz filers to
Calibrated Photodiode (outside)
and to **SiPM** (inside vessel)

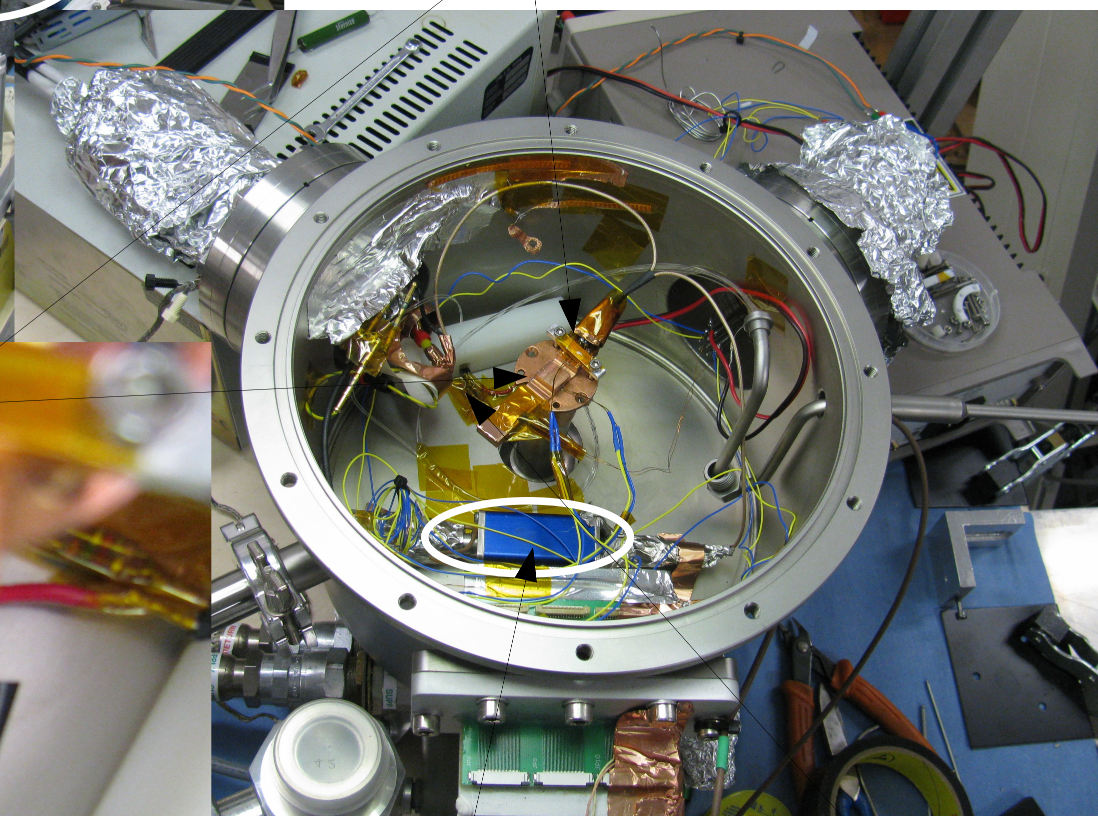

Cryocooler
(50K<T<300K)

Amplifier

UV LED (380nm)
+ fibers to SiPM

Experimental setup

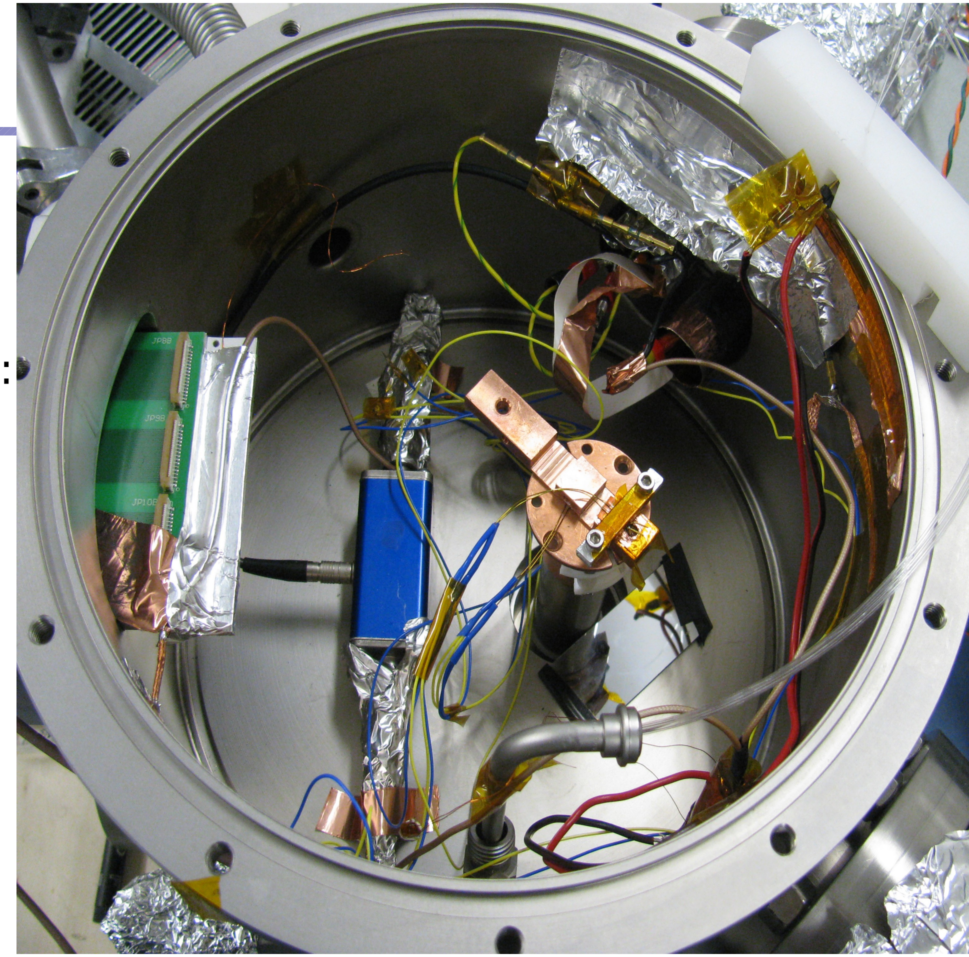

Temperature control/measurement

- Cryo-cooler + heating with low R resistor
- thermal contact (critical) with cryo-cooler head: SIPM within a copper rod
- T measurement with 3 pt100 probes
- Measurements on SiPM carried after thermalization (all probes at the same T)
- check junction T with forward characteristic

Voltage/Current bias/measurement

- Keytley 2148 for Voltage/Current bias/readout

Pulse measurement

- Care against HF noise → feed-throughts !!!
- Amplifier Photonique/CPTA (gain~30, BW~300MHz)

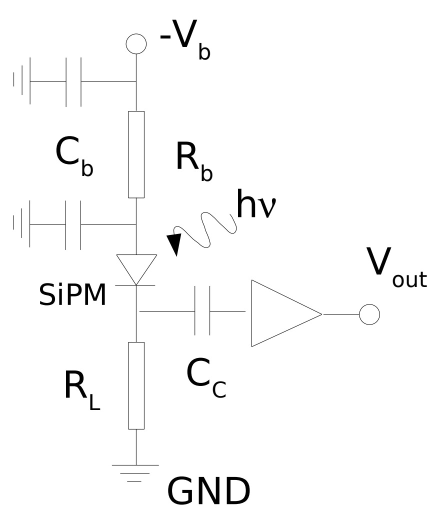

SiPM samples

- FBK SiPM runII – 1mm^2 (Vbr~33V, fill factor~20%)

Gain and pulse shape

If R_Q is high enough the internal current decreases at a level such that statistical fluctuations may quench the avalanche

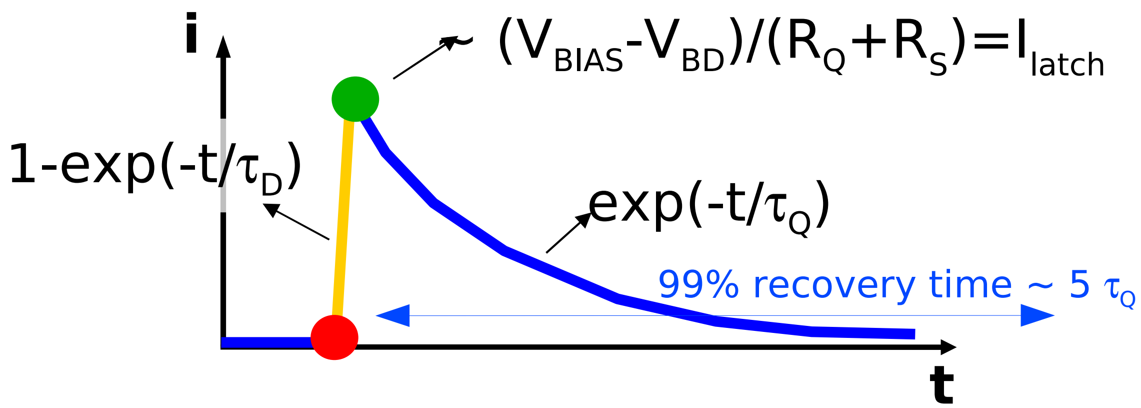

The leading edge of the signal is much faster than trailing edge:

1. $\tau_D = R_S C_D << R_Q C_D = \tau_Q$
2. turn-off mean time is very short (if R_Q is sufficiently high, I_{latch} ~ 10μA)

Recovery time:

increases at low T due to polysilicon R_Q while C_D is independent of T

$Gain \sim C_D\,\Delta V \rightarrow$ independent of T

at fixed Over-Voltage (ΔV)

Gain and pulse shape

The SiPM equivalent circuit has two time constants:

- $\tau_F = R_{Load}\ C_{TOT}$ (fast)
- $\tau_Q = R_Q\,(C_D + C_Q)$ (slow)

F. Corsi, et al. NIMA 572(2007)

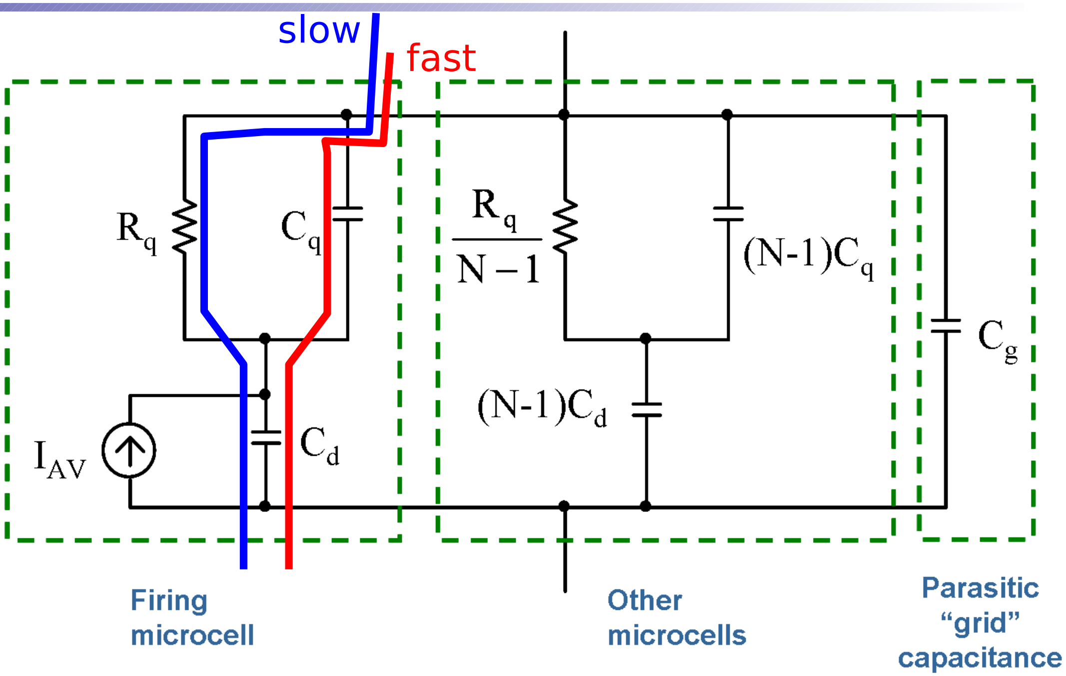

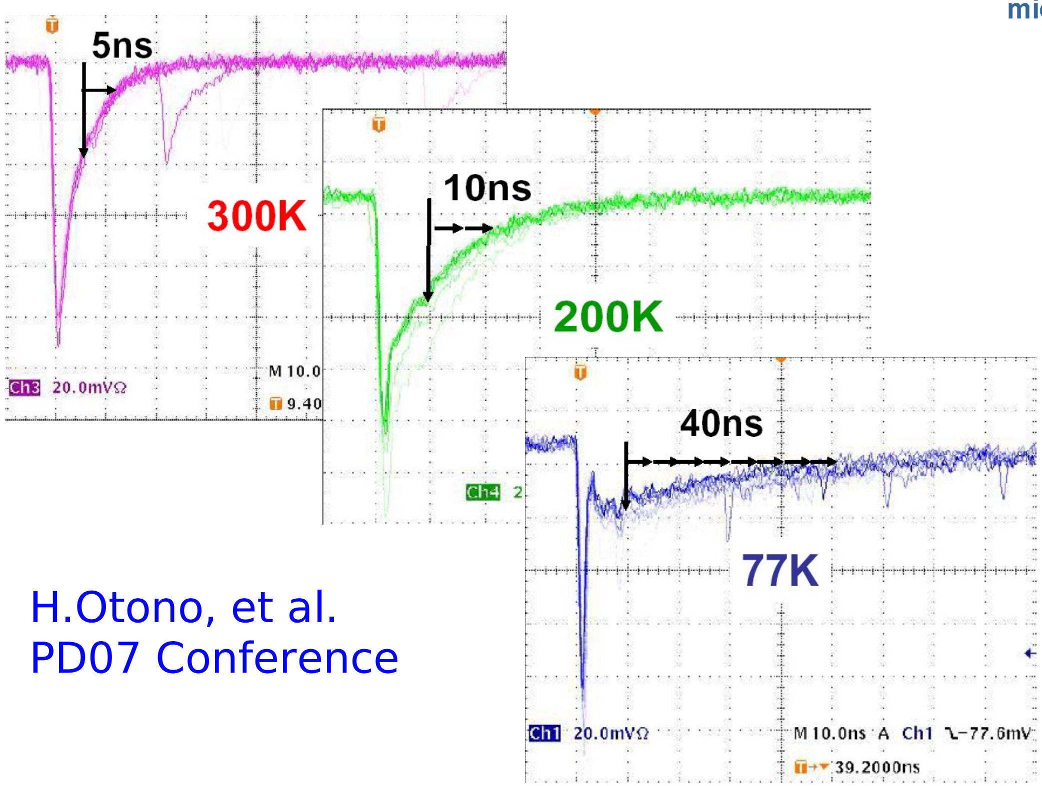

Waveform:

The two current components show different behavior with Temperature

(fast component is independent of T because stray C_Q couple with external R_{LOAD} independently of R_Q)

H.Otono, et al.
PD07 Conference

I-V measurements: forward bias

1 **Forward current** $J_F \sim \exp(V_d \frac{q}{\eta k T})$

Diffusion dominating: $\eta \to 1$
Recombination dominating: $\eta \to 2$

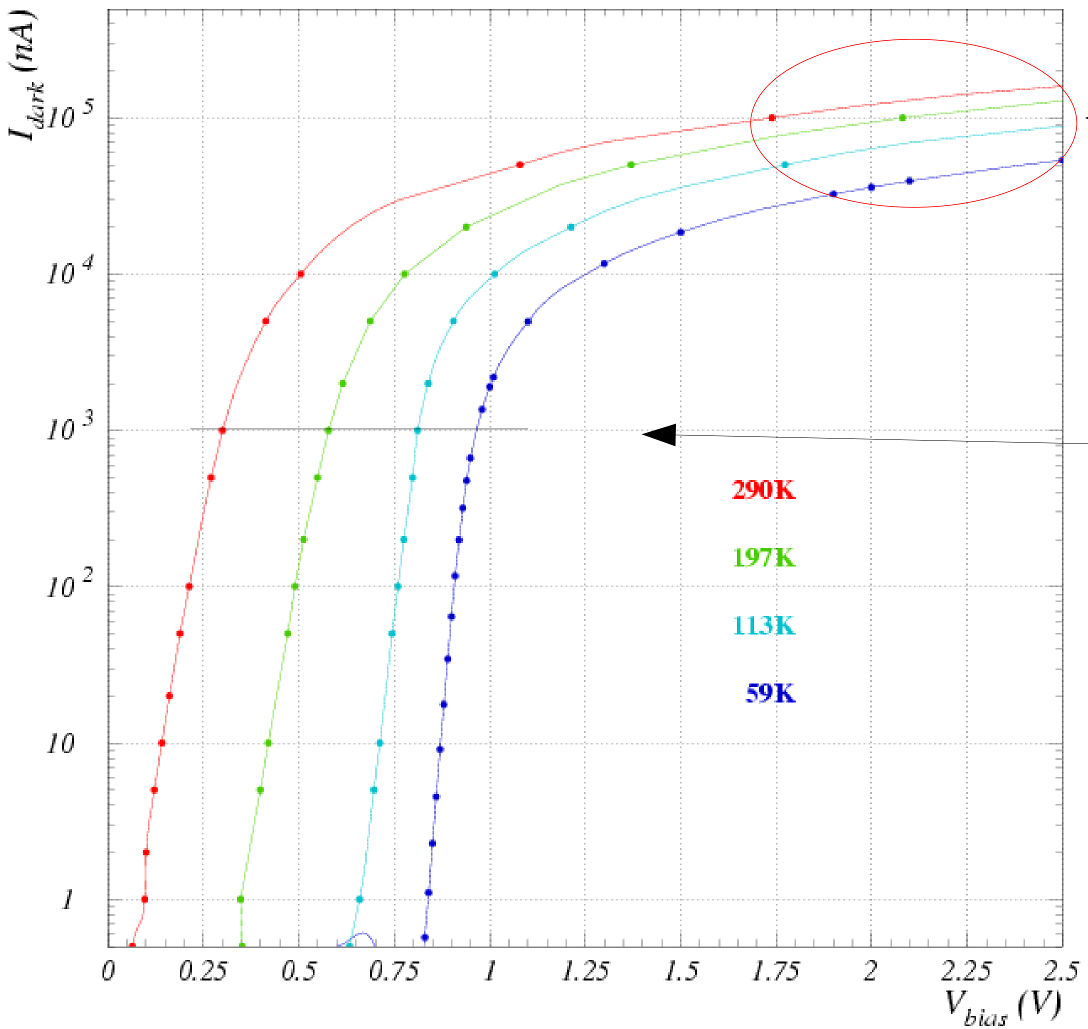

2 **Ohmic** behavior at high current

Linear fit → $R_{series} \sim R_Q / N_{cells}$

3 **Voltage drop** (V_d) increases with T decreasing (e.g. at 1μA)

I-V measurements: forward bias

Voltage drop at fixed forward current → precise **measurement of junction T**

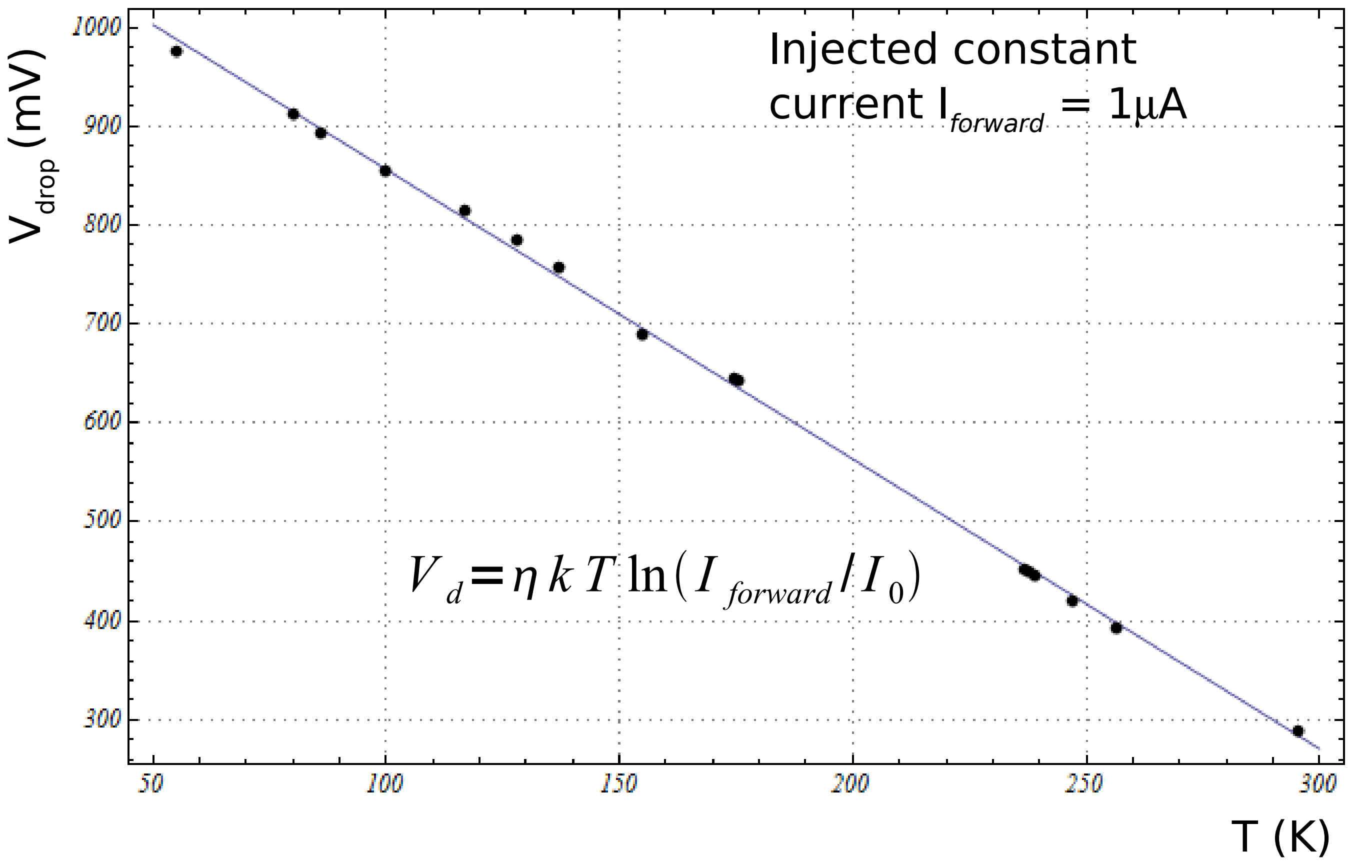

- linear dependence with slope $dV_{drop}/dT|_{1\mu A} \sim 3mV/K$
- precise calibration/probe for junction Temperature

Series Resistance vs T

1) Fit at high V of forward characteristic → **measurement of series resistance R_s**

2) Exponential recovery time (afterpulses envelope) → **measurement of R_s**

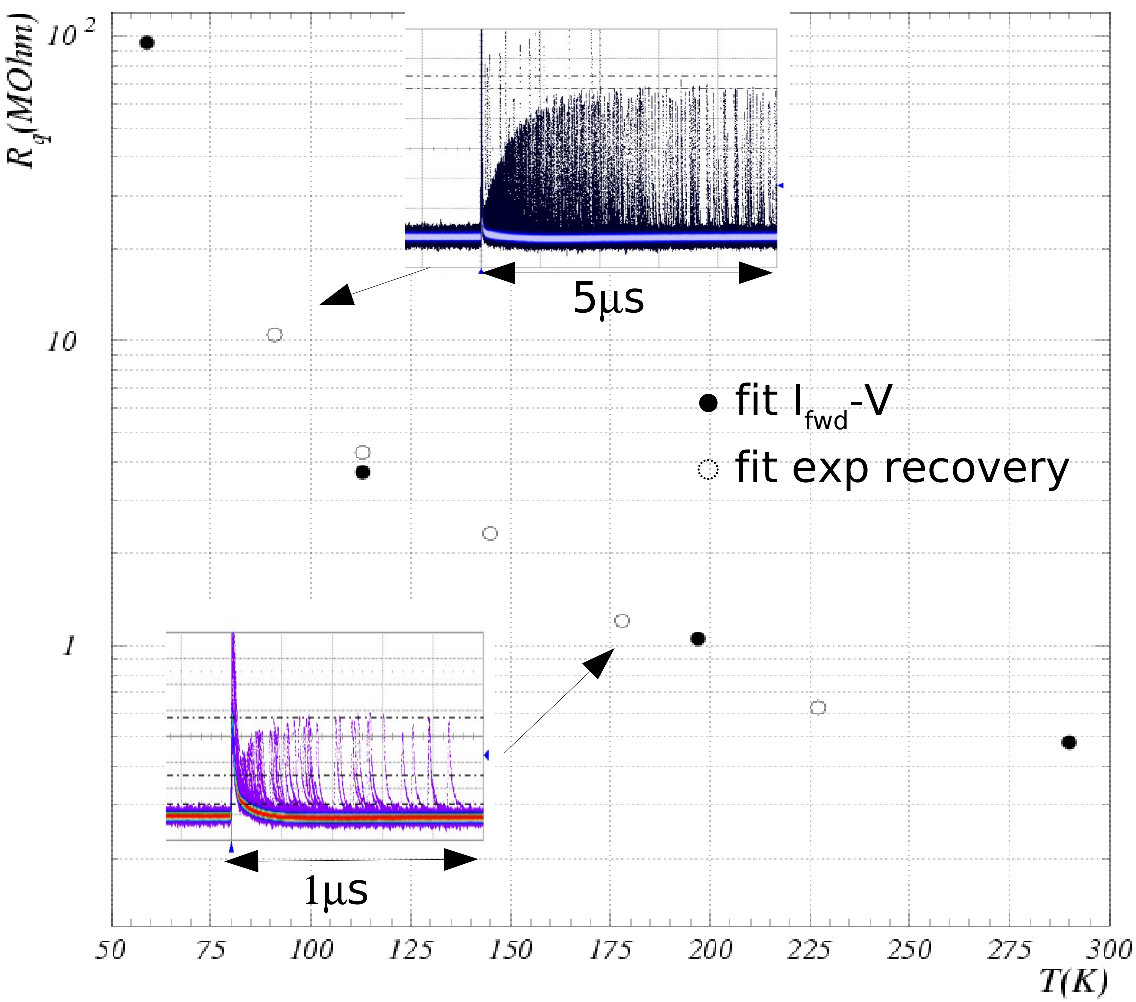

The two kinds of measurement are consistent
→ **dominant effect from quenching resistor R_Q**

NOTE: afterpulses envelope

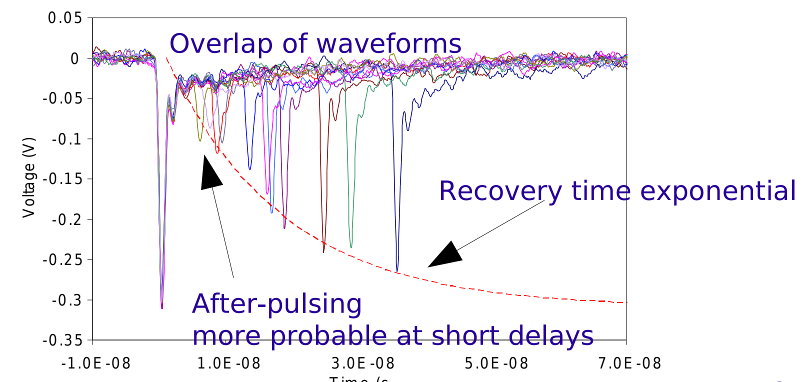

I-V measurements: reverse bias

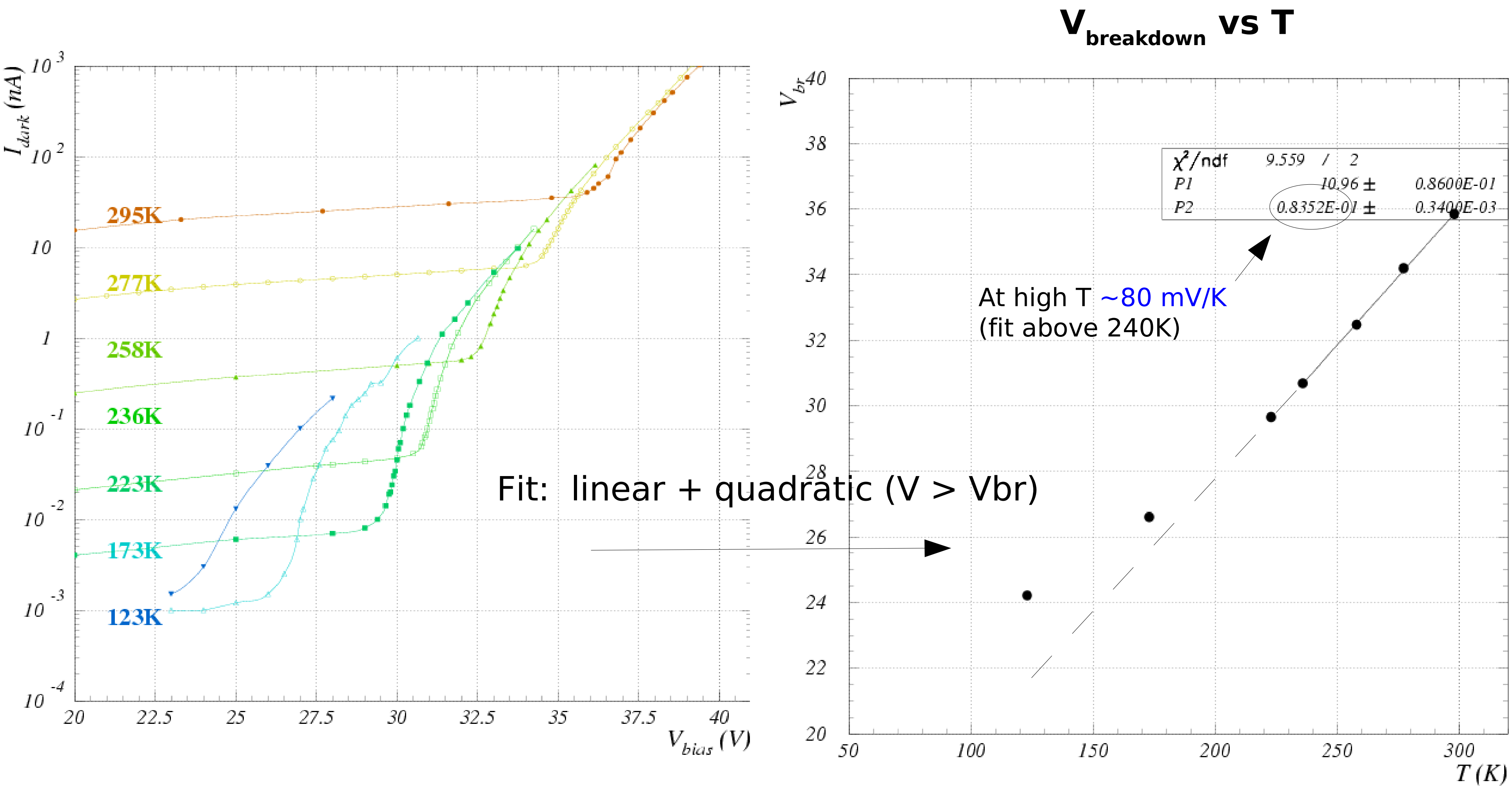

Avalanche breakdown voltage decreases due to increased carriers mobility at low T

V breakdown vs T

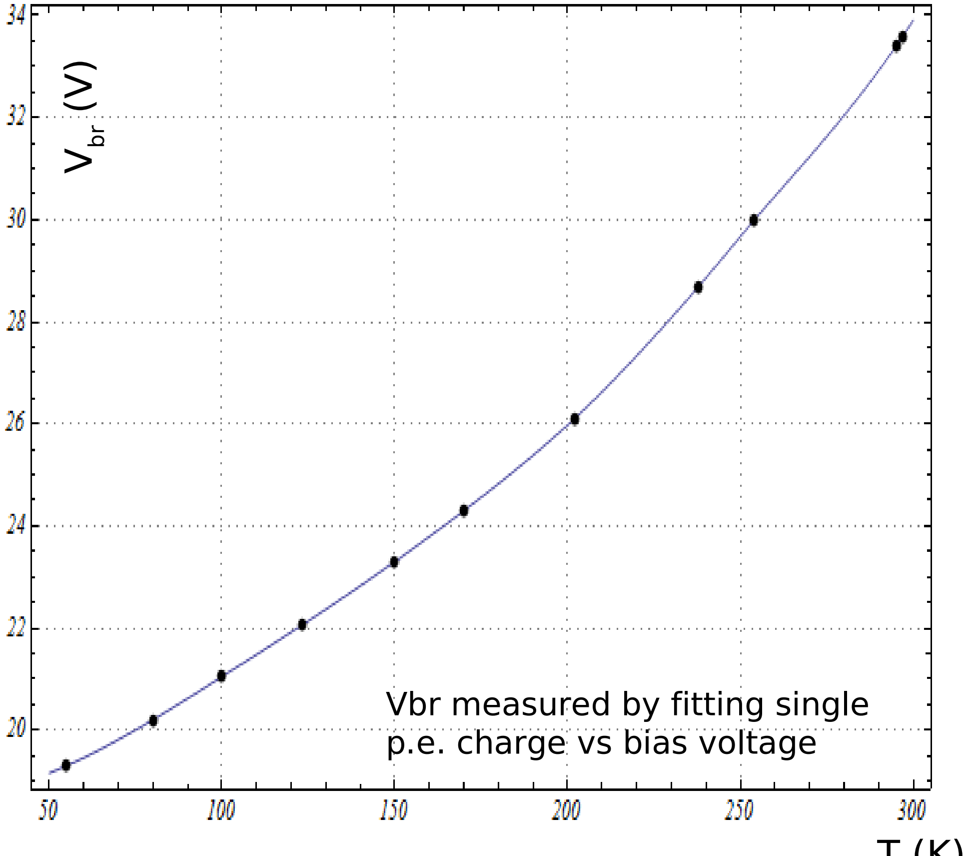

Consistent with Baraff model for doping profile of FKB SiPM

Temperature coefficient

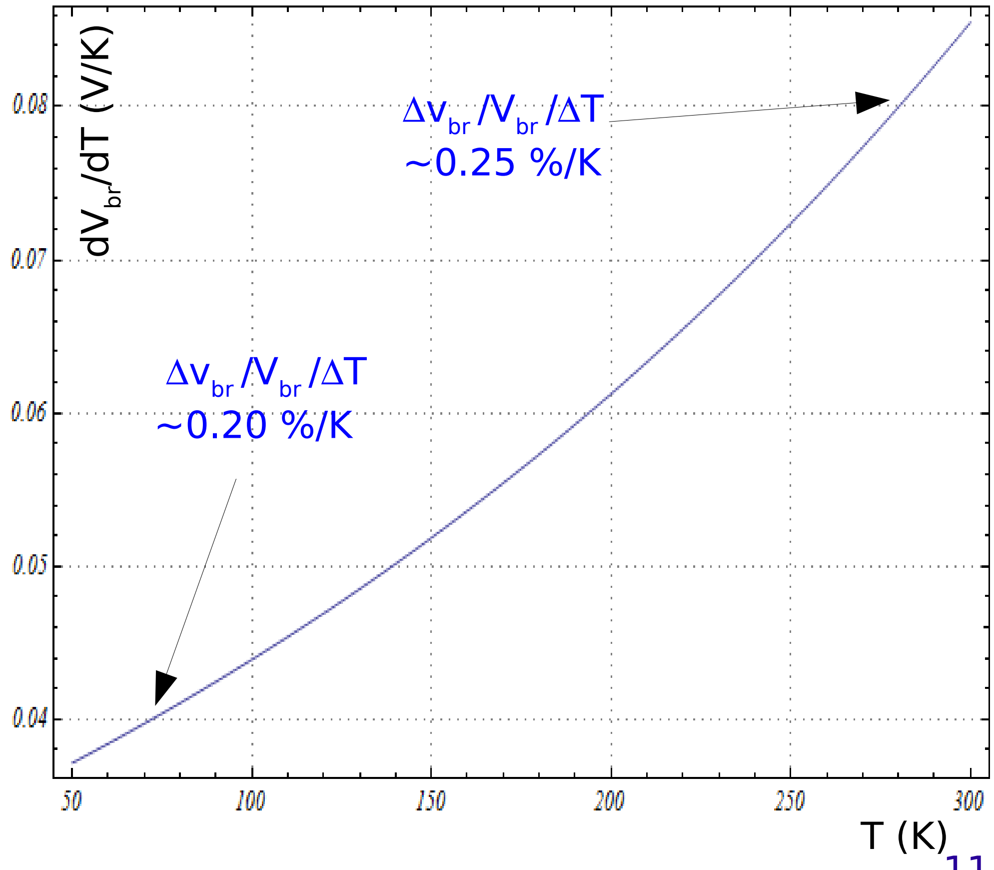

Improved stability at lower T

Dark current vs T at constant gain (i.e. fixed ΔV)

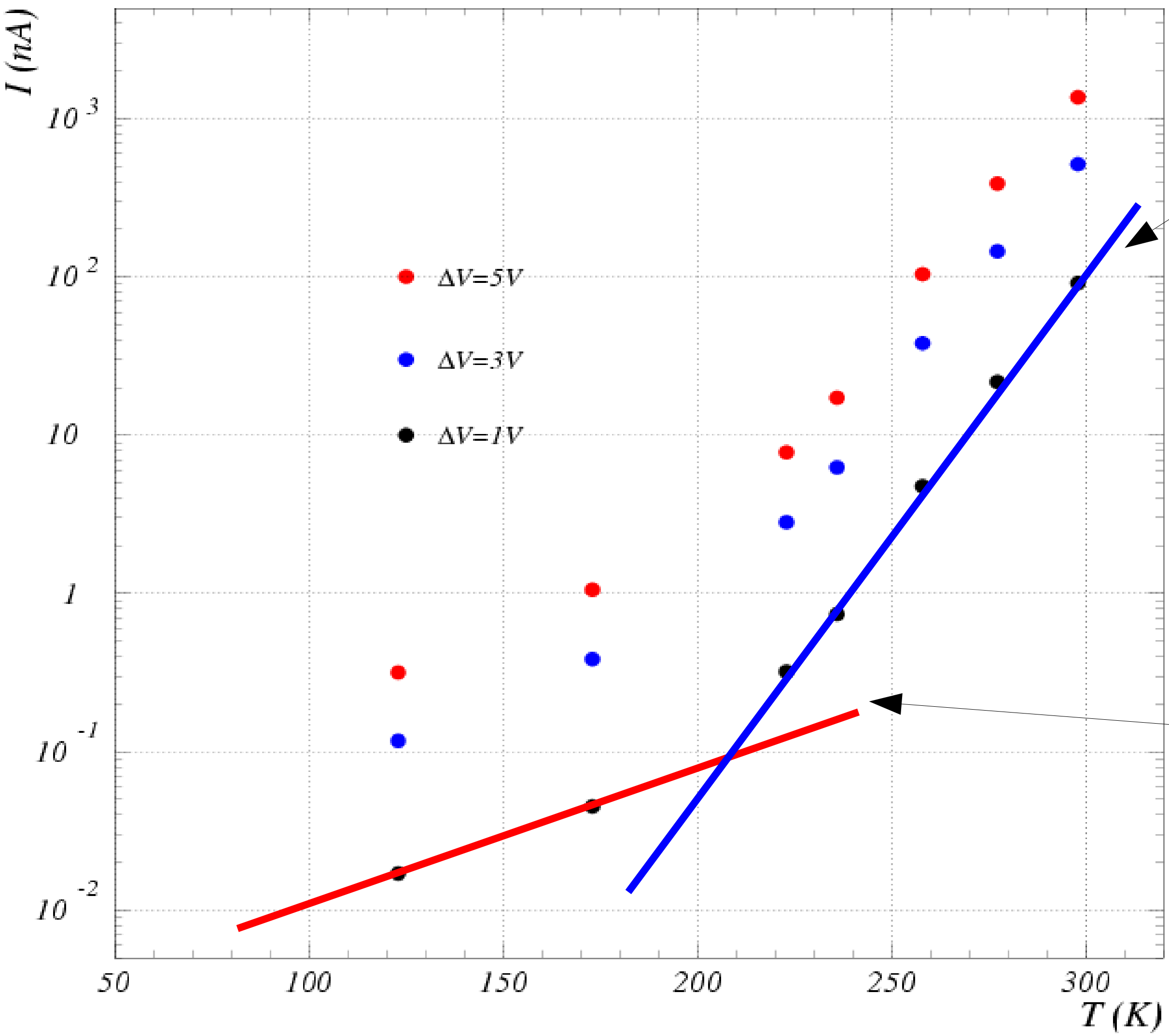

Main noise mechanisms:

1) Gereration/Recombination noise (SHR field enhanced)

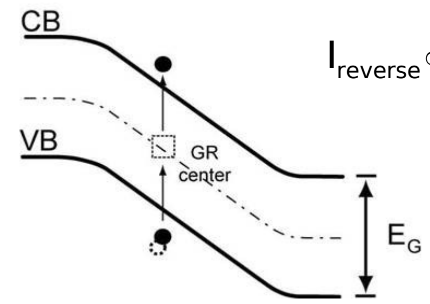

$$I_{reverse} \propto T^{1.5} \exp \frac{-E_g}{K_B T}$$

2) Band-to band Tunnel noise (strong dependence on the Electric field profile)

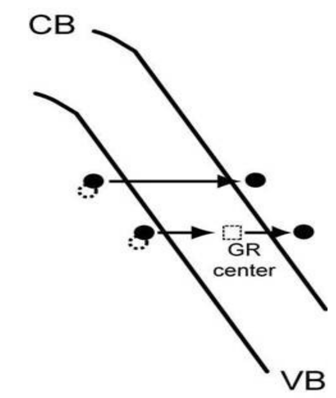

Tunnel noise dominating for T<200K (FBK devices)

Dark counts rate vs T at constant gain (i.e. fixed ΔV)

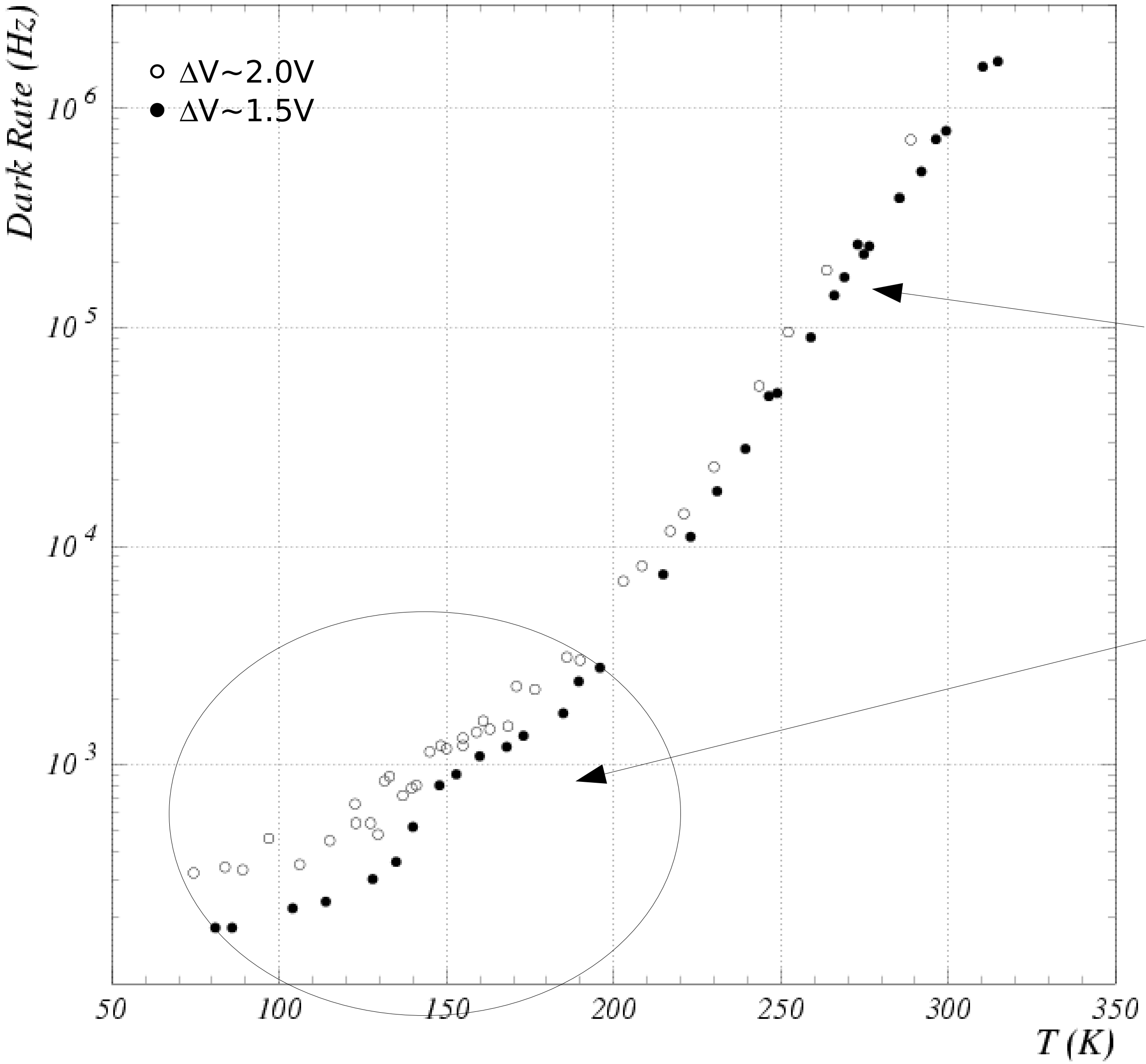

Measurement: **rate of ≥1p.e.** at fixed gain (i.e. ~fixed ΔV)

Activation energy
Eg~0.358eV

Two tunneling mechanisms ?
to be understood

After-pulsing

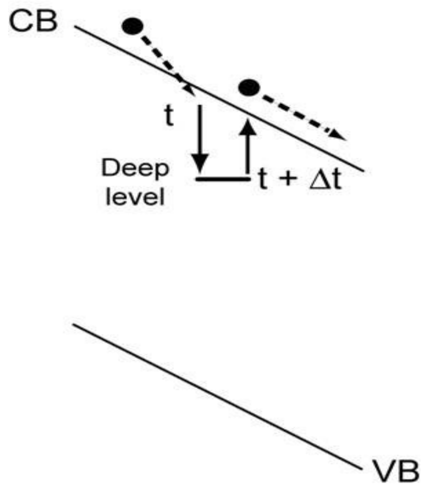

Carrier trapping and delayed release

$$P_{after-pulse}(t) = P_c \cdot \frac{\exp(-t/\tau)}{\tau} \cdot P_{01} \propto \Delta V^2$$

P_{01} : trigger probability
∝ ΔV(t) (over-voltage, recovery)

τ : trap lifetime
depends on trap level position

quadratic dependence on ΔV

P_c : trap capture probability
∝ carrier flux (current) during avalanche ∝ ΔV (over-voltage)
∝ N traps

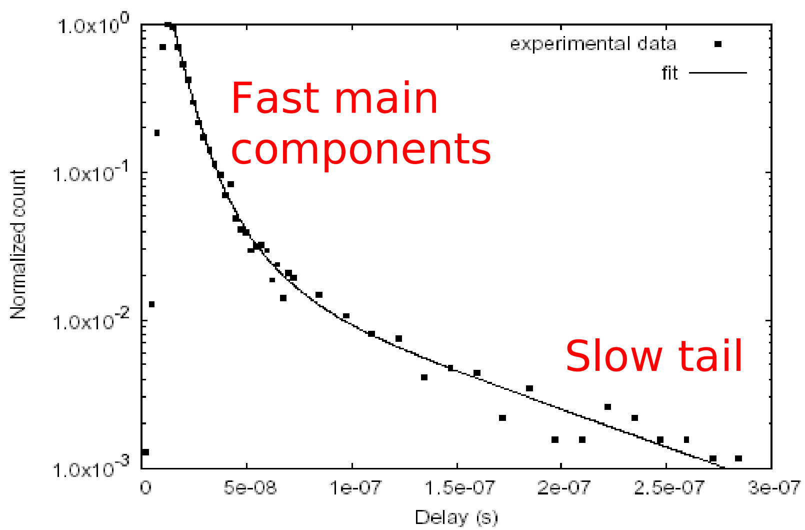

Fig. 10. Spectrum of the delay time from the primary pulse to the after-pulse.

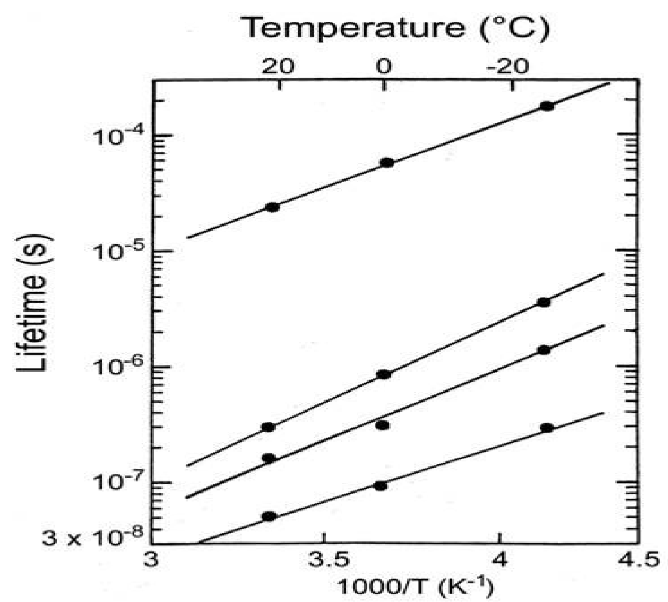

S.Cova, A.Lacaita, G.Ripamonti, IEEE EDL (1991)

It can be reduced to % in a wide ΔV range… at 300K

After-pulses vs T (constant gain, ie ΔV)

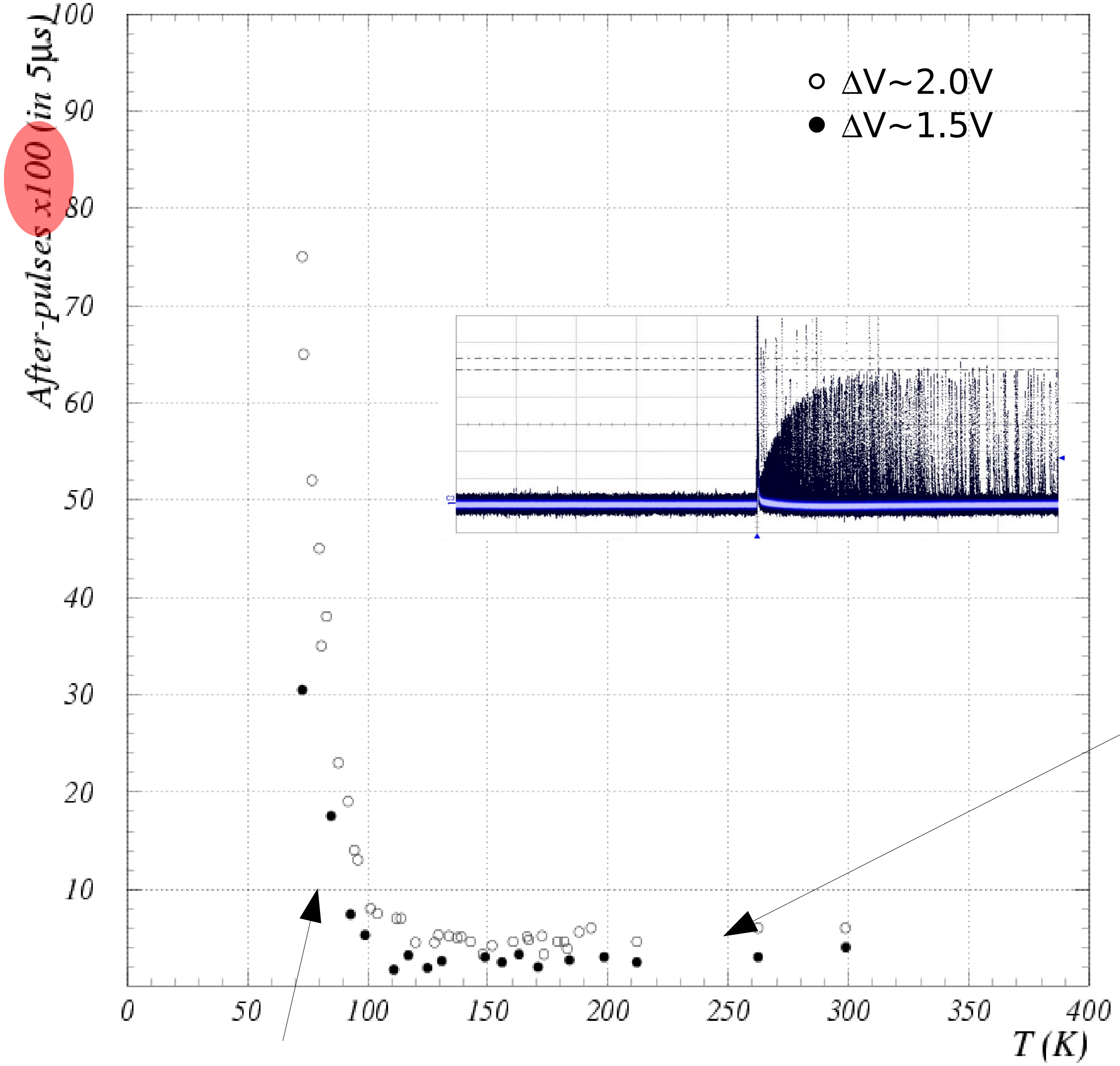

Measurement:
of **average number of after-pulses** counted in the **5μs time window** following the trigger (1 p.e.) at fixed gain (i.e. ~fixed ΔV) (dark noise subtracted)

- Few % at room T
- quite constant down to ~120K

T decreasing: increase of characteristic time constants of traps (τ_{traps}) is compensated by increasing cell recovery time (R_Q)

- Several % below 100K

T<100K: new traping centers active (to be studied in more detail)

ΔV scan (fixed T) – DR, AP, Gain, X-TALK

Dark Noise Rate
decreasing at low T

After-Pulsing
increasing at low T

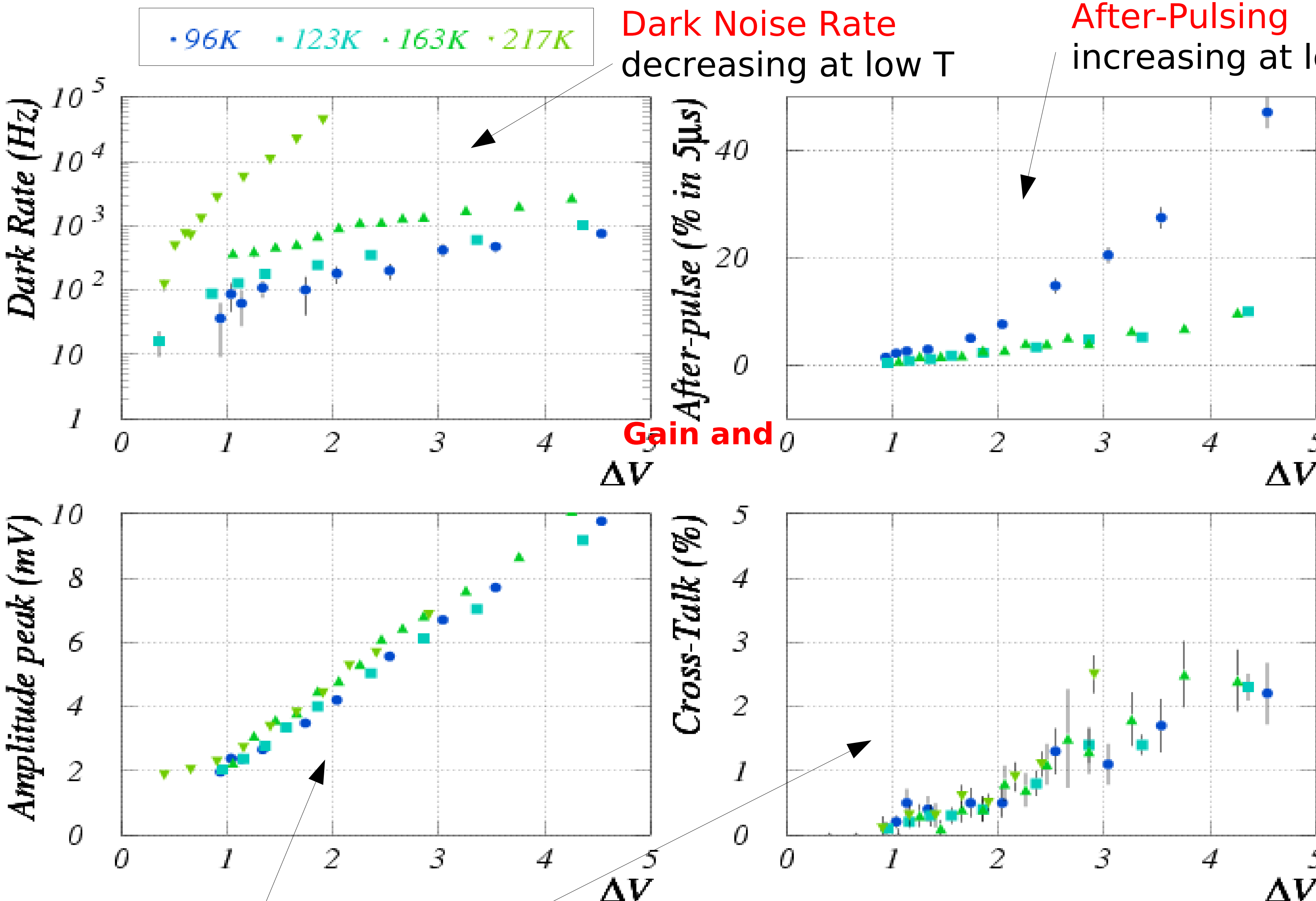

Gain and

Gain and Cross-Talk independent of Temperature

PDE vs ΔV and λ (room T)

device with ε_{geom} ~50%

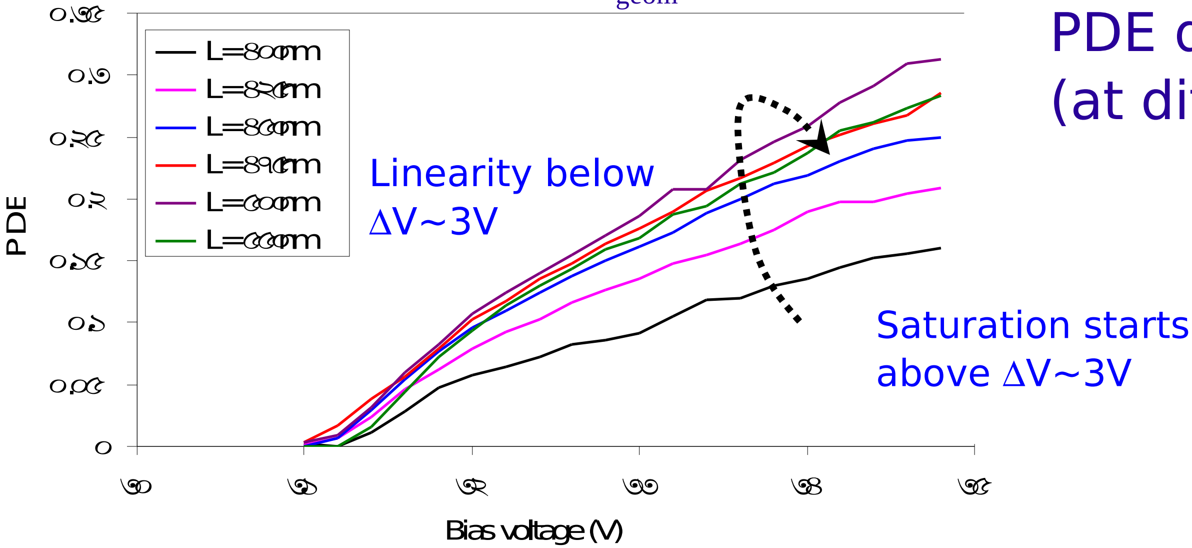

PDE dependence on ΔV (at different λ)

device with ε_{geom} ~ 22%

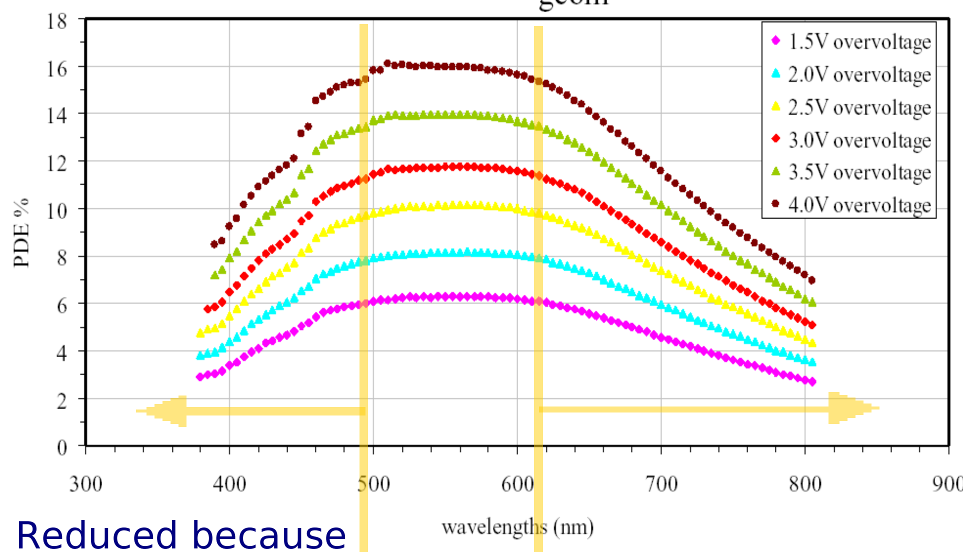

Reduced because avalanche triggered by holes (and ARC)

Reduced because low QE

PDE dependence on λ (at different ΔV)

PDE at various λ - ΔV scan (at constant T)

PDE vs ΔV measured as Current/Gain → PDE (a.u.) ≡ I_{SiPM} / I_{calib} / ΔV

Normalization to calibrated photo-diode current (not absolute # of photons)

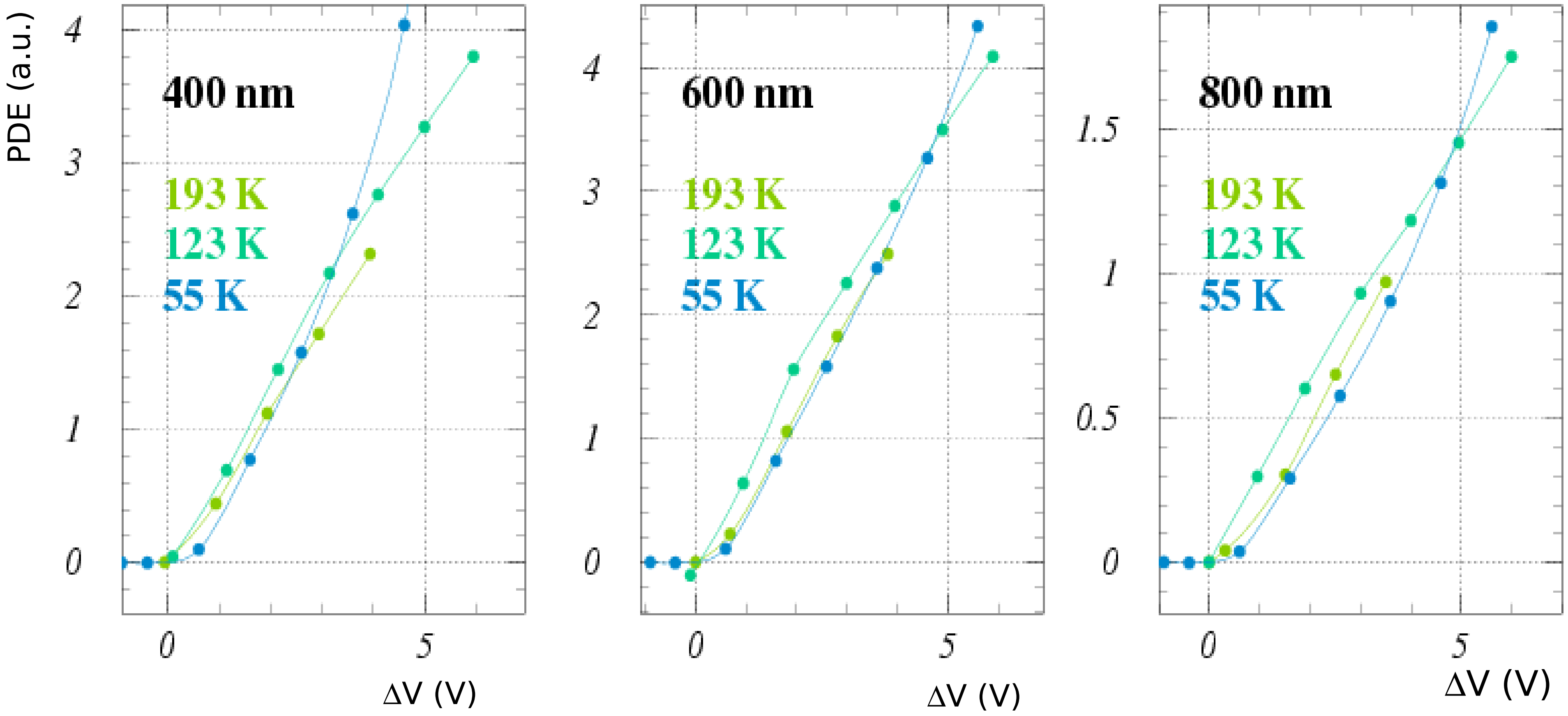

- 193K and 123K measurements not affected by after-pulses → saturation visible
- 55K affetcted by after-pulses (not corrected; cross-talk is not subtracted too)

(Dark rate subtracted - small effect)

PDE with LED (380nm) - ΔV scan (const. T)

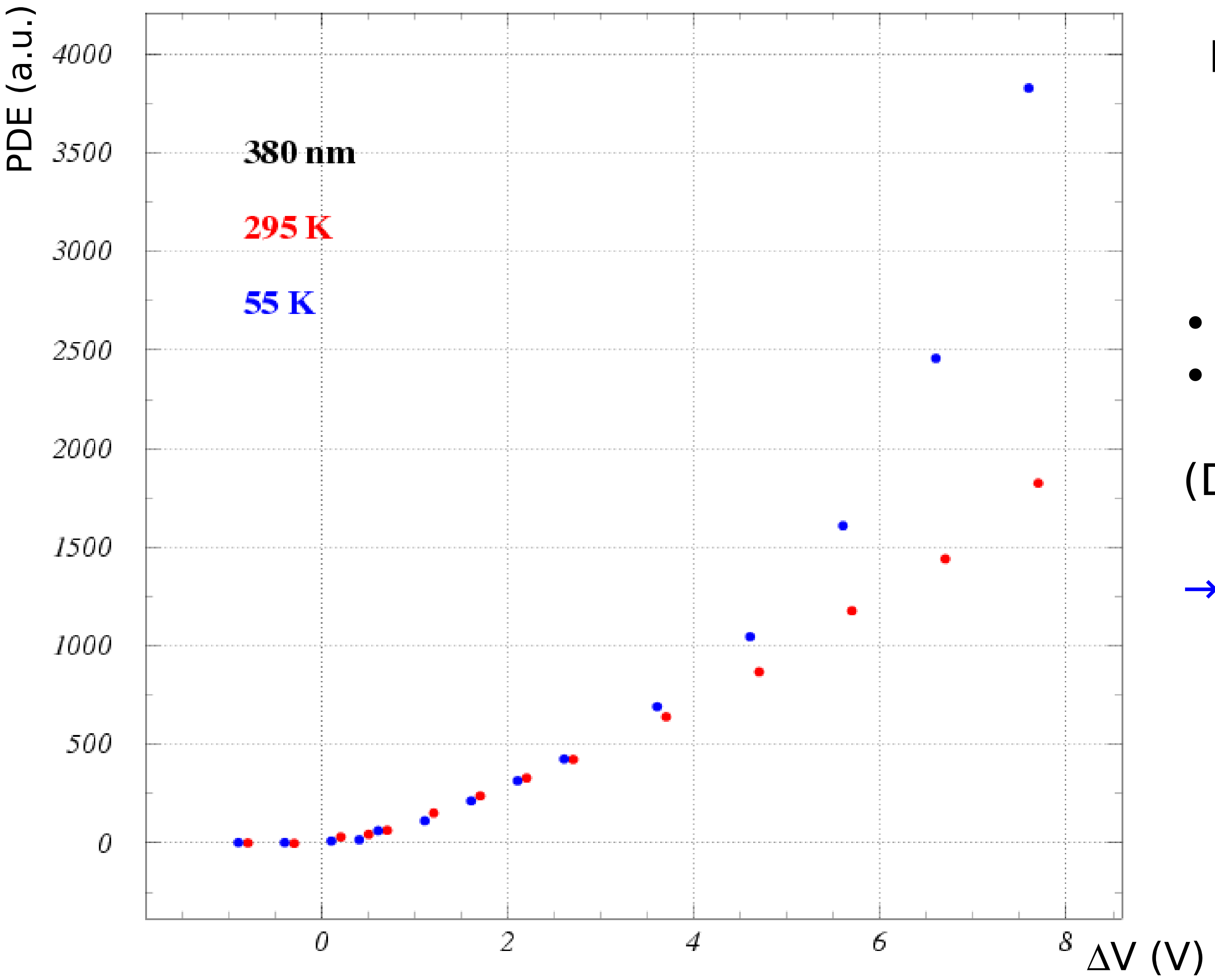

PDE (a.u.) ≡ $I_{SiPM} / I_{LED} / \Delta V$

- 55K affected by After-Pulses
- 295K less affected by A-P

(Dark rate subtracted)

→ Slope PDE/ΔV (at small ΔV) independent of T

PDE with LED (380nm) - T scan ($\Delta V=2V$)

PDE dependence on T at fixed gain. Normalization with PDE at T=300K

$PDE(T) \equiv I_{SiPM}(T) / I_{LED}$

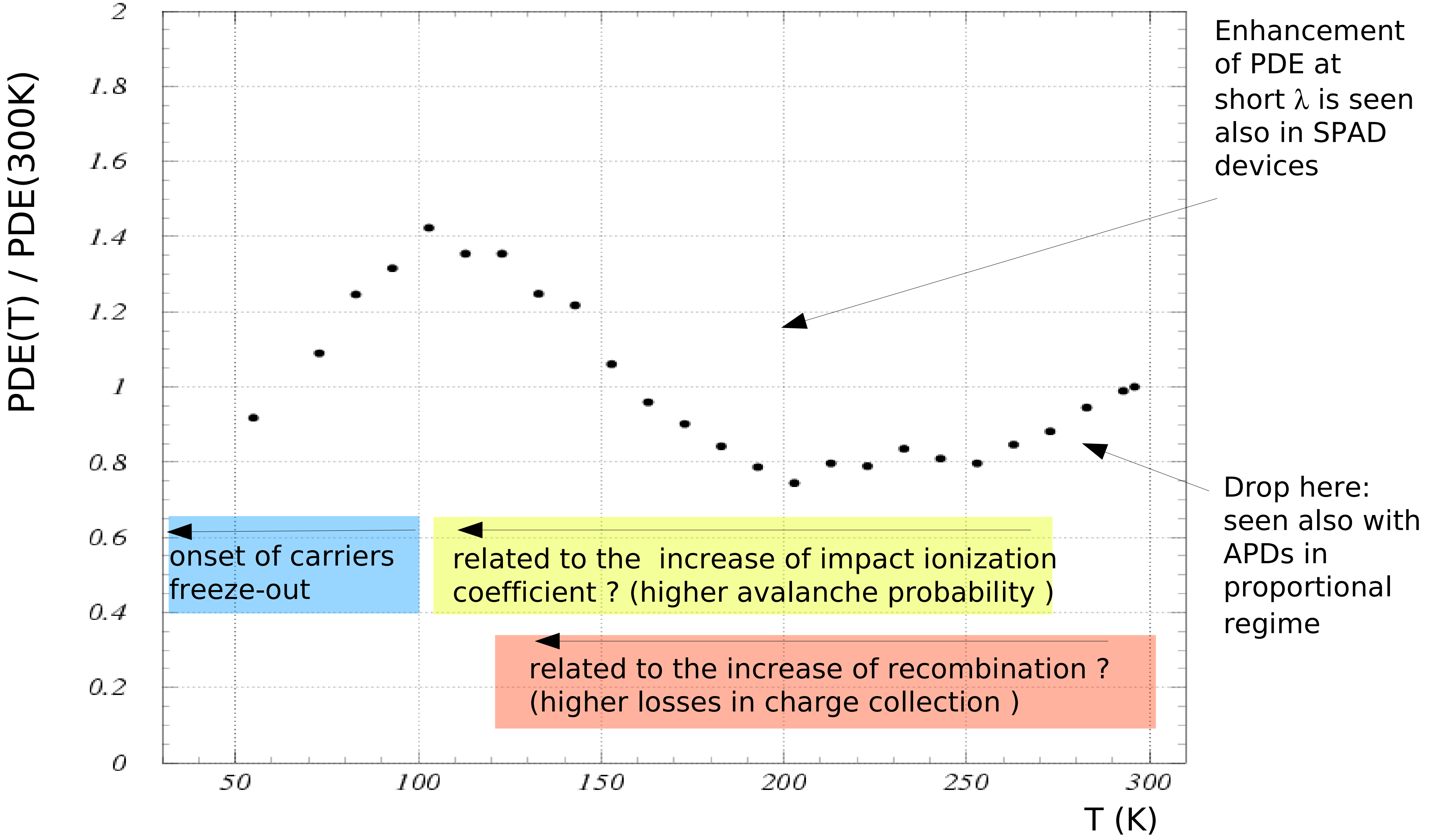

Studies ongoing for better understanding this shape

PDE at various λ – T scan (ΔV =2V)

PDE dependence on T at fixed gain. Normalization with calibrated photo-diode current and with PDE at T=300K (double ratio)

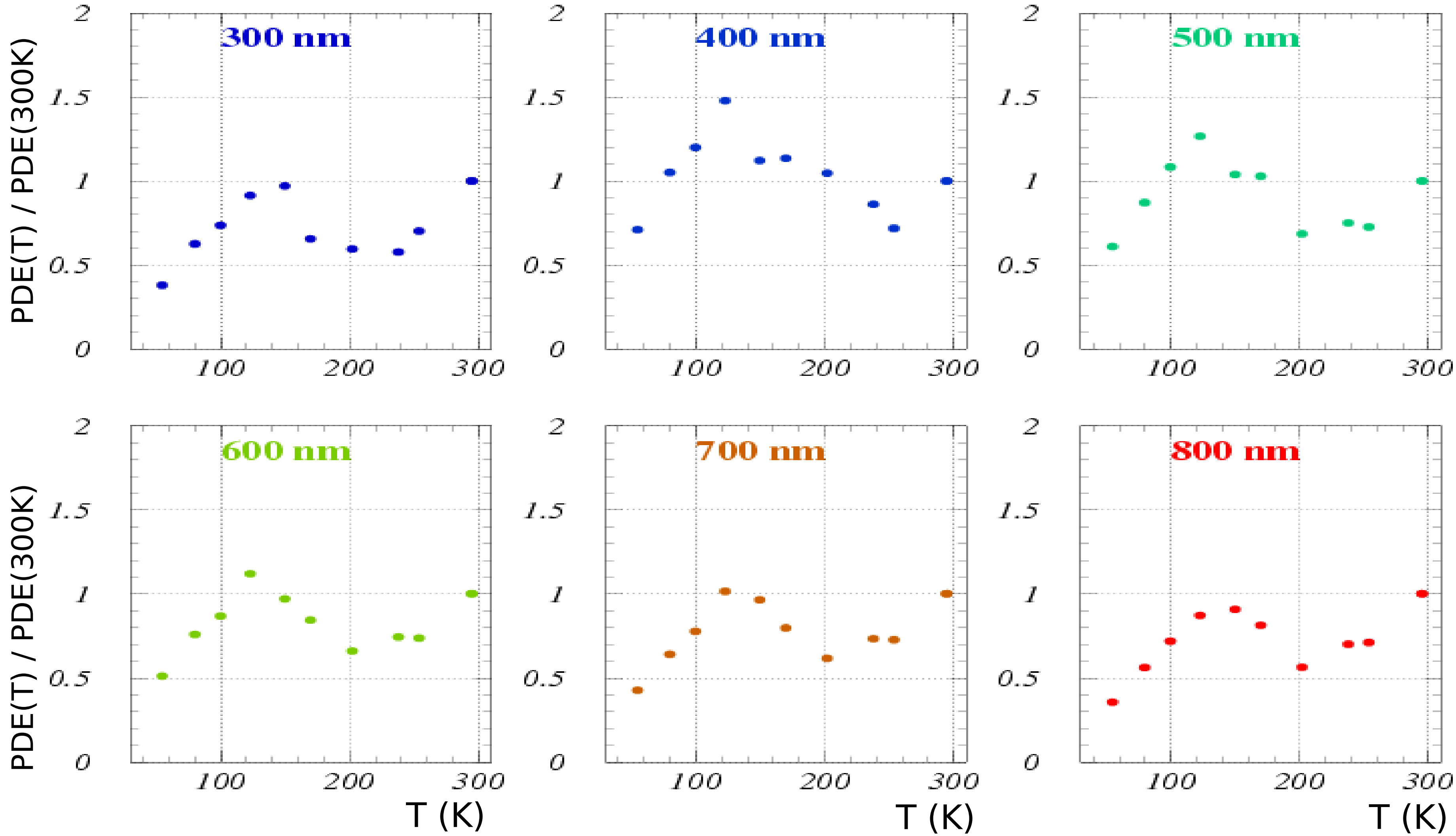

$PDE(T) \equiv I_{SiPM}(T) / I_{calibrated\ P\text{-}D}$

- shape similar at different λ → related to properties of multiplication /recombination
- lower efficiency at low T for longer λ → due to absorption length ~ 1/T (with constant depletion width)

SiPM Timing – overview

GM-APD timing: fast and slow components

1) Fast component: gaussian with time scale O(10ps)

Statistical fluctuations in the avalanche:

- Longitudinal build-up (minor contribution)
- Transversal propagation (main contribution):
  - via Multiplication assisted diffusion (dominating in few um thin devices) A.Lacaita et al. APL and El.Lett. 1990
  - via Photon assisted propagation (dominating in thick devices - O(100um)) PP.Webb, R.J. McIntyre RCA Eng. 1982 A.Lacaita et al. APL 1992

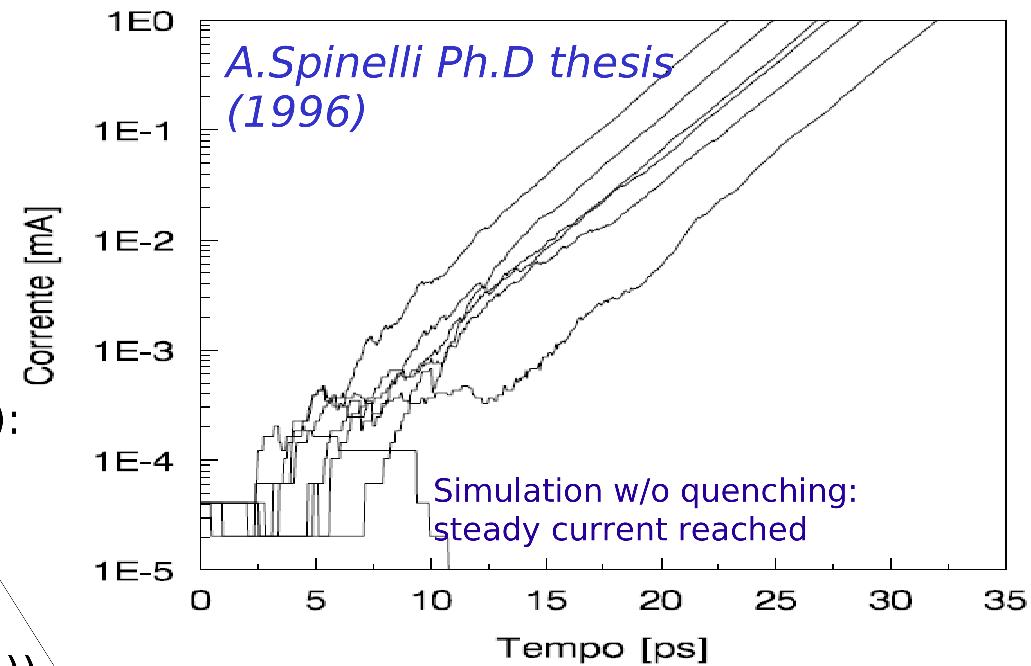

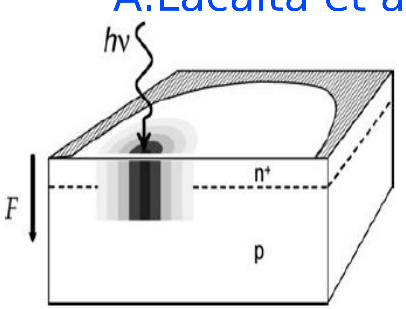

Multiplication assisted diffusion

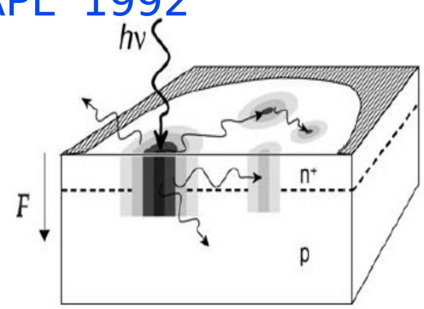

Photon assisted propagation

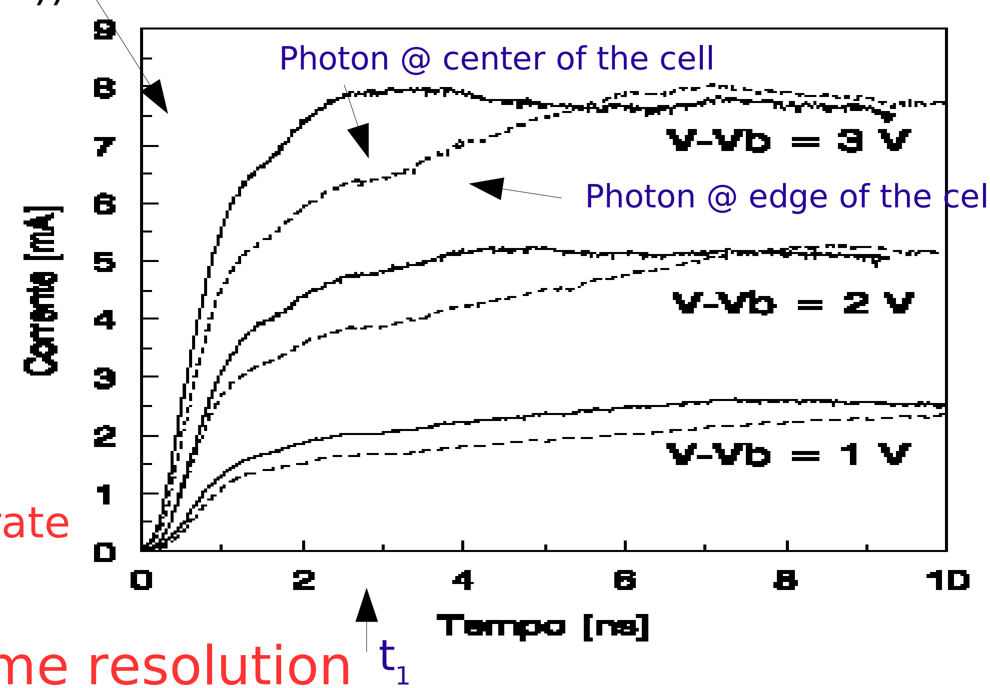

Dependence of avalanche build-up rate on the impact position ($\rightarrow$ cell size)

Higher overvoltage $\rightarrow$ improved time resolution

GM-APD timing: fast and slow components

2) Slow component: minor non gaussian tails with time scale O(ns)

Carriers photogenerated in the neutral regions beneath the junction and reaching the electric field region by diffusion

G.Ripamonti, S.Cova Sol.State Electronics (1985)

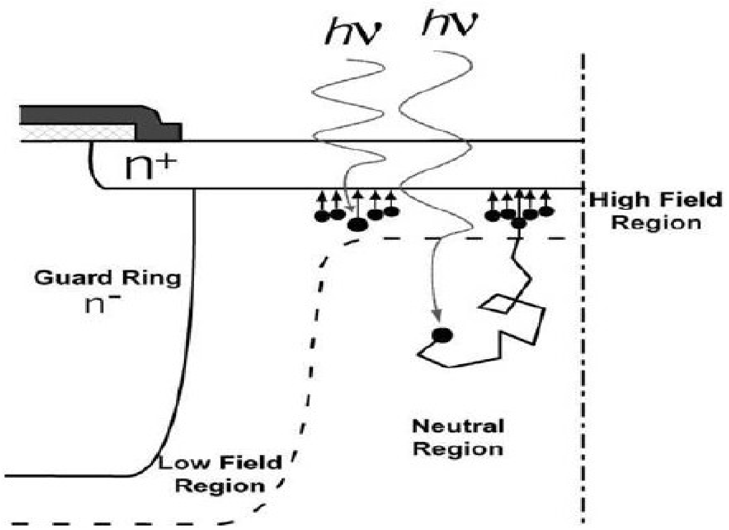

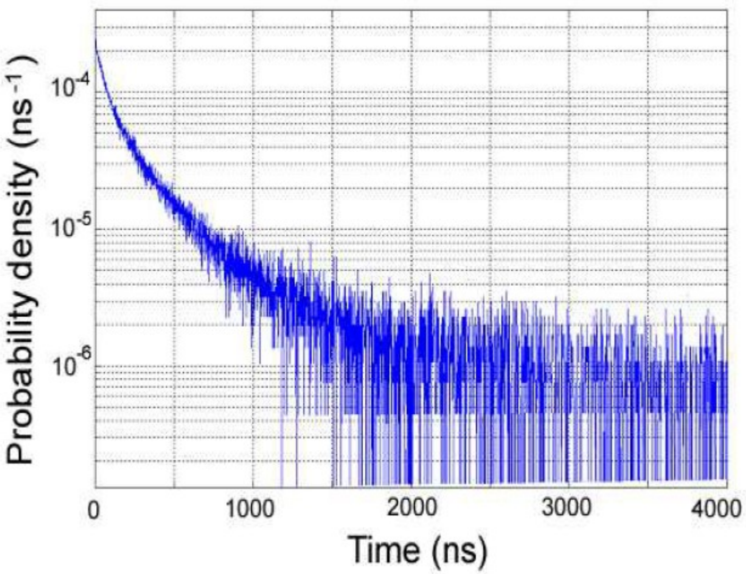

tail lifetime: $\tau \sim L^2 / \pi^2 D$
L = effective neutral layer thickness
D = diffusion coefficient

S.Cova et al. NIST Workshop on SPD (2003)

Shorter wavelengths $\rightarrow$ higher resolution (reduced tails)

Waveform analysis: method

(1) Selection of candidate peaks:
- single photon peaks
- proper signal shape
- low instantaneous intensity (no activity before/after within 50ns)
- low noise during the previous 10 ns (typical noise ~ 1mV rms)

(2) Peak reconstruction
- optimum time reconstruction
- amplitude and width (baseline shift correction)

(3) Time difference Δt between consecutive peaks

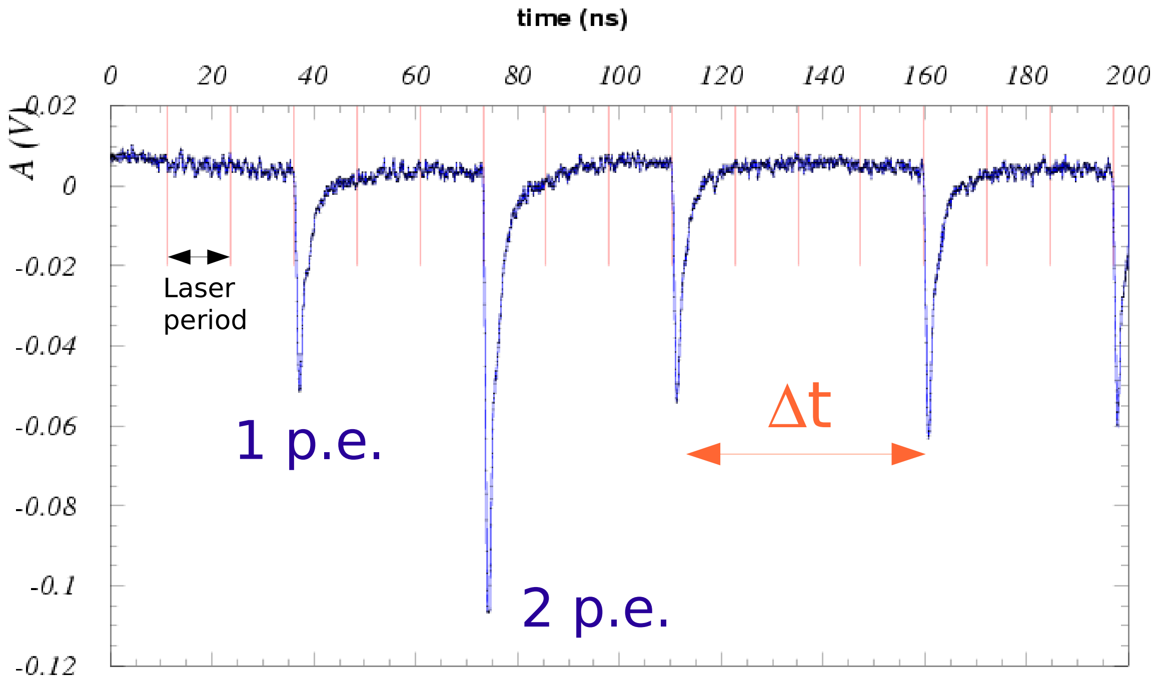

NOTE: working fine at 20MHz counting rate

Waveform analysis: optimum timing filter

Different methods to reconstruct the time of a peak:

✗ parabolic fit to find the peak maximum
✗ average of time samples weighted by the waveform derivative
✔ digital filter: weighting by the derivative of a reference signal
$\rightarrow$ best against noise (signal shape known)

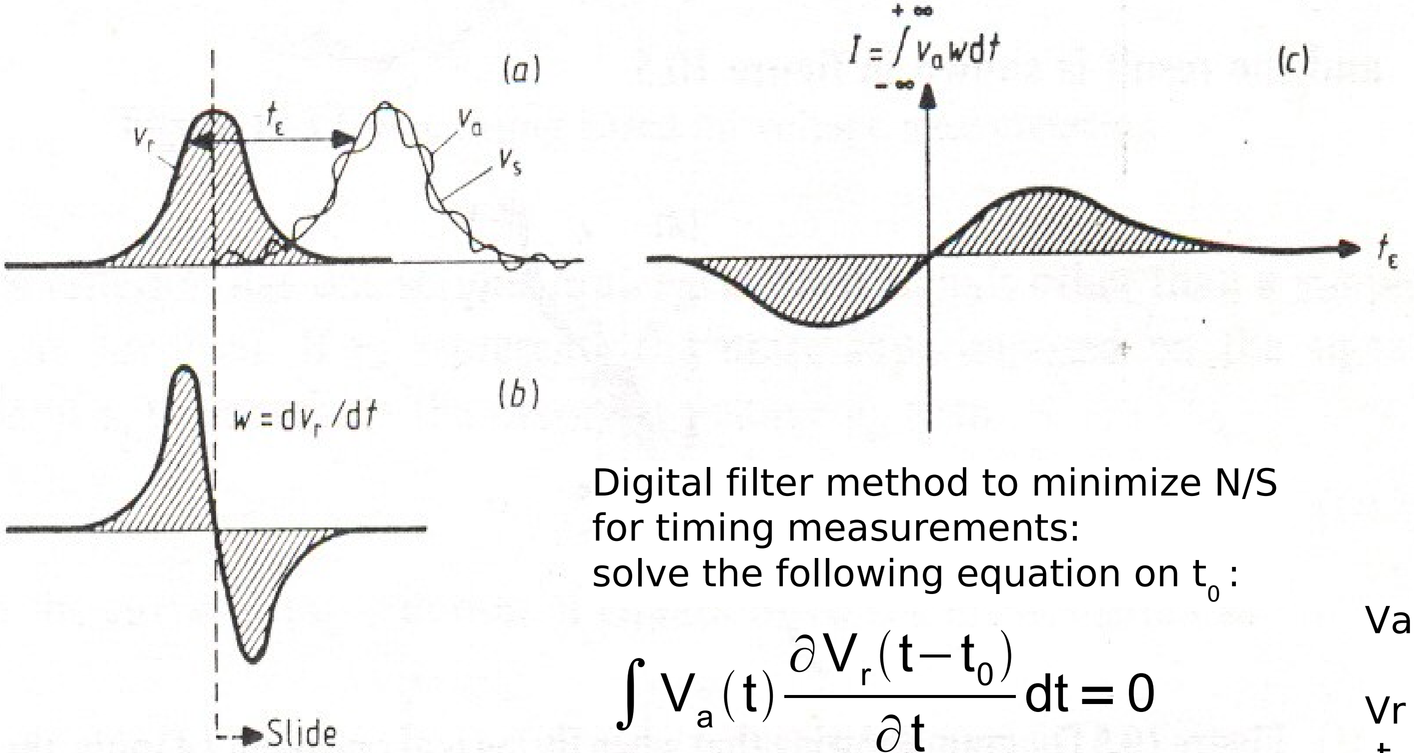

Digital filter method to minimize N/S for timing measurements:
solve the following equation on t_0 :

$$\int V_a(t) \frac{\partial V_r(t-t_0)}{\partial t} dt = 0$$

Va = measured signal (includes noise)
Vr = reference signal
t_0 = reference time

Single Photon Timing Resolution (SPTR)

Analysis of the distributions of the t difference between successive peaks (modulo the laser period T_{laser}=12.367ns)

Gaussian + **Tails (long λ)**
rms~50-100 ps
~ exp (-t / O(ns))
contrib. several % for long wavelengths

Data at λ=400nm
fit gives reasonable χ^2 with gaussian (σ_t^{fit}) + constant term (dark noise contribution)

The detector resolution is obtained by $\sigma_t^{fit}/\sqrt{2}$

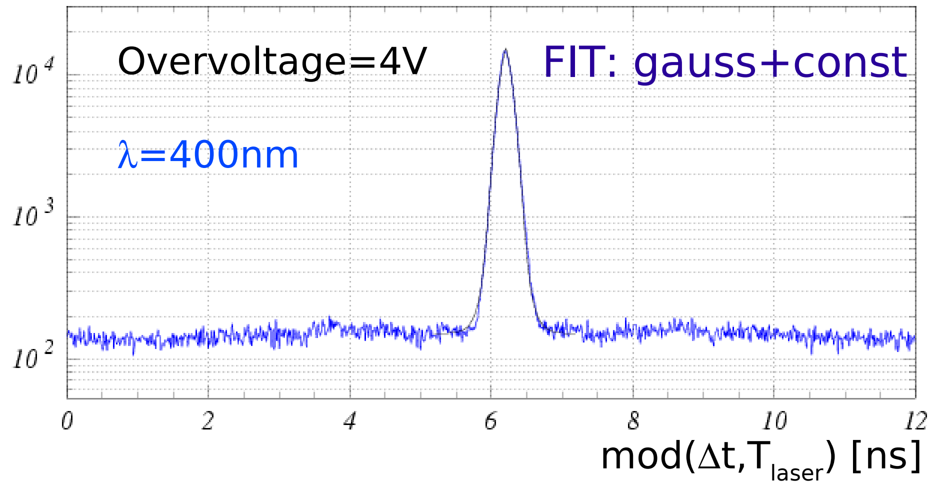

Data at λ=800nm
fit gives reasonable χ^2 with an additional exponential term exp(-Δt/τ)

- τ ~ 0.2÷0.8ns in rough agreement with diffusion tail lifetime: $\tau \sim L^2 / \pi^2 D$ if L is taken to be the diffusion length
- Contribution from the tails ~ 10÷30% of the resolution function area

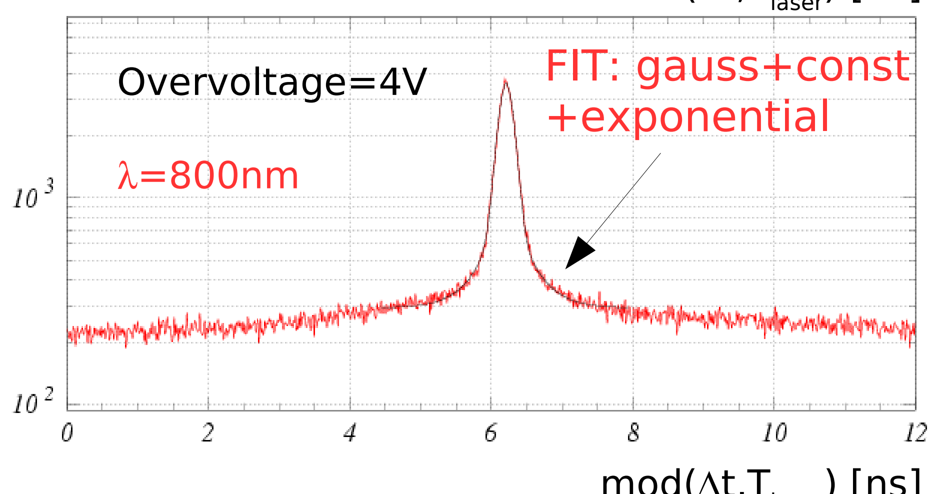

Distributions of the difference in time between successive peaks (modulo the measured laser period T_{laser}=12.367ns)

IRST – single photon timing res. (SPTR)

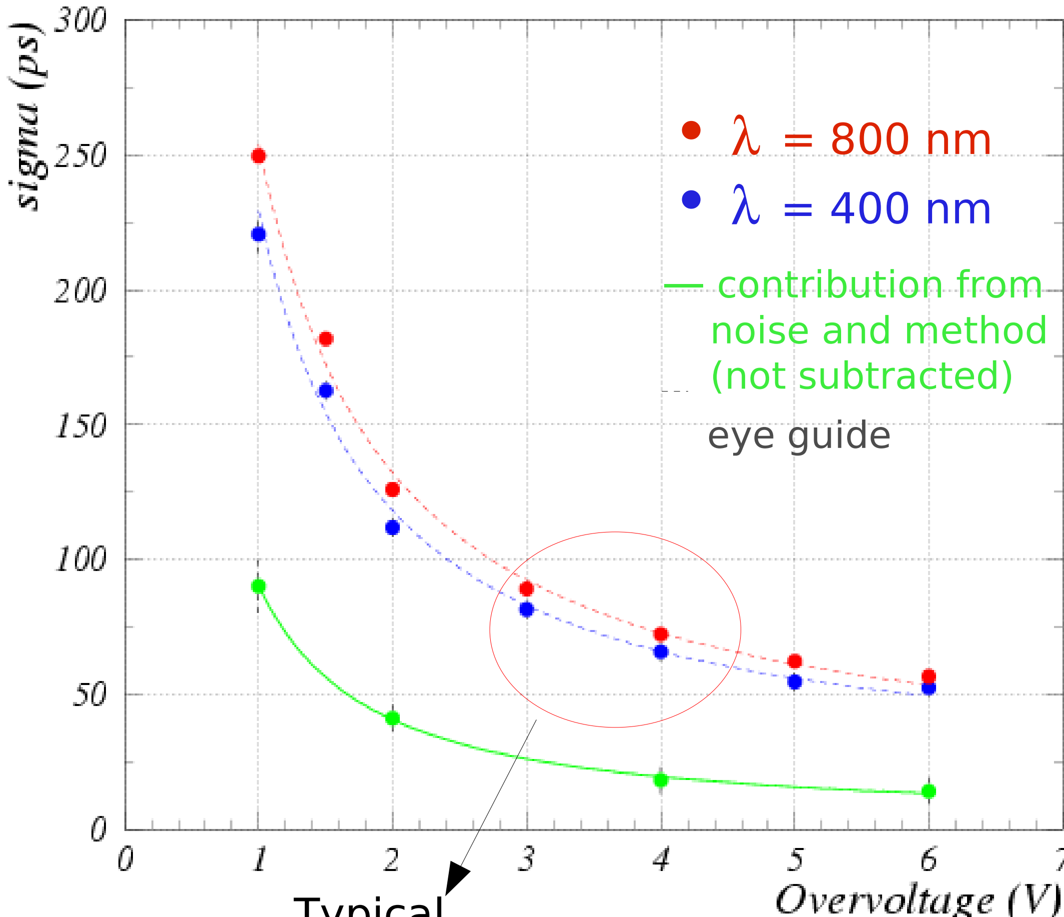

Typical working region

Better resolution for short wavelengths: carriers generated next to the high E field region

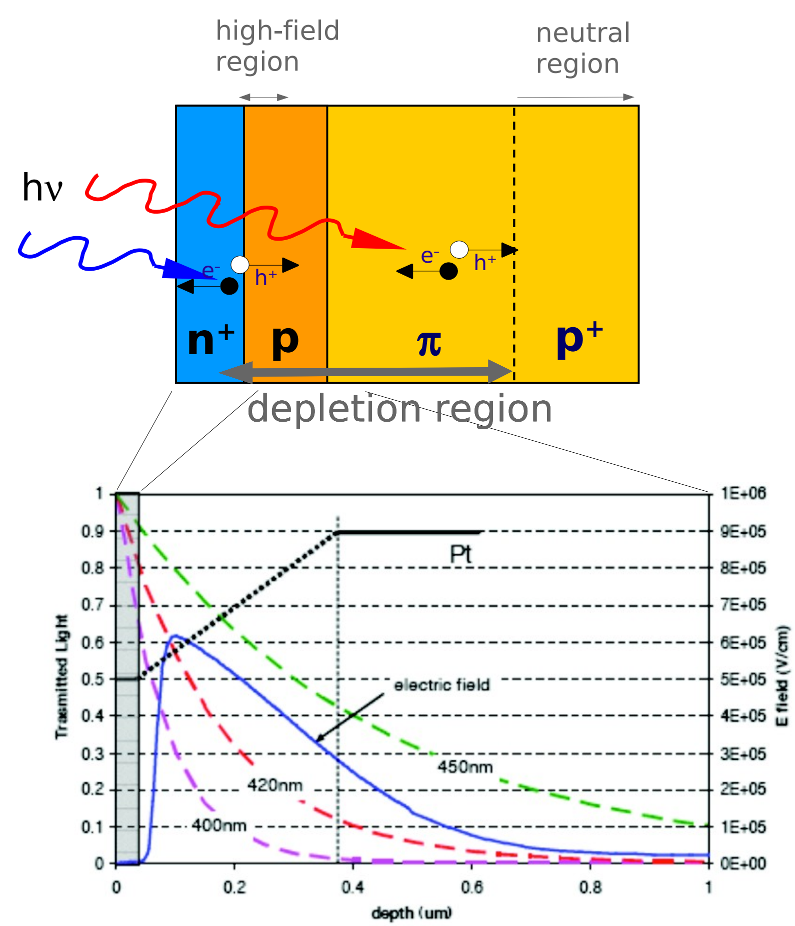

G.Collazuol et al NIMA 581 (2007) 461

IRST devices (different types)

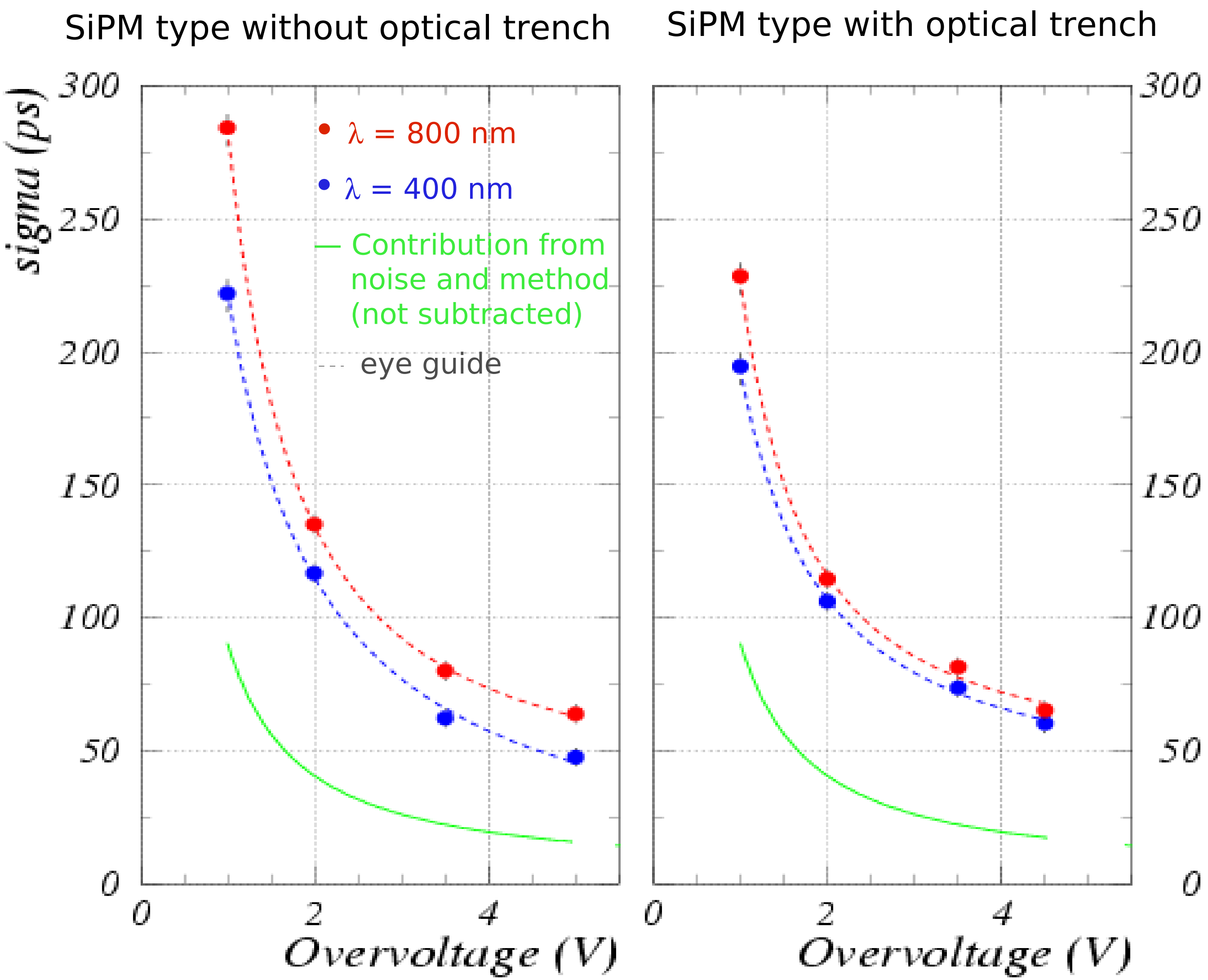

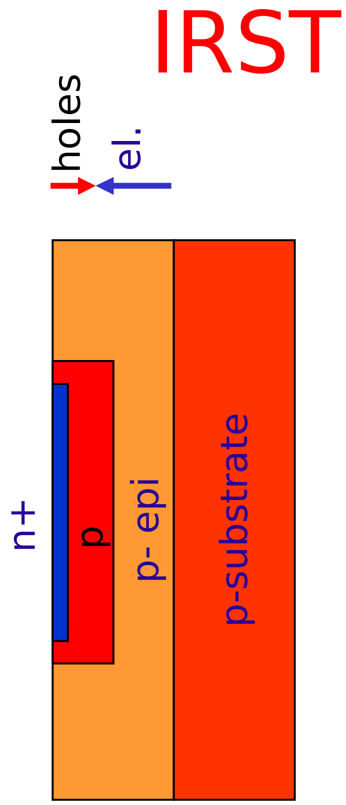

Results in fair agreement for devices with the same structure

Hamamatsu – single photon timing res.

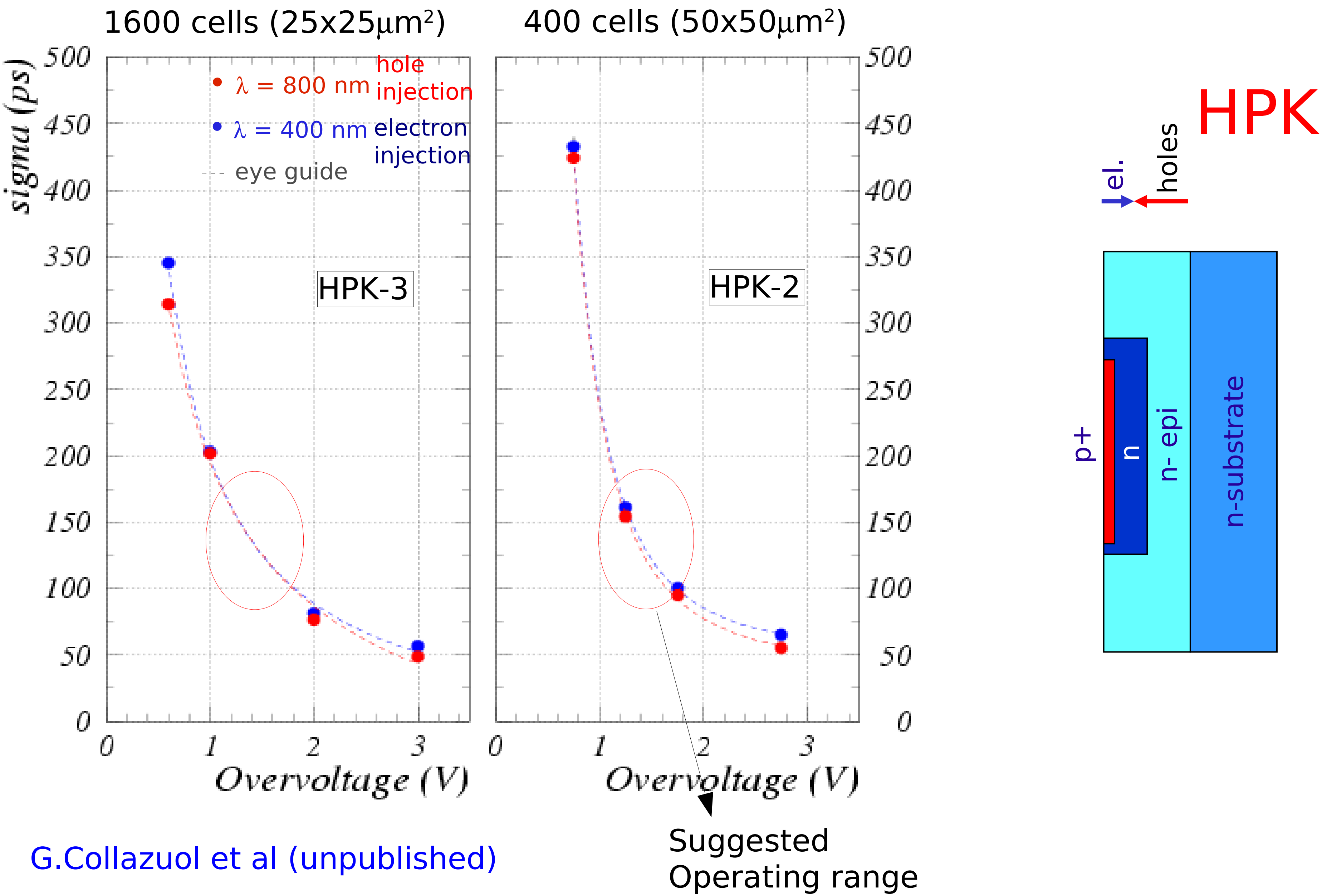

G.Collazuol et al (unpublished)

CPTA/Photonique – single photon timing res.

a) Green-Red sensitive
SSPM 050701GR_TO18

b) Blue sensitive
SSPM 050901B_TO18

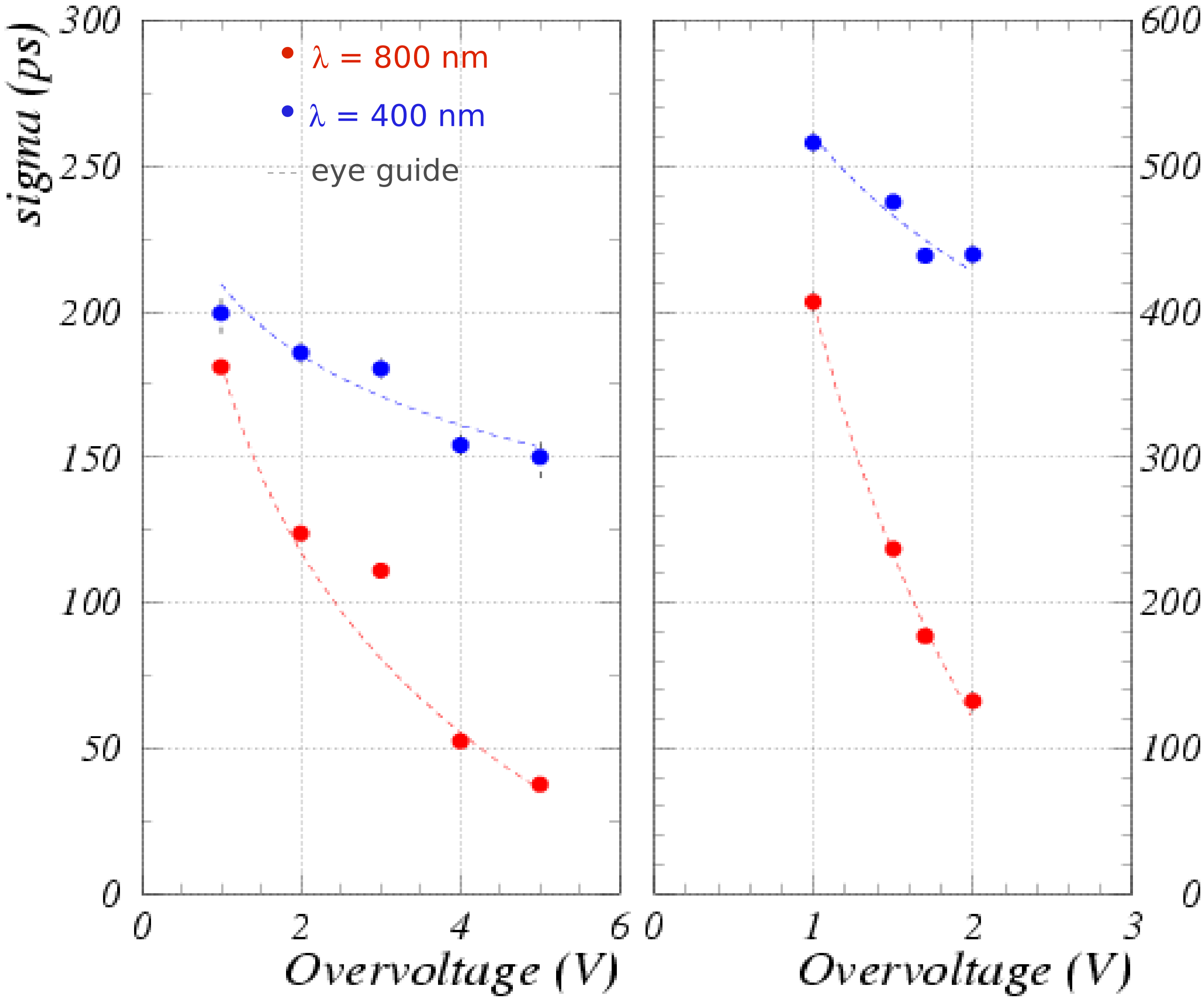

Two different structures:
a) thick n^+/p
b) p^+/n deep junction

G.Collazuol et al (unpublished)

Timing studies

Dependence of SiPM timing on the number of simultaneous photons

Poisson statistics: $\sigma_t \propto 1/\sqrt{N_{pe}}$

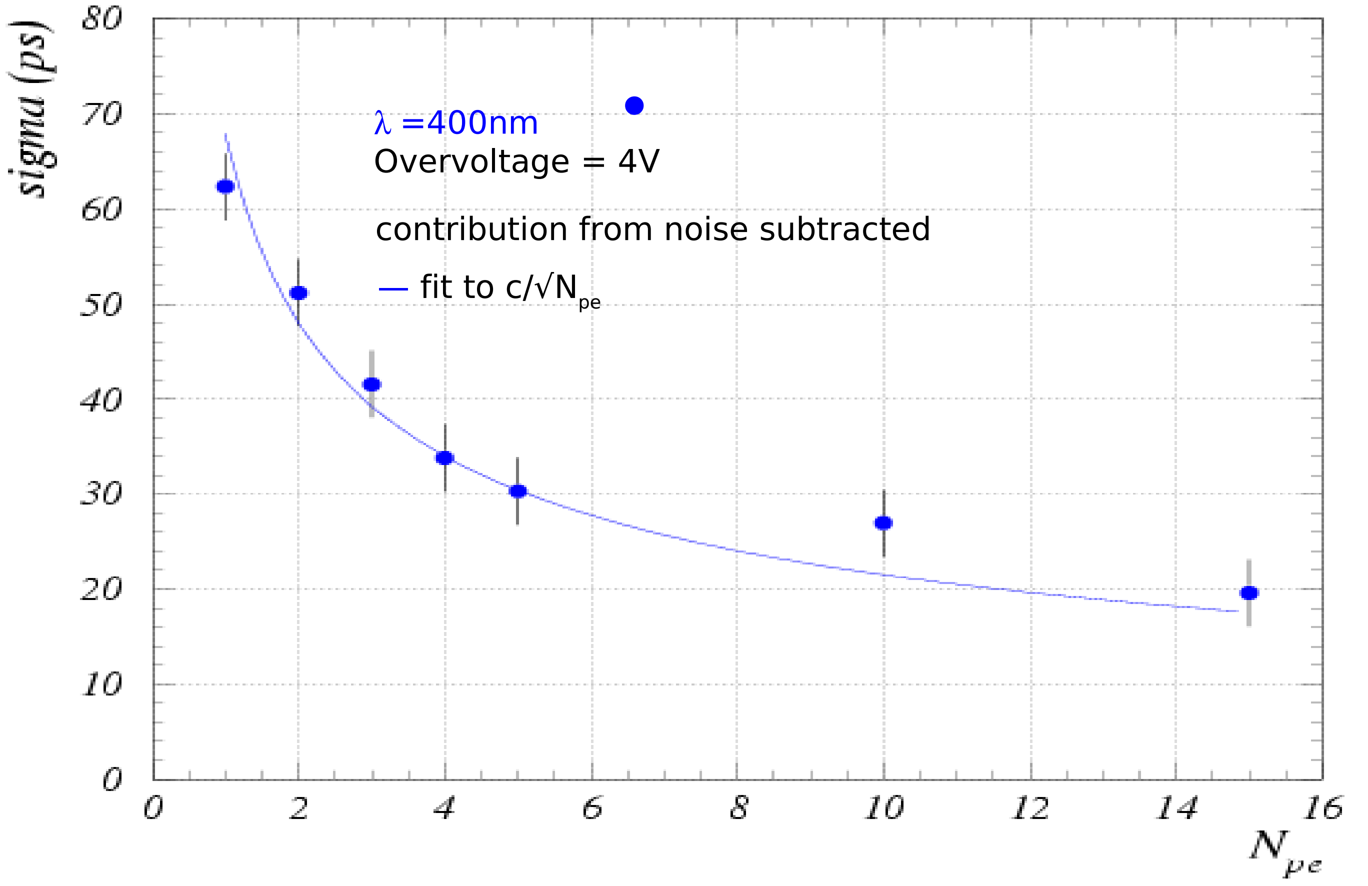

N of simultaneous photo-electrons

SPTR: position dependence

Yamamoto et al (Hamamatsu)

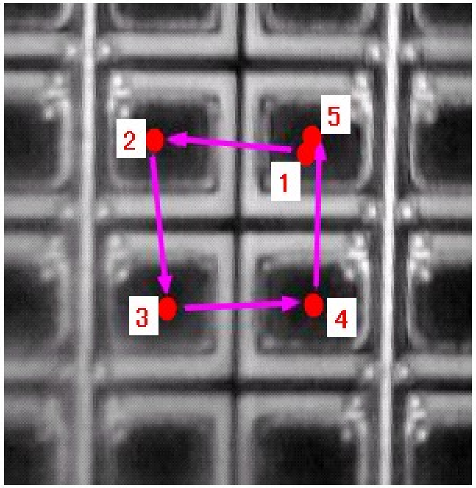

	FWHM (ps)	FWTM (ps)
1	199	393
2	197	389
3	209	409
4	201	393
5	195	383

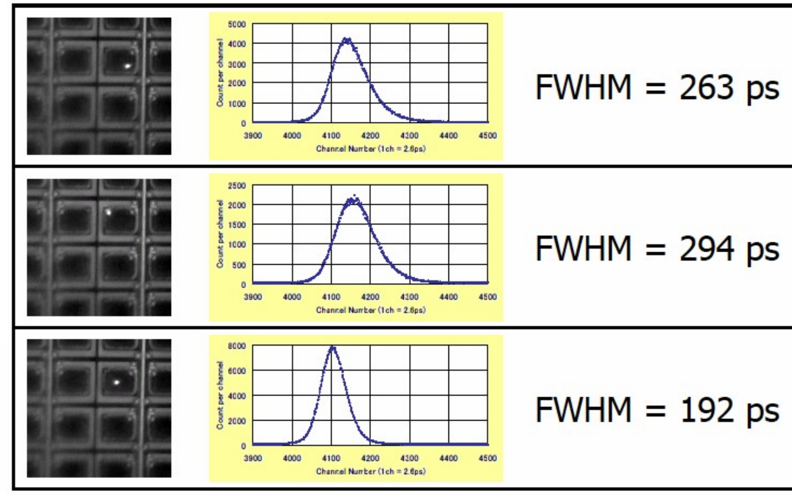

K.Yamamoto PD07

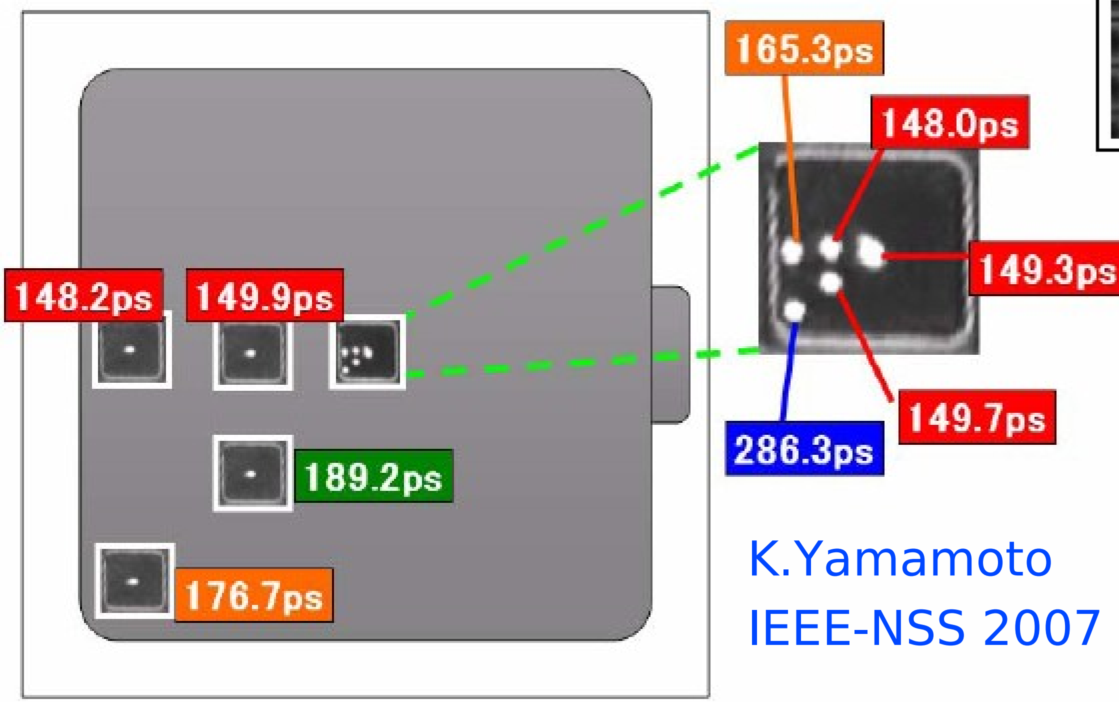

K.Yamamoto IEEE-NSS 2007

Lower jitter if photoproduction at the center of the cell

Data include the system jitter (common offset, not subtracted)

NOTE: when laser is impinging only on one cell it is not easy to be sure that only one photons is in the cell: while the amplitude is invariant (many photons = one photon), timing is much affected by the number of photons (A.Ronzhin)

Conclusions

SiPM behave very well at low T, even better than at room T

In the range 100K<T<200K SiPM perform optimally;
→ excellent alternatives to PMTs in cryogenic applications (eg Noble liquids)

- Breakdown V decreases non linearly with T
  → stability of devices wrt T is even better at low T
- Dark rate reduced by orders of magnitude
  → different (tunneling) mechanism(s) below ~200K
- After-pulsing increases swiftly below 100K
- Cross-talk and Gain (detector capacity) are independent of T (at fixed Over-V.)
- PDE higher than at T room at low T for short λ

I just carried on **additional measurements at low T** with short laser pulses for:
- accurately measuring of after-pulsing characteristic time constant(s) vs T
- cross-checking PDE (pulsed vs current method)
- measuring timing resolution vs Temperature (expected to improve at low T)
- checking Gain resolution at low T

Simulations and modeling going on to understand better After-Pulsing and PDE features at low T

We measured also the **excellent SiPM intrinsic timing resolution (<100ps for 1p.e.)**
Recent additional measurements to be analyzed (time to avalanche, different devices, ...)
Simulations and modeling work going on to understand timing data in more detail

Additional material

Setup: vacuum vessel + cryo-cooler

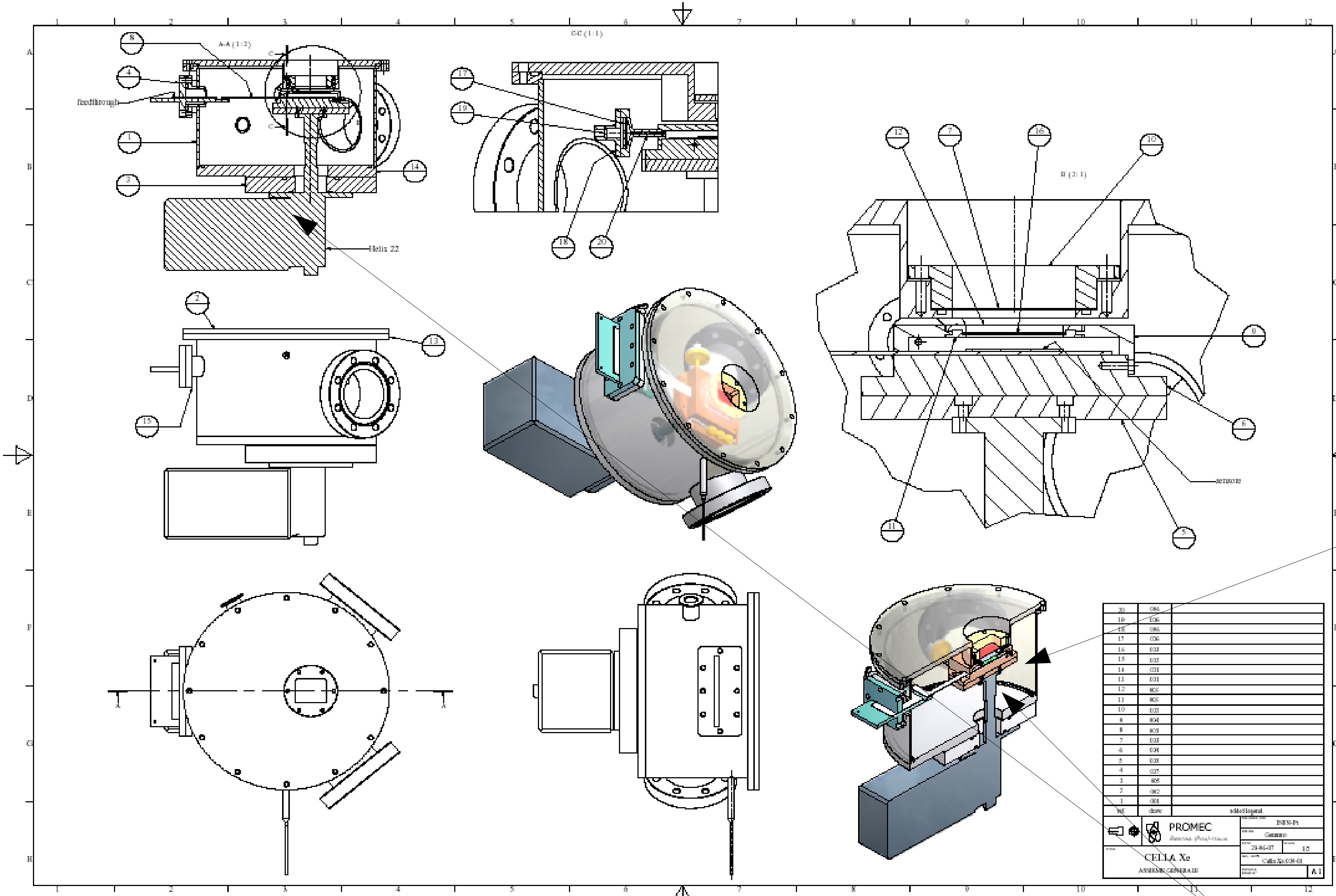

Vacuum vessel

cryo-cooler

Acknowledgments: A.Brez, A. Baldini, G.Signorelli (Pisa)

SiPM's are in thermal contact with a cooled Cu rod

Close up of a cell

Doping and Field profiles (IRST)

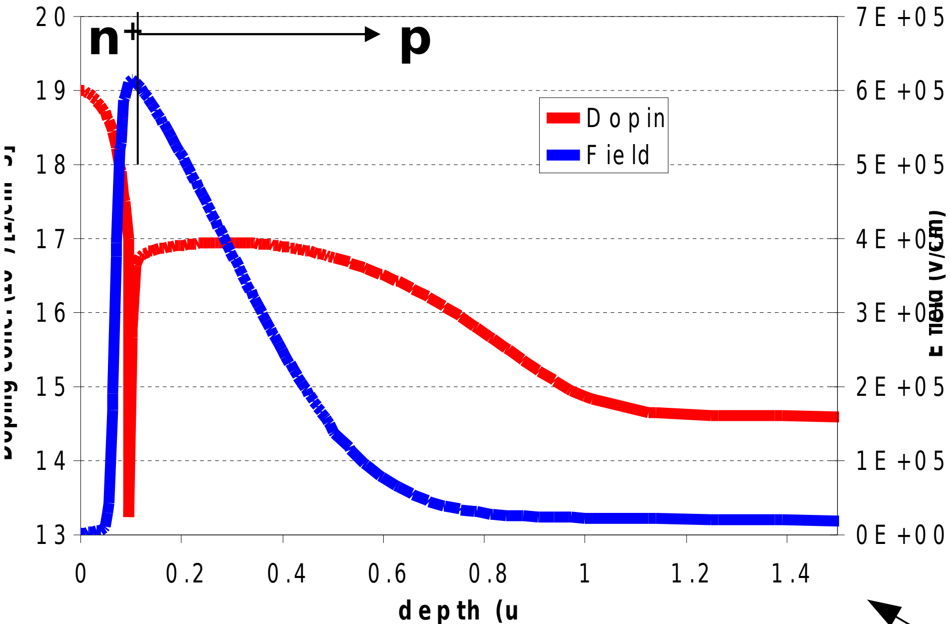

Light absorption in Silicon

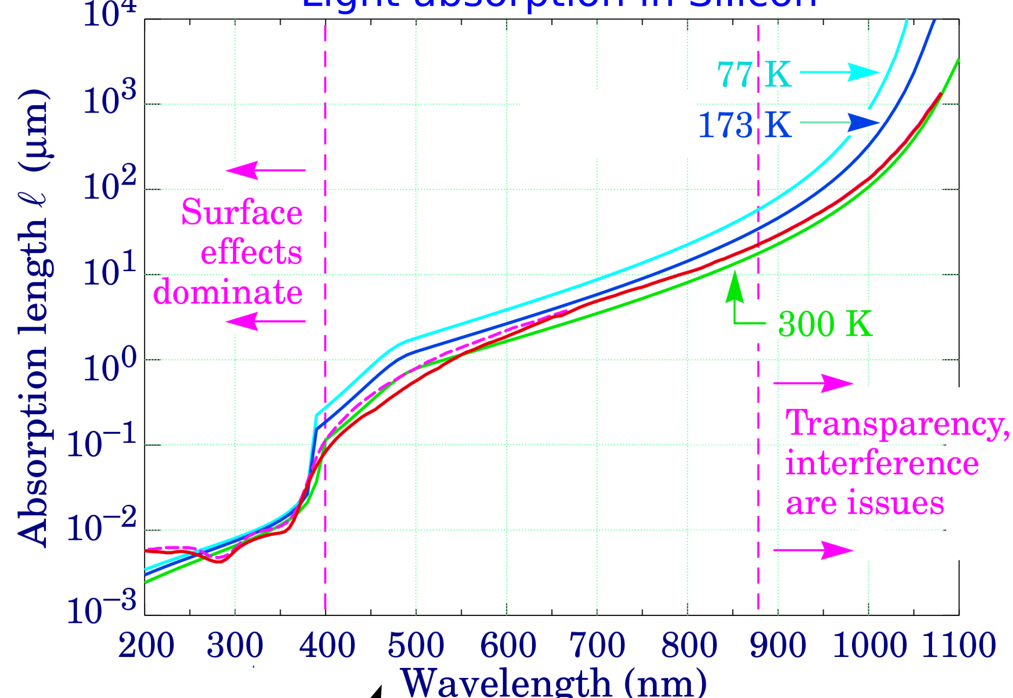

V_{BD} versus doping concentration

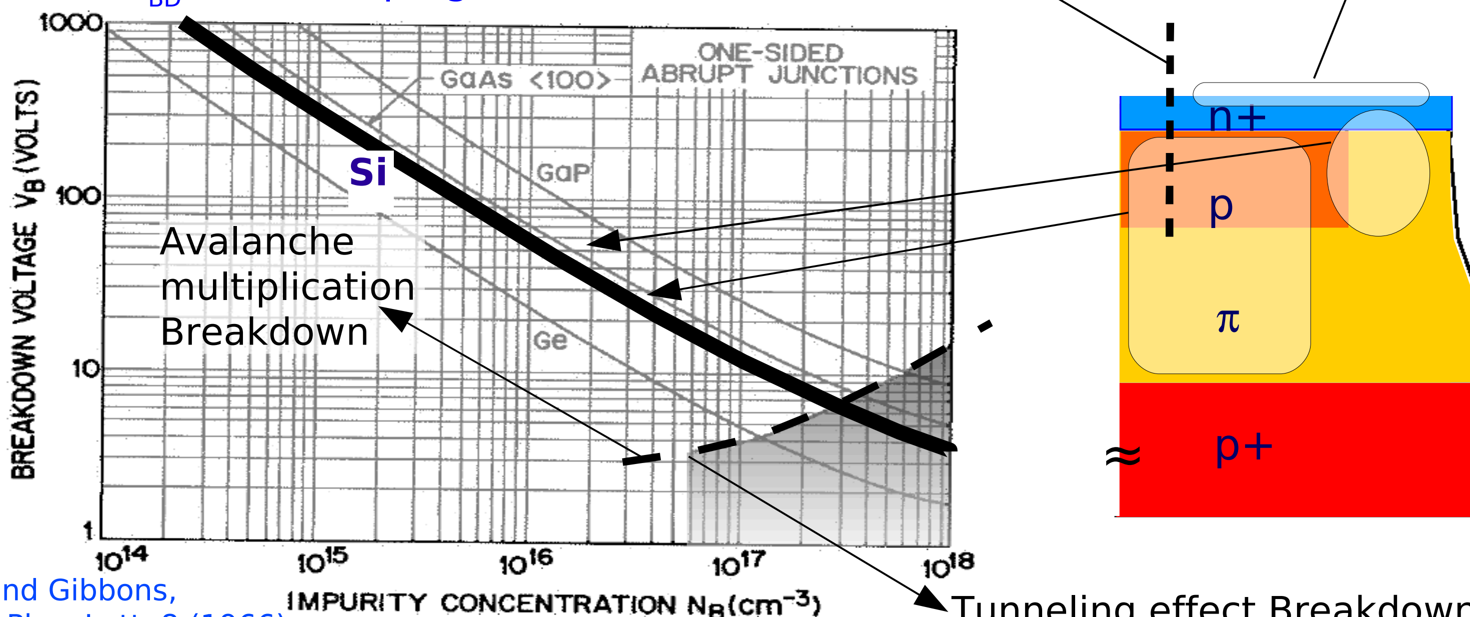

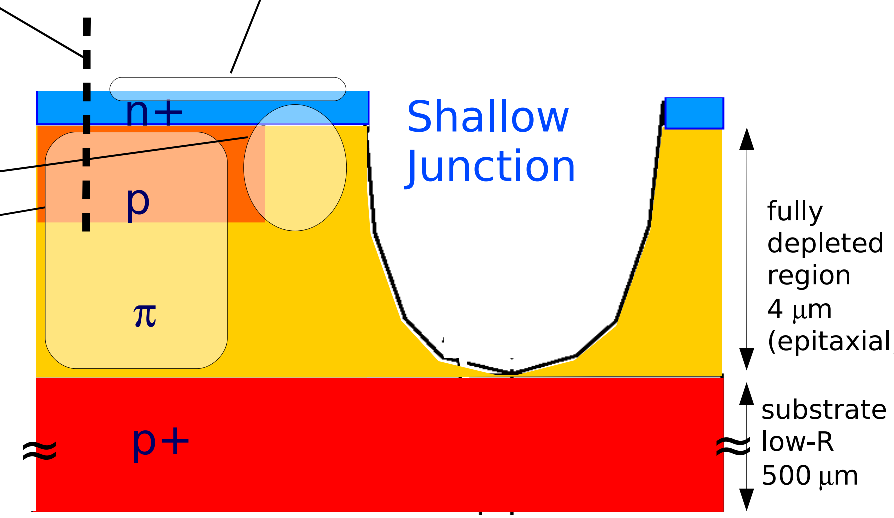

Sze and Gibbons, Appl. Phys Lett. 8 (1966)

Electrical model of a SiPM

R_q: quenching resistor
(hundreds of kΩ)
C_d: junction capacitance
(few tens of fF)
C_q: parasitic capacitance in parallel to R_q (few tens of fF, $C_q < C_d$)
I_{AV}: SiPM ~ ideal current source
current source modeling the total charge delivered by a cell during the avalanche $Q=\Delta V(C_d+C_q)$
C_g: parasitic capacitance due to the routing of Vbias to the cells (metal grid, few tens of pF)

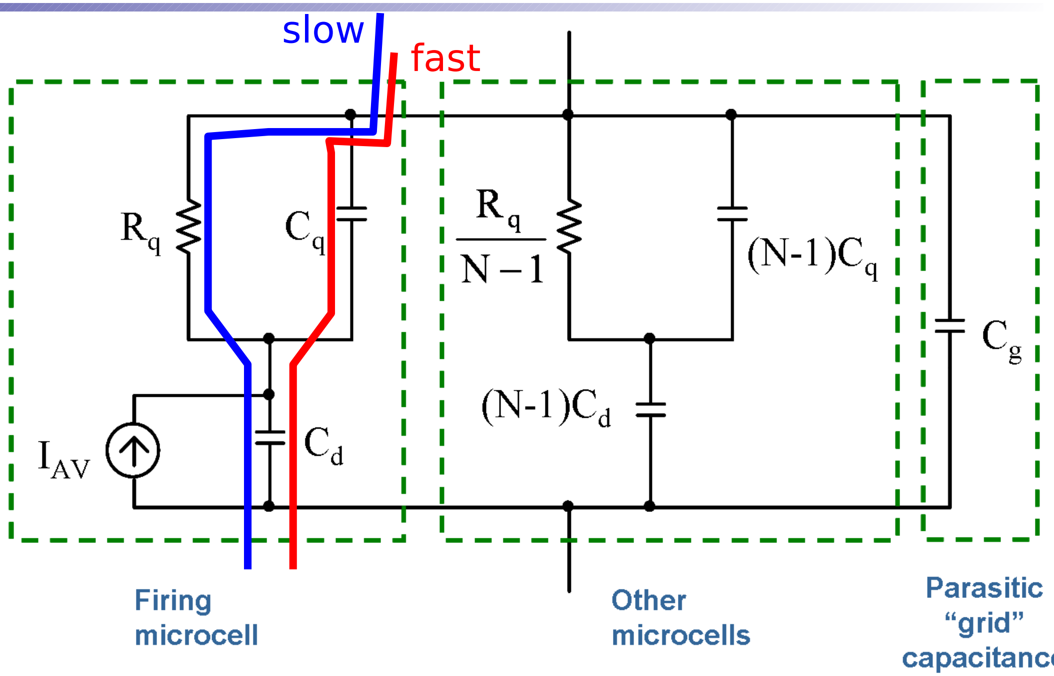

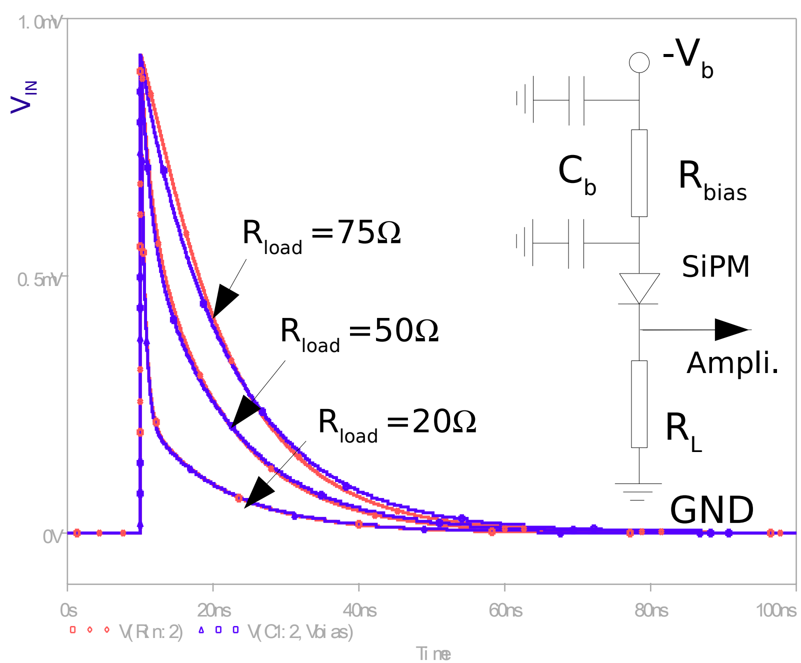

1) the peak of V_{IN} is independent of R_s

A constant fraction Q_{IN} of the charge Q delivered during the avalanche is instantly collected on $C_{tot}=C_g+C_{eq}$.

2) The circuit has two time constants:

- $\tau_{IN}= R_L C_{tot}$ (fast)
- $\tau_r = R_q (C_d+C_q)$ (slow)

Decreasing R_s, the time constant τ_{IN} decreases, the current on R_s increases and the collection of Q is faster

F. Corsi, C. Mazzocca et al.

Silicon properties at low T: higher mobility

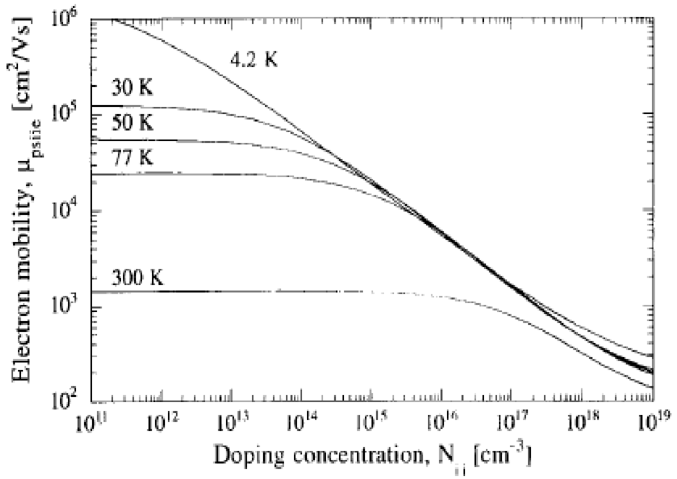

FIGURE 1.16. Calculated electron mobility due to phonon and ionized impurity scattering mechanisms. The five plots correspond to $T = 300, 77, 50, 30$, and 4.2 K.

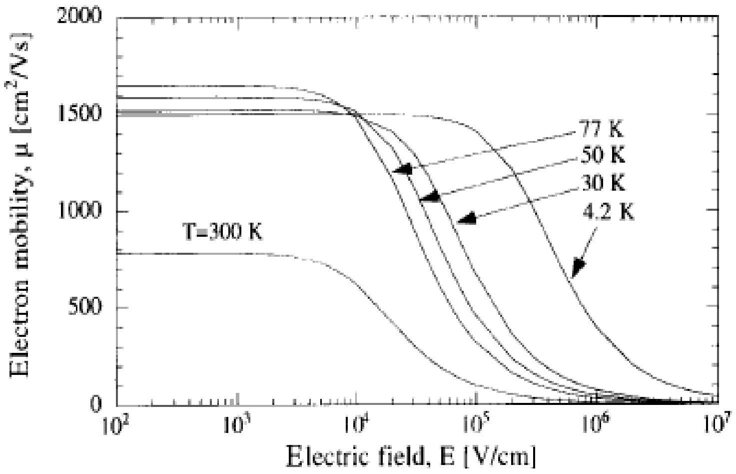

FIGURE 1.17. Calculated electron mobility, due to phonon, ionized impurities, and velocity saturation effects, as a function of the electric field for five temperatures; $N_{ii} = 10^{17}\ \mathrm{cm}^{-3}$.

Silicon propt's at low T: carriers freeze-out

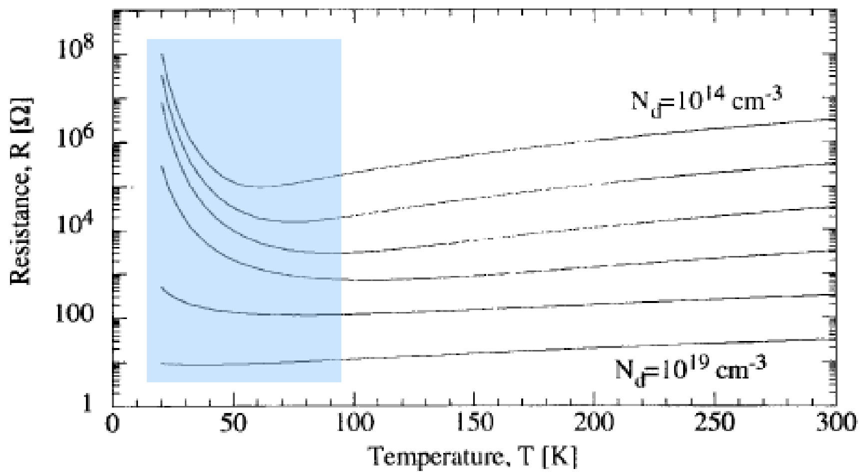

FIGURE 1.14. Calculated electrical resistance of a silicon slab of $(W/L) = 20/50\ \mu m$ and depth of $1\ \mu m$ for different doping concentration levels.

For T<100 K, the ionized impurities act as shallow traps (provided the impurity doping concentration below of 10^{18} atoms/cm^2) and carriers begin to occupy these shallow levels.

For T<30 K, practically no carriers remain in the bands

Plots from Guiterrez, Dean, Claeys - "Low Temperature Electronics: Physics, Devices, Circuits and Applications", Academic Press 2001

Silicon propt's at low T: impact ionization

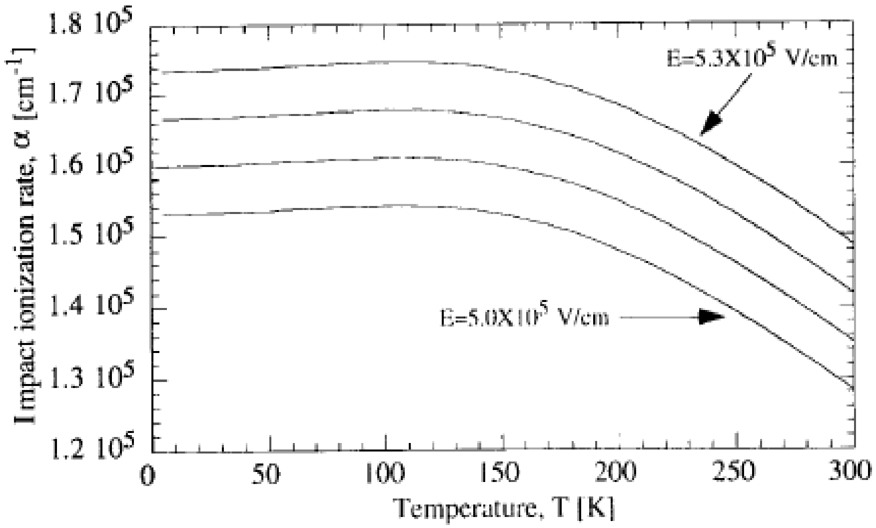

FIGURE 1.43. The impact ionization rate α as a function of temperature T_A with the electric field E as a parameter calculated from Okuto and Crowell's *(85)* model.

For T<77K no data are available → modeling is quite difficult...

Silicon propt's at low T: absorption length

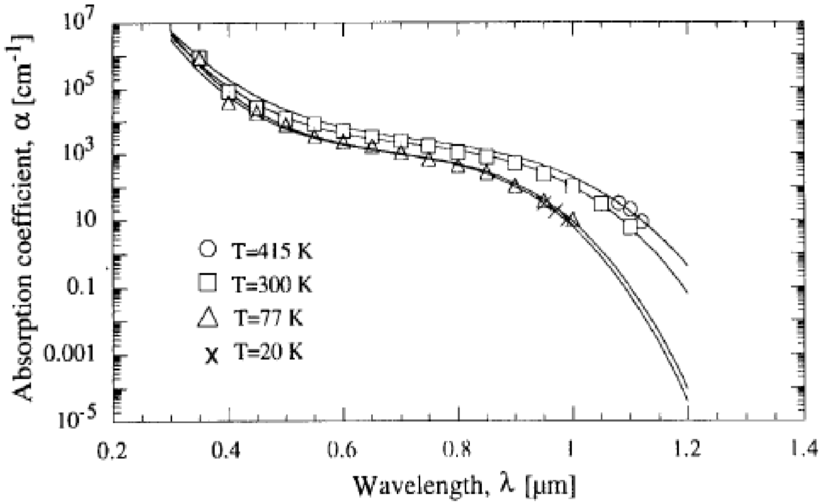

FIGURE 1.53. Experimental (symbols) and fitted (lines) absorption coefficient α of silicon at $T = 415$, 300, 77, and 20 K [replotted from Rajkanan *et al.* *(109)*].

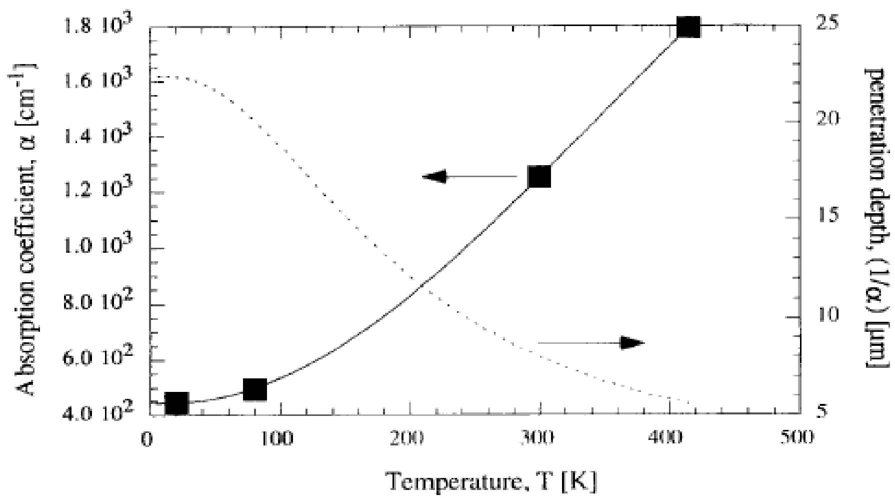

FIGURE 1.54. Measured absorption coefficient α (■) *(101)* and fitted α (solid line) versus temperature *T*. On the right axis the fitted penetration depth (1/α) is also shown.

Avalanche breakdown vs T

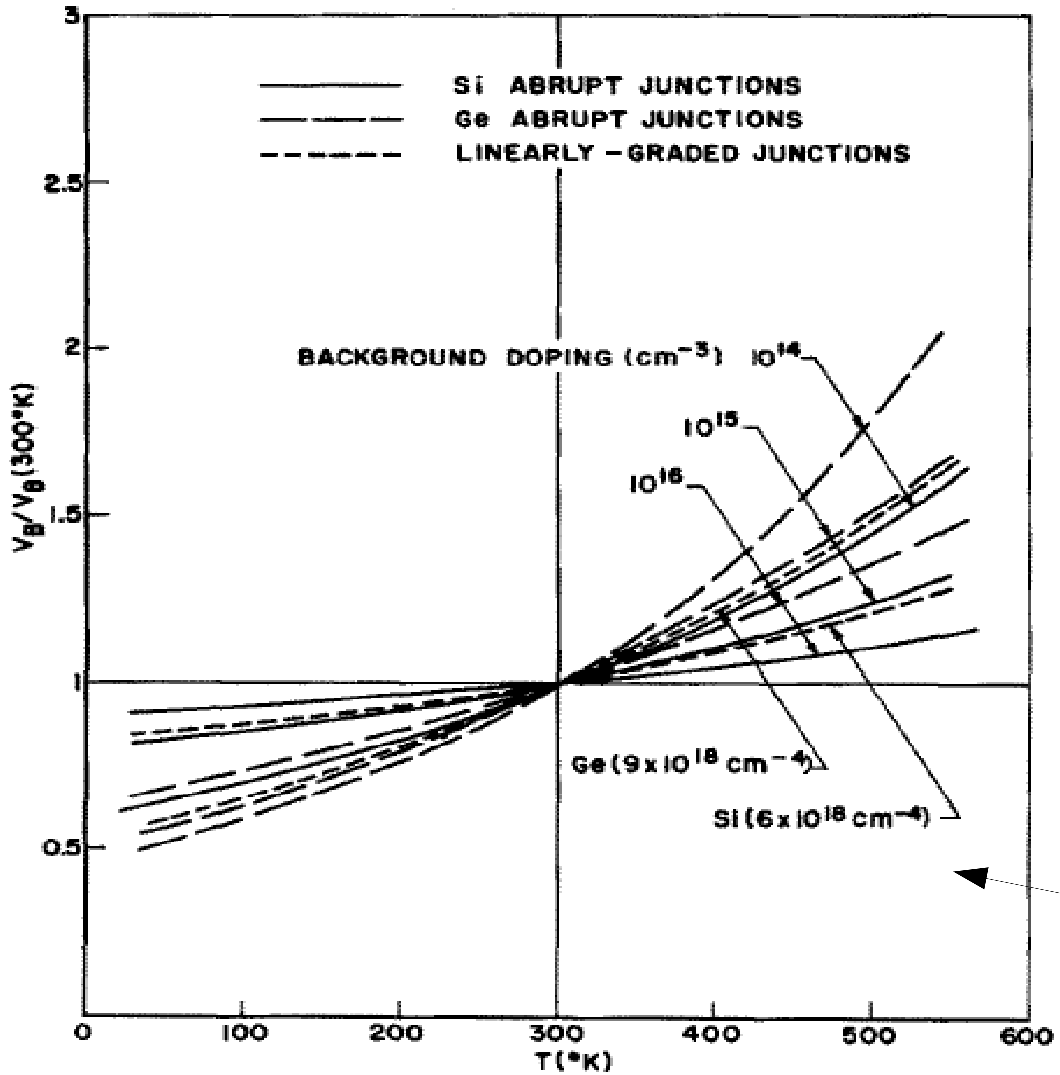

Fig. 4. Breakdown voltage vs temperature for Si and Ge *p-n* junctions. $V_B(300°K)$ is 2000, 330, and 60 V for Si and 950, 150, and 25 V for Ge for dopings of 10^{14}, 10^{15}, and 10^{16} cm^{-3} respectively. The linear-graded junctions have $V_B(300°K)$ the same as those for doping of 10^{15} cm^{-3}.

Avalanche breakdown V is expected to show a **non linear dependence on T** (depending of the junction type and doping concentration)

Breakdown V decreasing with T due to increasing mobility

NOTE: in freeze-out regime Zener (tunnel) breakdown could be relevant. → negative Temperature coefficient (increasing with decreasing T)

Crowell and Sze

More recent model by Crowell and Okuto after Shockley, Wolff, Baraff, Sze and Ridley.

p-n junction characteristics: forward bias

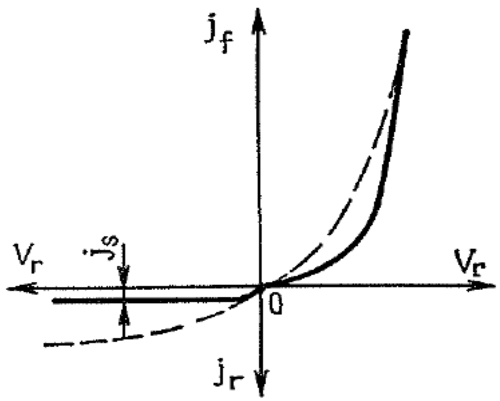

Fig. 8.16. The current-voltage characteristic of a *pn* junction

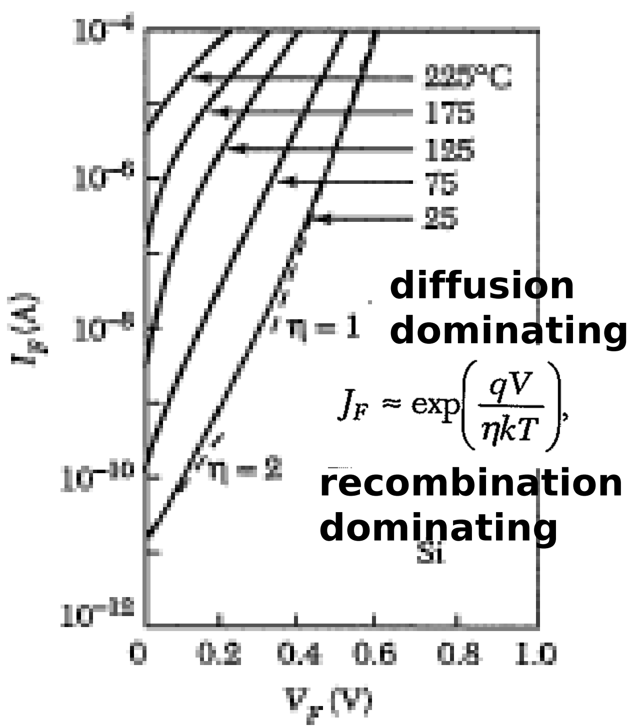

Sze - "Semiconductor devices"

E.Johnson (RMD) at IEEE 2009

"Characterization of CMOS APD at cryogenic T"

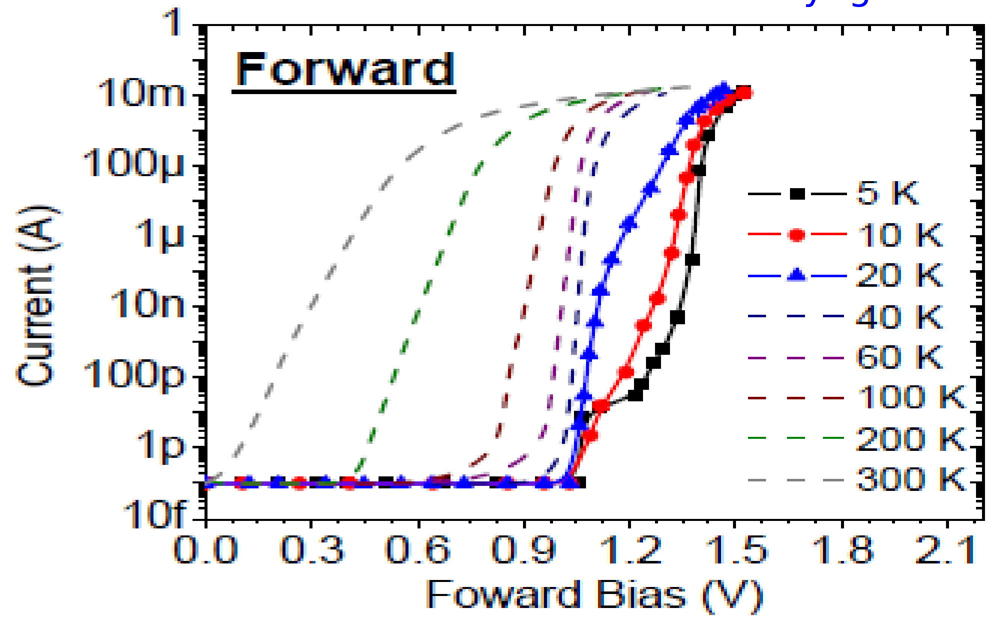

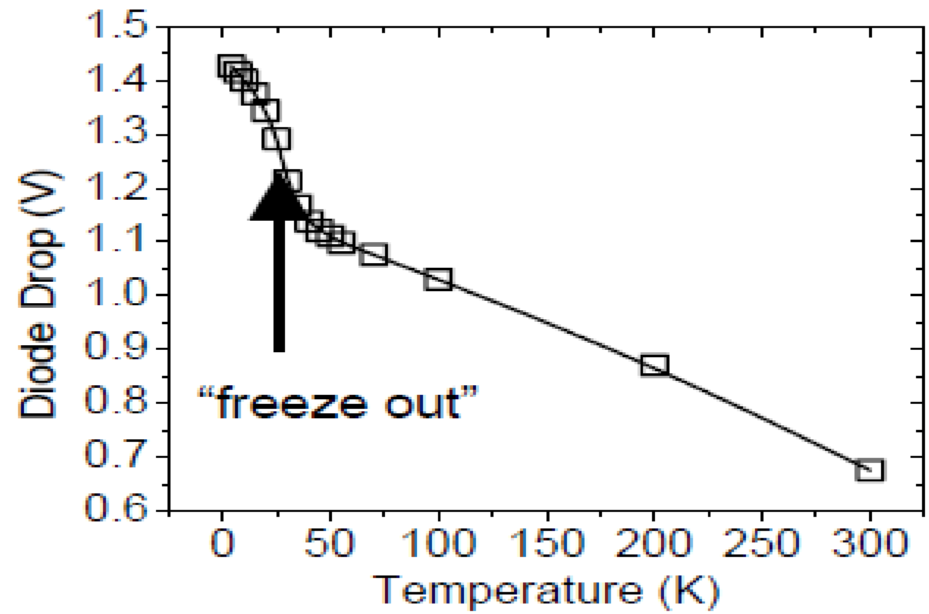

Dark count rate vs T (at fixed gain)

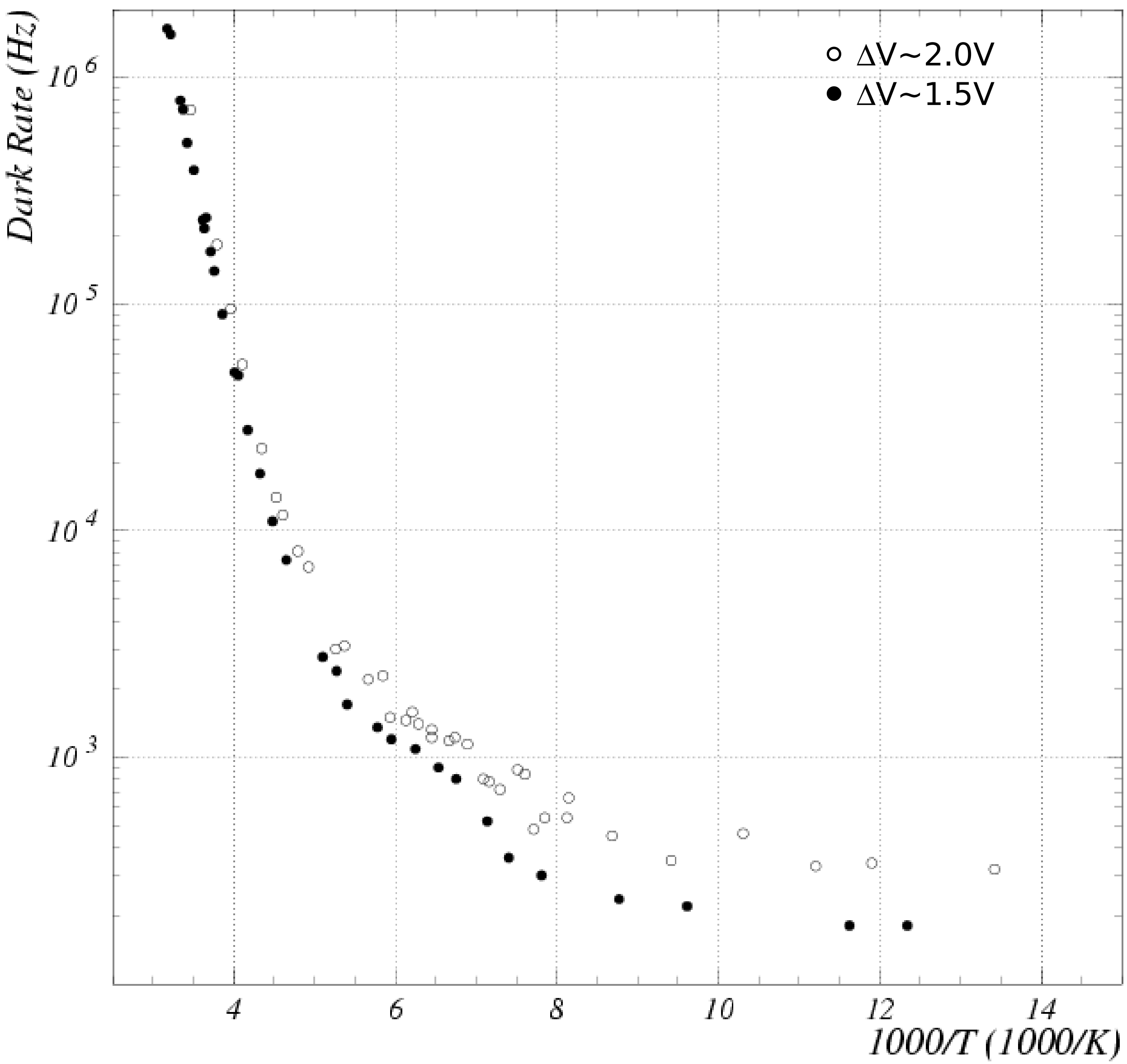

Measurement: **rate of ≥1p.e.** at fixed gain (i.e. ~fixed ΔV)

T dependence: Dark Rate

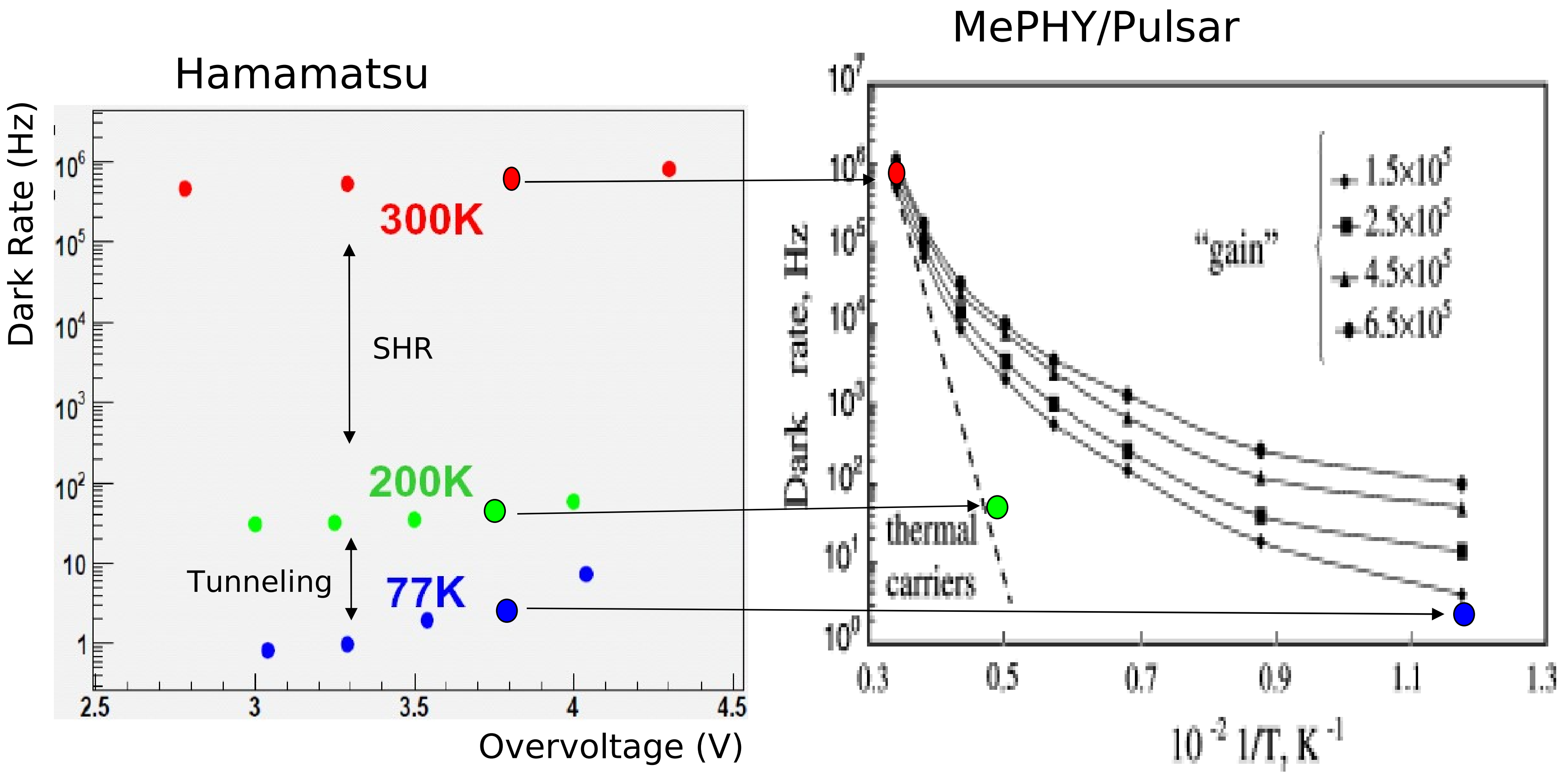

H.Otono – PD07

Dolgoshein et al, NIM A 442 (2000)

Electric field engineering and silicon quality
make huge differences in dark noise as a function of T

T dependence: PDE (SPAD/APD devices)

PDE dependence on T
(Over-voltage fixed)

Combination of various effects:

- P_{01} increases at low T because of increased impact ionizazion
- Optical attenuation length increased (Energy gap increases) at low T
- Depletion region widening in APDs, but not in SiPM which are fully depleted

Similar effect expected also for SiPM

SPAD: Cova el al, Rev.Sci.Instr. 7 (2007)

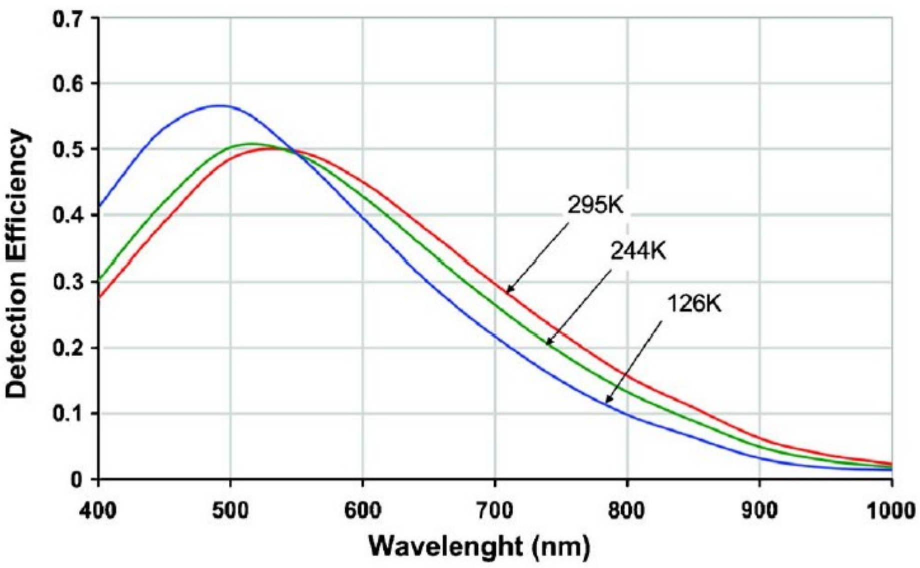

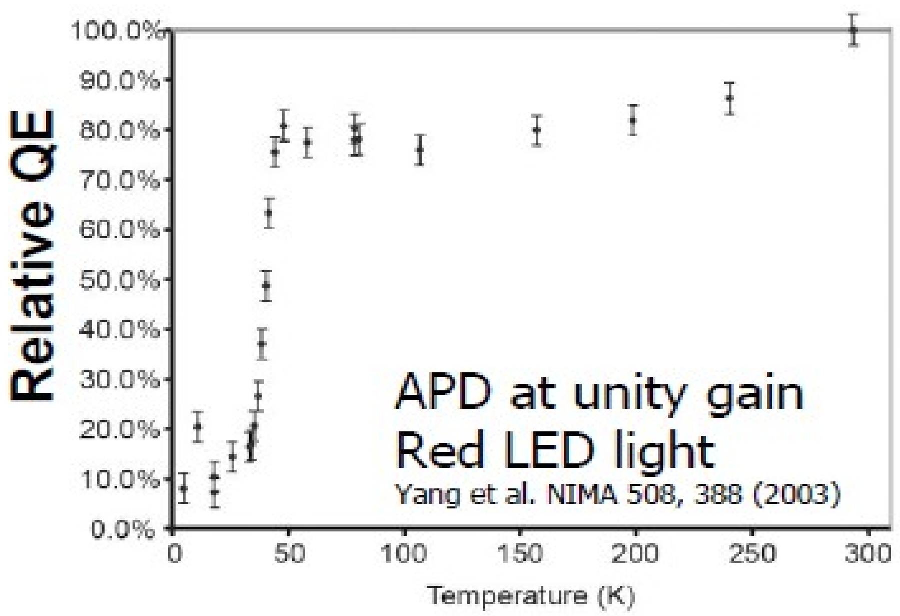

APD: Johnson et al (RMD) IEEE 2009

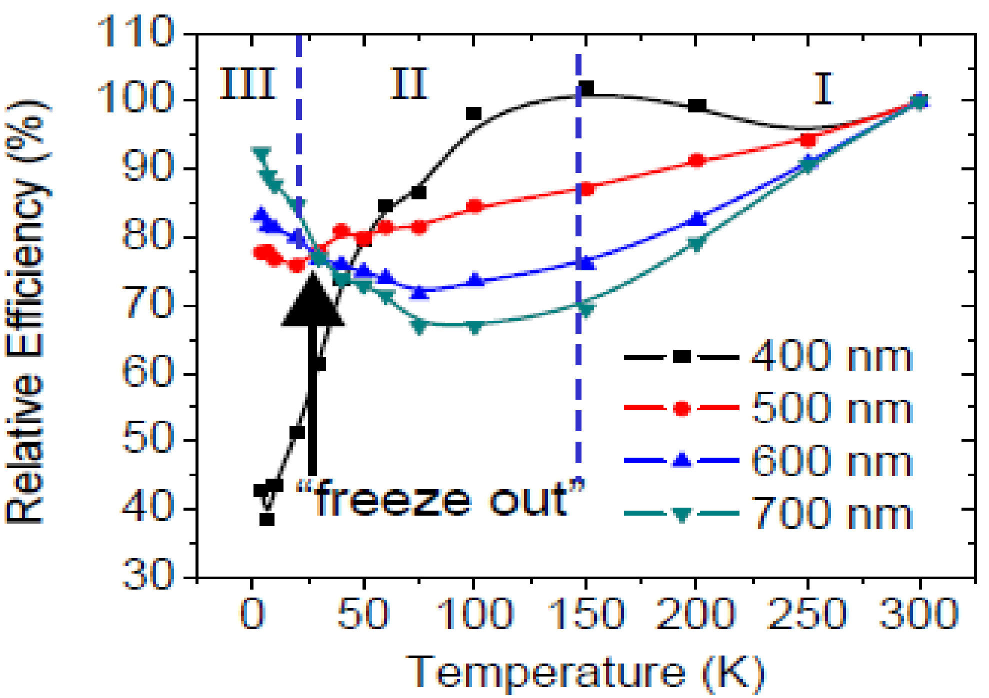

Photo-detection efficiency (PDE)

$$PDE = N_{pulses} / N_{photons} = QE \bullet P_{01} \bullet \varepsilon_{geom}$$

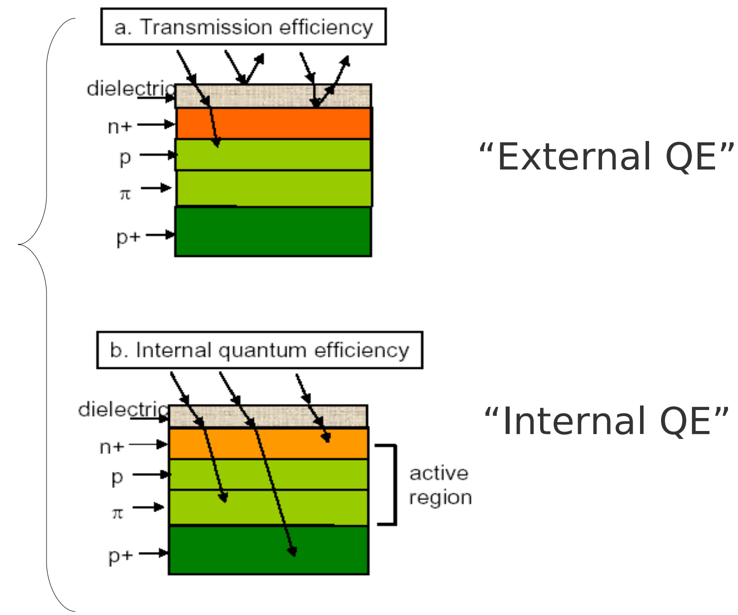

Carrier Photo-generation

(QE = probability for a photon to generate a carrier that reaches the high field region)

*

Avalanche triggering

(P_{01} = probability for a carrier traversing the high-field to generate the avalanche)

*

Geometrical fill factor

(ε = fraction of dead area due to structures between the cells, eg. guard rings, trenches)

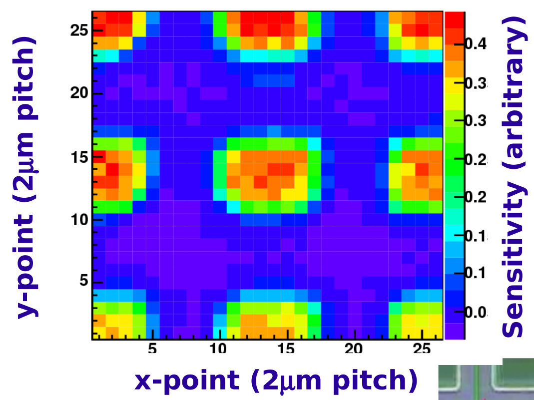

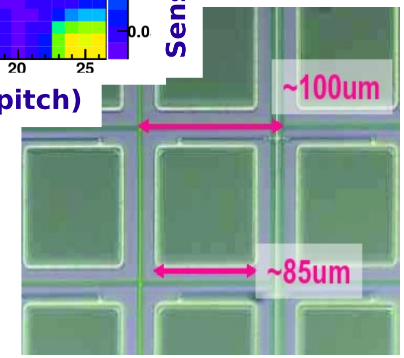

Hamamatsu SiPM close up

W.Oldham et al. IEEE TED (1972)

QE: Efficiency of a single cell

Two factors in QE:

(1) transmittance of the entrance window (dielctric on top of silicon surface)

(2) probability of a photon inside to generate a e-h pair in the active layer (internal quantum efficiency)

Only the depleted region is fully active to efficiently photo-generate because of high recombination probability in the un-depleted regions.

Only a small layer ($\lambda_{diffsion} \sim \sqrt{D\tau_{recomb}}$) at the edge of un-depleted regions contributes to the photo-generation (critical for UV light)

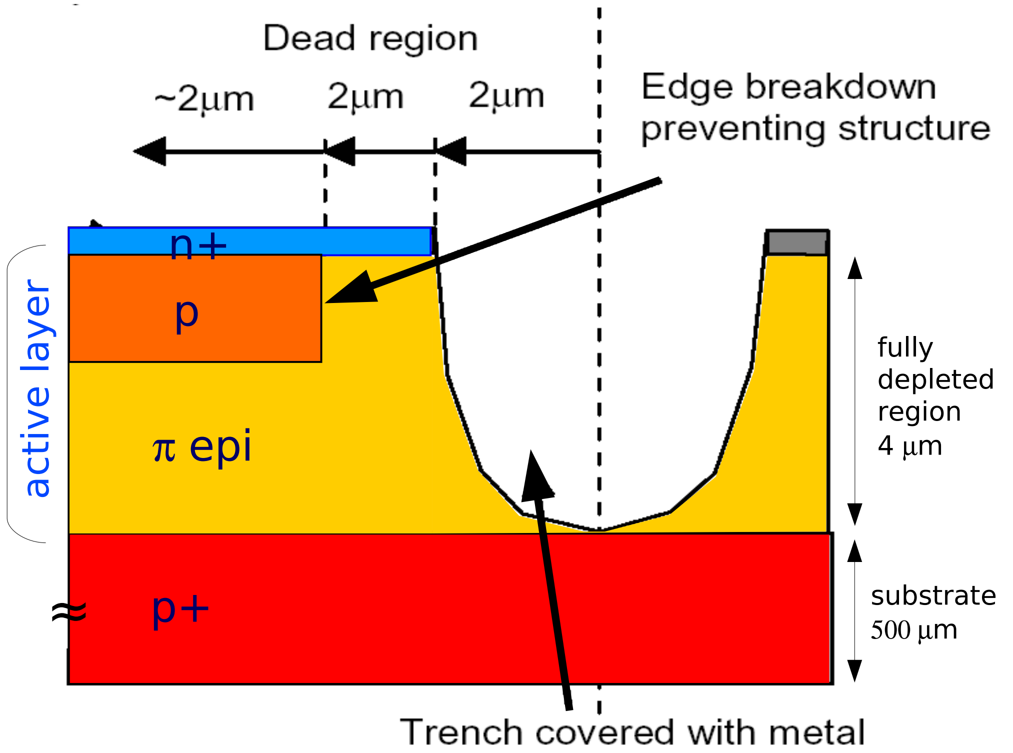

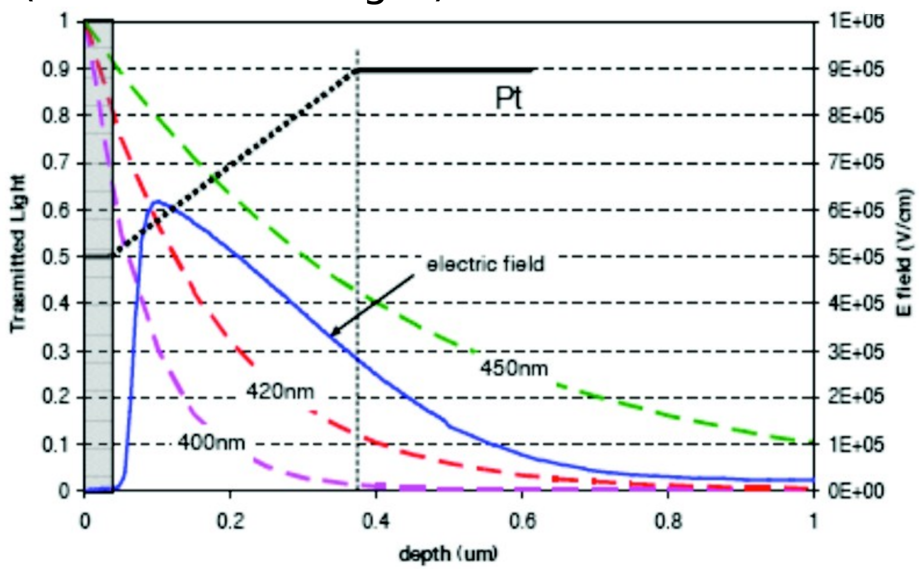

QE optimization

- Anti-reflective coating (ARC)
- Shallow junctions for short λ
- Thick epi layers for long λ

QE: Efficiency of a single cell

Direct access to internal QE and transmittance through ARC by measuring photo-voltaic regime (V_{bias}~ 0 V) the photon detection efficiency of a diode with the same n^+/p junction structure and same ARC

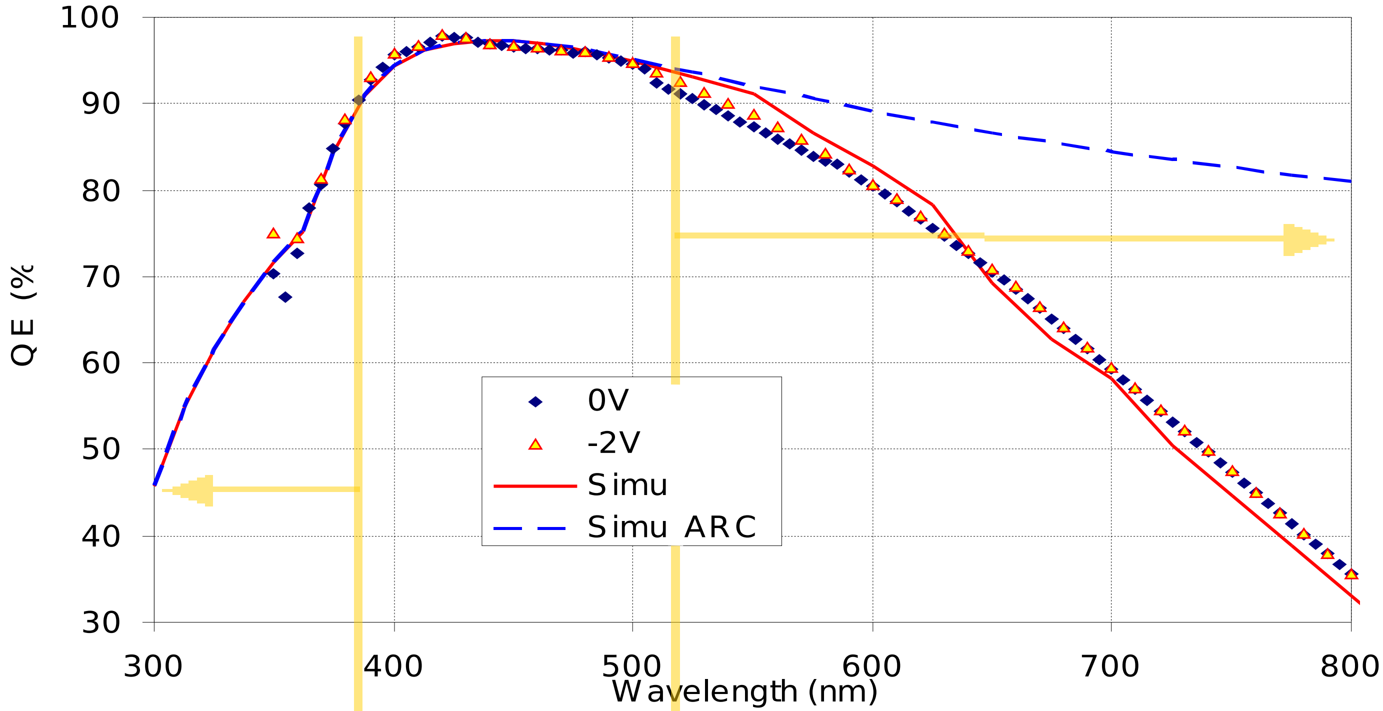

Reduced by ARC Transmittance

Reduced by the small π layer thickness

IRST devices

Avalanche trigger probability (P_{01})

P_{01} dependence on position

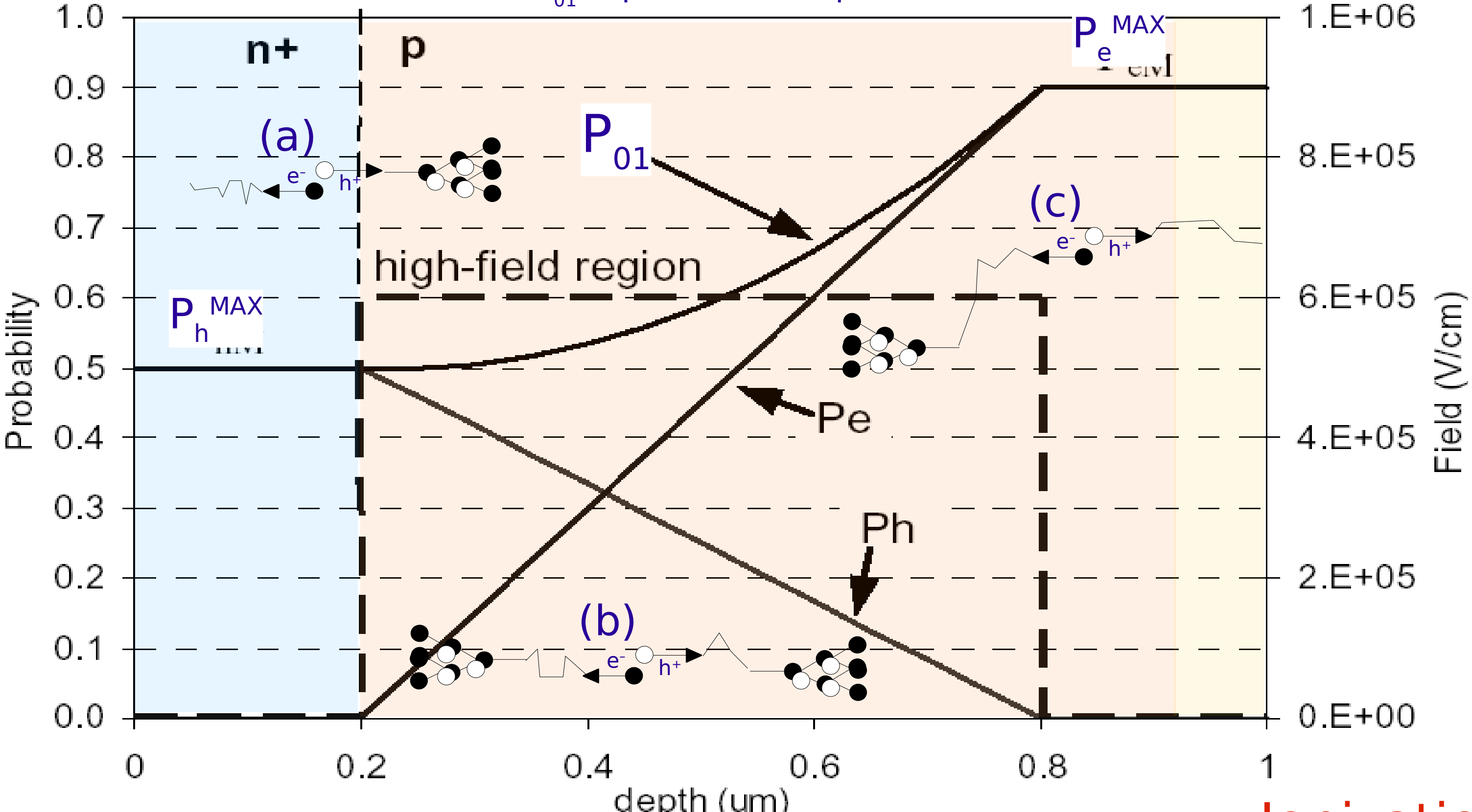

C.Piemonte
NIM A 568
(2006) 224

Example with constant high-field:

(a) only holes may trigger the avalanche

(b) both electrons and holes may trigger
(but in afraction of the high-field region)

(c) only electrons may trigger

Ionization rate in Silicon

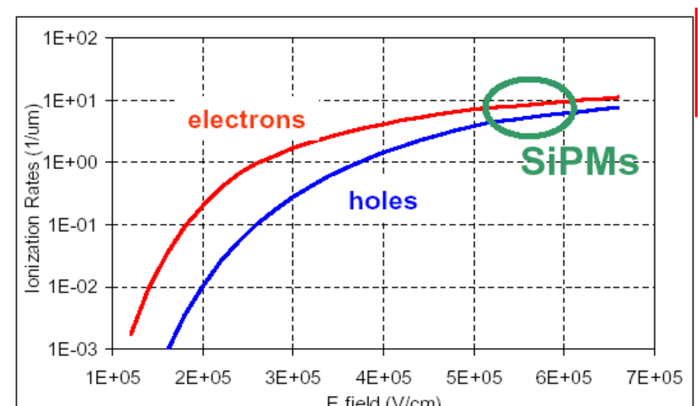

P_{01} optimization

- high over-voltage
- photo-generation in the p-side of the junction

Avalanche trigger probability (P_{01})

$P_{01} = PDE / QE / \varepsilon_{geom.}$

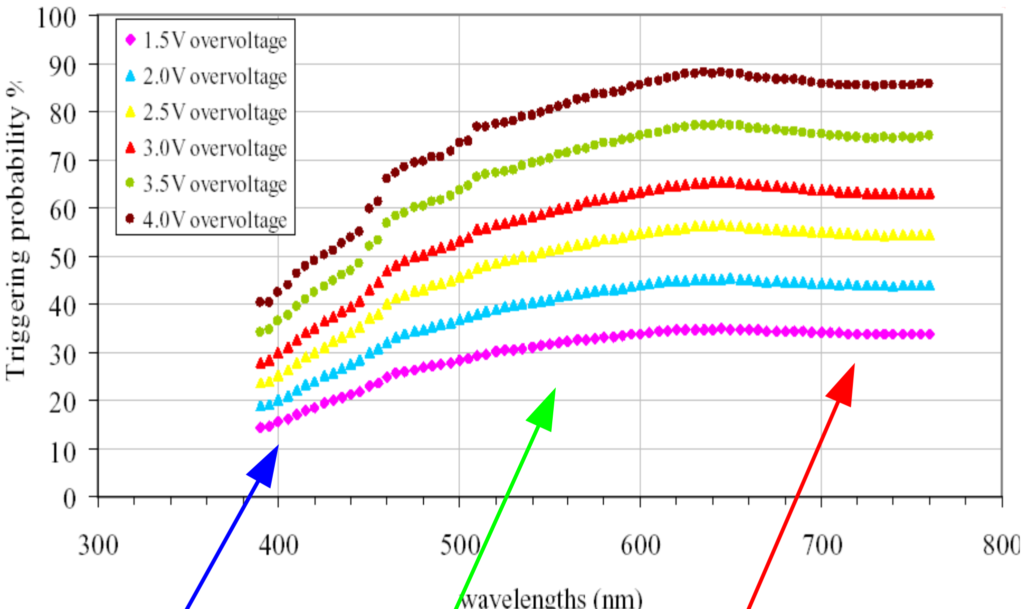

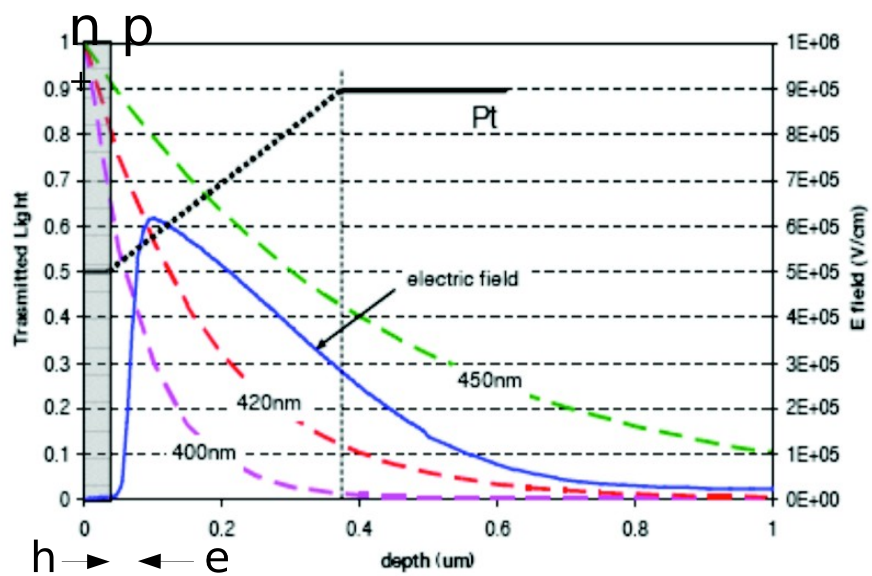

Only e⁻ cross the high E field region and trigger the avalanche

Both h⁺ and e⁻ might trigger the avalanche (but cross only a fraction of high field region)

Only h⁺ cross the high E field trigger the avalanche

IRST devices

PDE vs ΔV

"Statistics of Avalanche Current Buildup Time in Single-Photon Avalanche diodes"
C.H.Tan, J.S.Ng, G.J.Rees, J.P.R.David (Sheffield U.)
IEEE J.Quantum Electronics 13 (4) (2007) 906

RPL model Courtesy of C.H.Tan

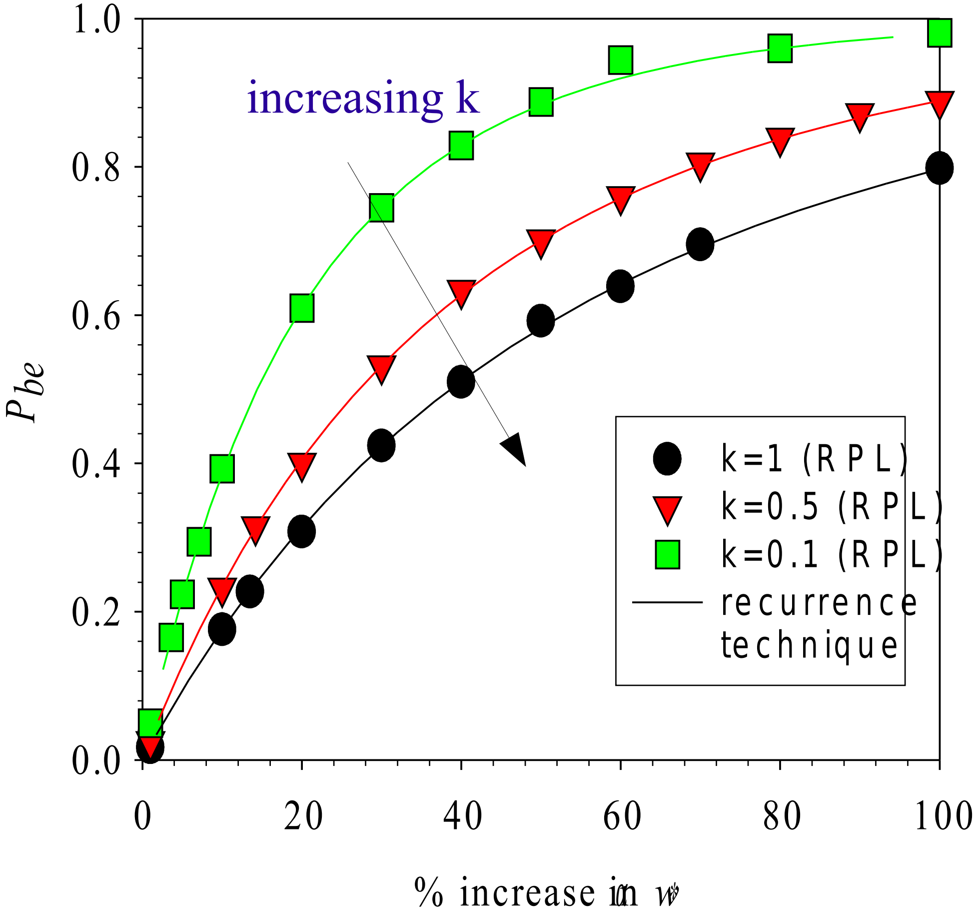

~ΔV/V

p-on-n structure

n-on-p structure

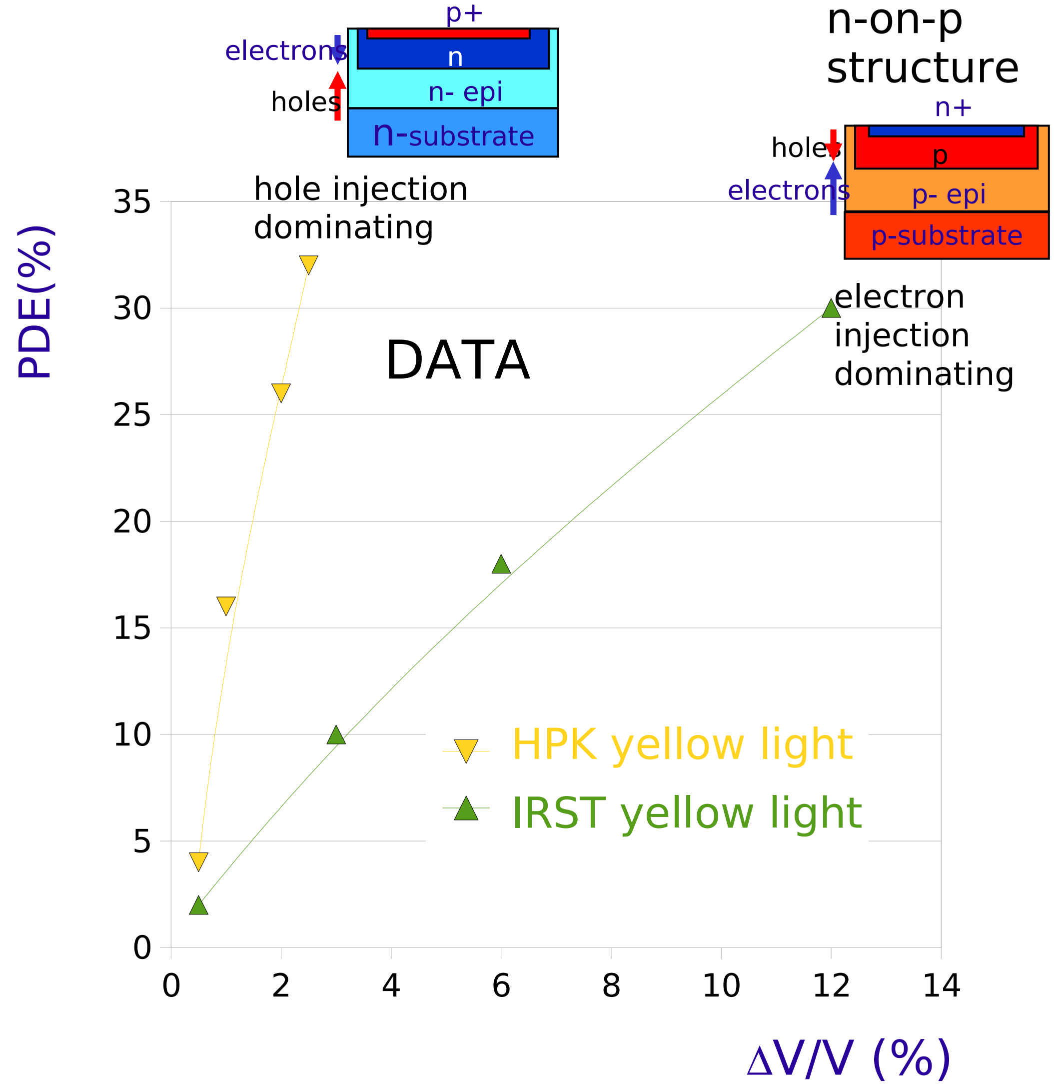

PDE vs λ

N.Dinu et al. NIM A (2008) to be published

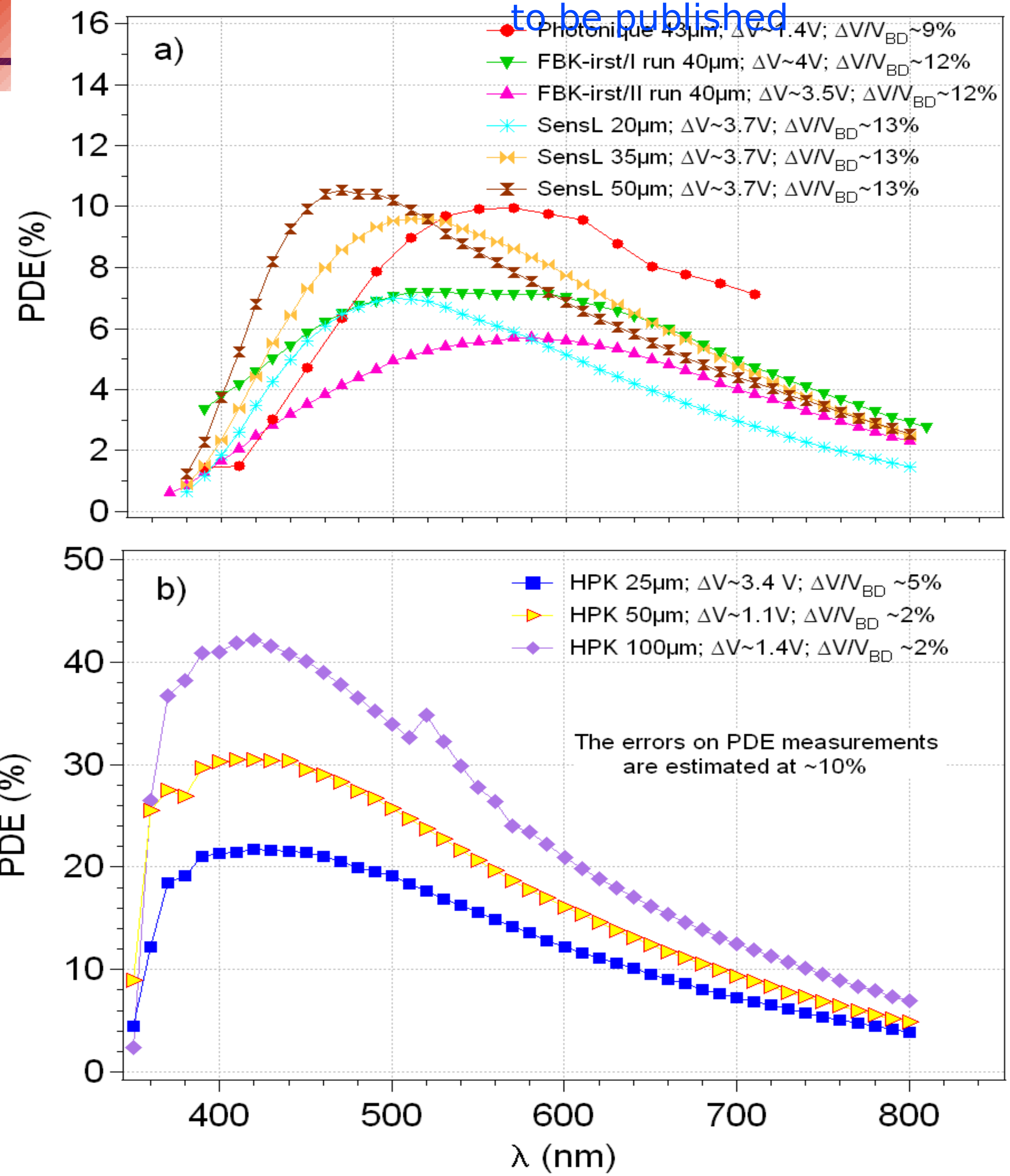

Fig. 5a) The PDE vs. λ of the Photonique, FBK-irst and SensL devices and b) HPK

n-on-p structures

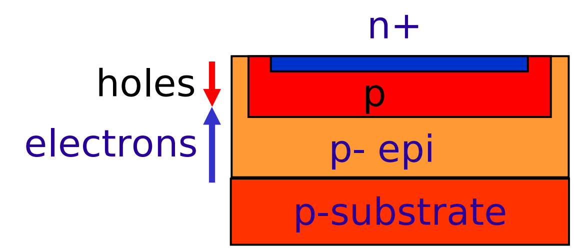

p-on-n structure

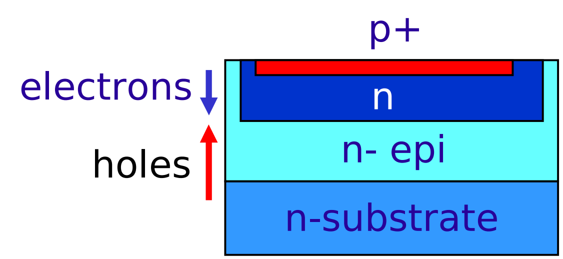

Note:
1) geometrical fill factor included
2) PDE in HPK catalog is 20%-30% more than the real PDE due to after-pulses and cross-talk

Experimental Setup

Pump Laser
Millenia V (Spectra-physics)
solid state CW visible laser

Crystal for Second Harmonic Generation (SHG)
conversion 800 nm → 400 nm
efficiency at % level

Low noise LV suppliers

Dark box

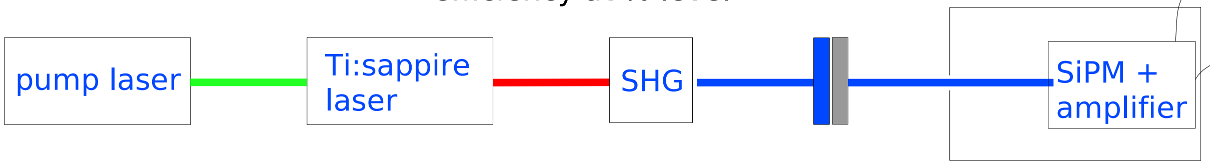

LeCroy SDA 6020
Analog bandwidth: 6GHz
Sampling rate: 20GS/s
Vertical resolution: 8 bits

(Aknowledments:
E.Marcon, LeCroy)

External trigger from Ti:sappire laser signal

Mode-locked Ti:sapphire Laser
Tsunami (Spectra-physics)
femtosecond pulsed laser

Filters
blue + neutral
for rejecting IR light and tune intensity

wavelength: tuned at 800±15 nm
pulse width: ~ 60 fs FWHM
pulse period: ~ 12 ns
pulse timing jitter < 100 fs

Electronics
I → V conversion via R_L (500Ω)
Two stage voltage amplification (= x50) based on high-bandwidth low-noise RF amplifier: gali-5 (MiniCircuit)
Z_{in} = 50Ω

(Aknowledments:
F.Morsani and L.Zaccarelli, INFN-Pisa)

Data taking conditions:
- different V_{bias}
- both at 800 nm and 400 nm
- with different light intensities (counting rates in the range 10÷20 Mhz ie 15÷30 KHz per single cell)

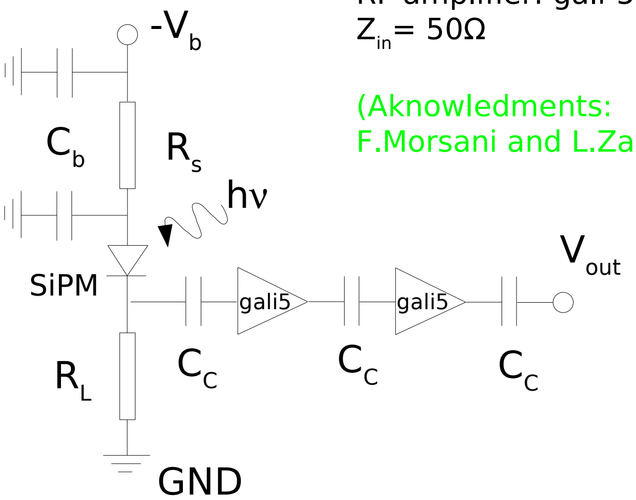

SPTR: HPK/CPTA comparison

T.Iijima – PD07
Nagoya and Lubiana groups

SiPM - HPK
(MPPC)

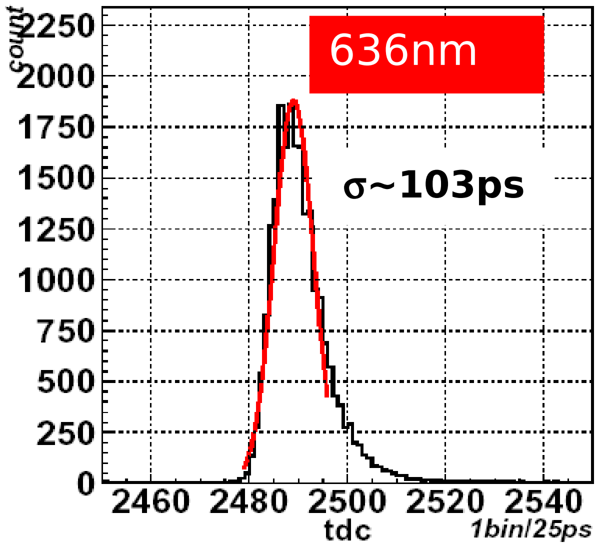

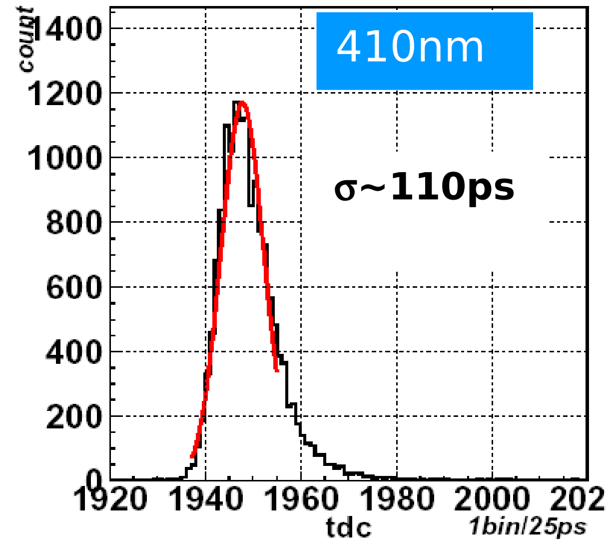

SIPM - CPTA
(MRS-APD)

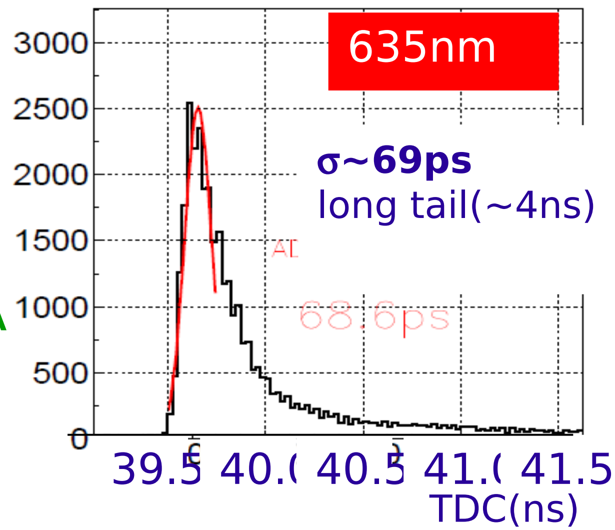

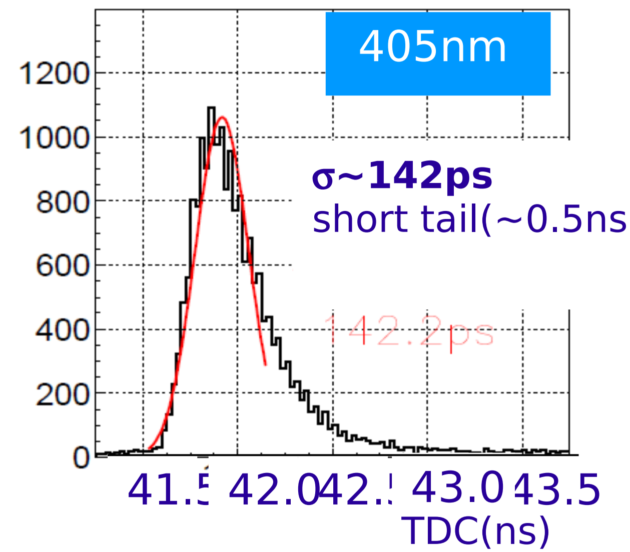

Method: CFD + TDC + Time walk corrections

Compatible with DASIPM measurements

SPTR: cell and sipm size dependence

B.Dolgoshein – LIGHT07

SiPM – MePhI/Pulsar:
576 cells (25x25μm^2)
Area = 1x1 mm^2

SiPM – MePhI/Pulsar:
1600 cells (100x100μm^2)
Area = 5x5 mm^2

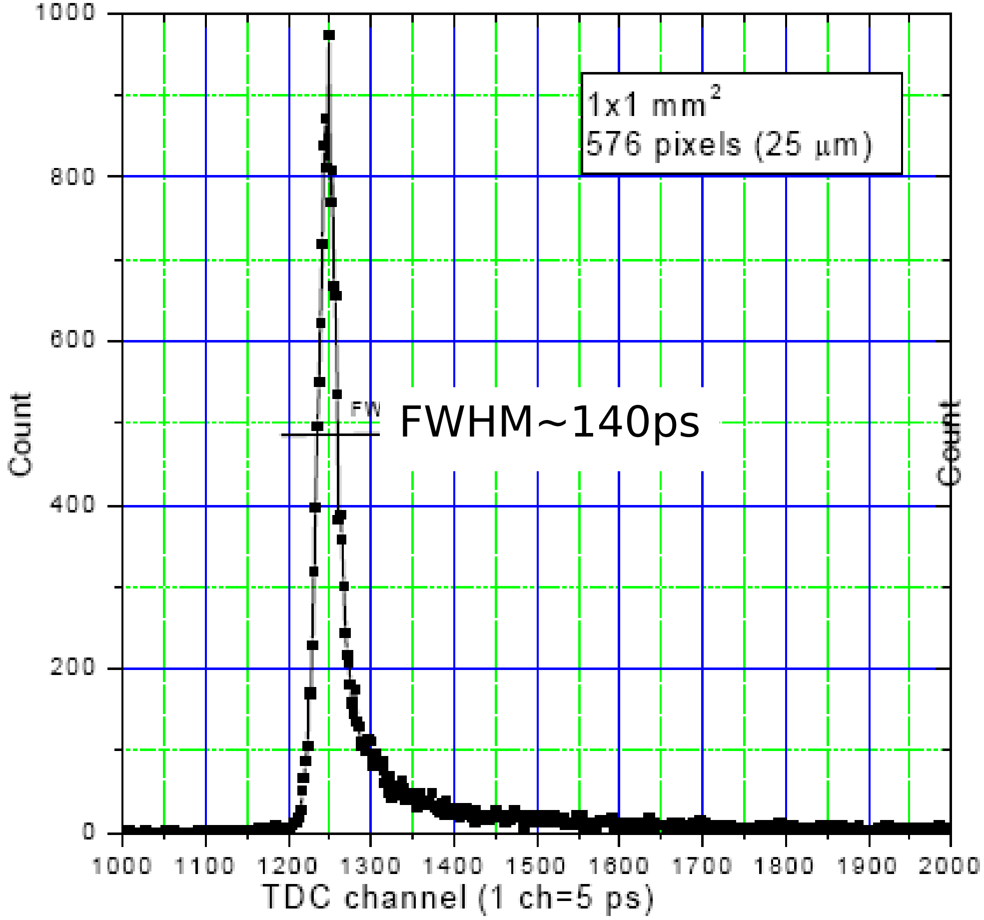

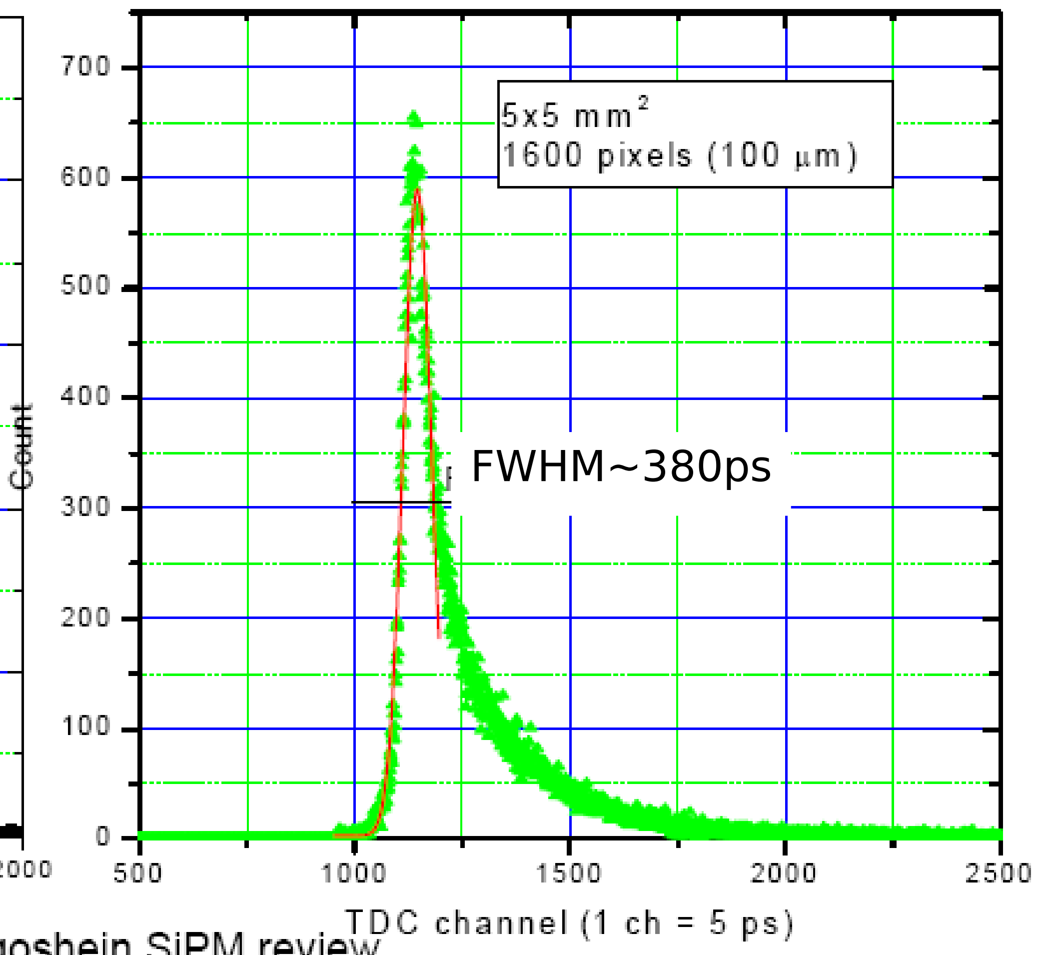

B.Dolgoshein,SiPM review

G.Collazuol - IPRD08 4/10/2008

SiPM signal: effect of C_{tot} and Z_{load}

SiPM – MePhI/Pulsar:
1600 cells ($100 \times 100 \mu m^2$)
Area = $5 \times 5\ mm^2$
$C_{tot} \sim 160pF$

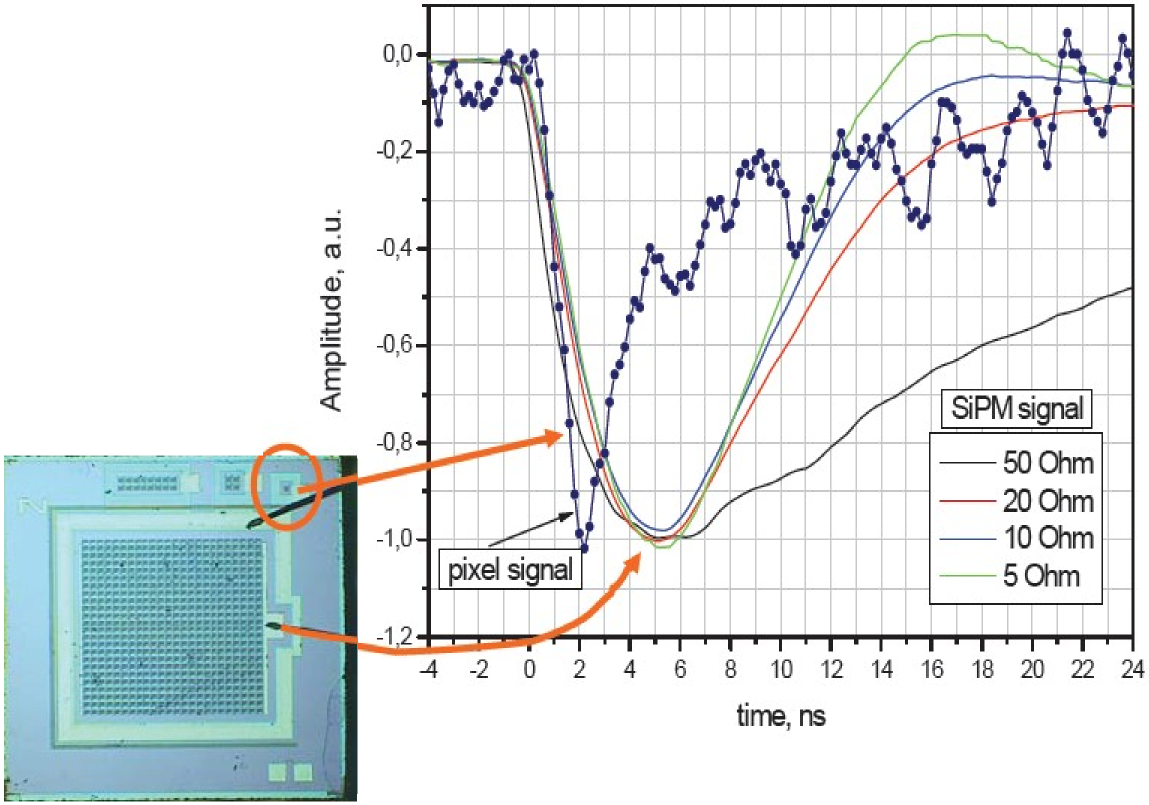

B.Dolgoshein and E.Popova
LIGHT07

Zin~50Ω
FWHM~1.5ns

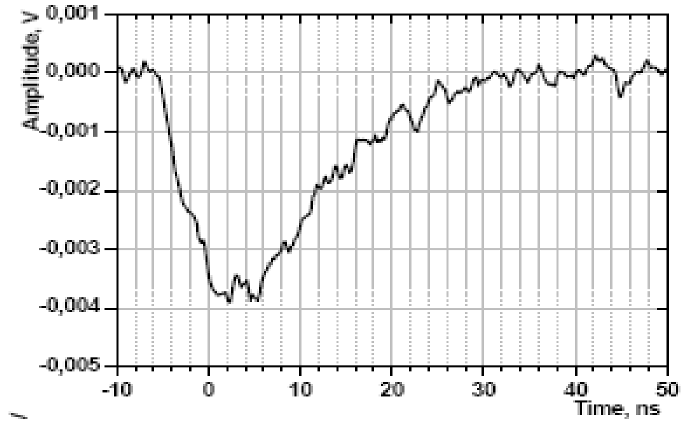

Zin~7Ω + shaper
FWHM~2.5ns

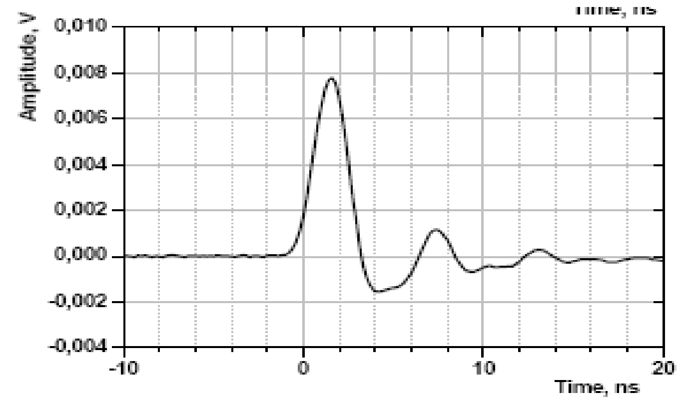

Trans-impedance amplifier

RPL model vs data: comparison ... not yet

Example of RPL simulation of pure electron injection in Si SPAD

Courtesy of C.H.Tan

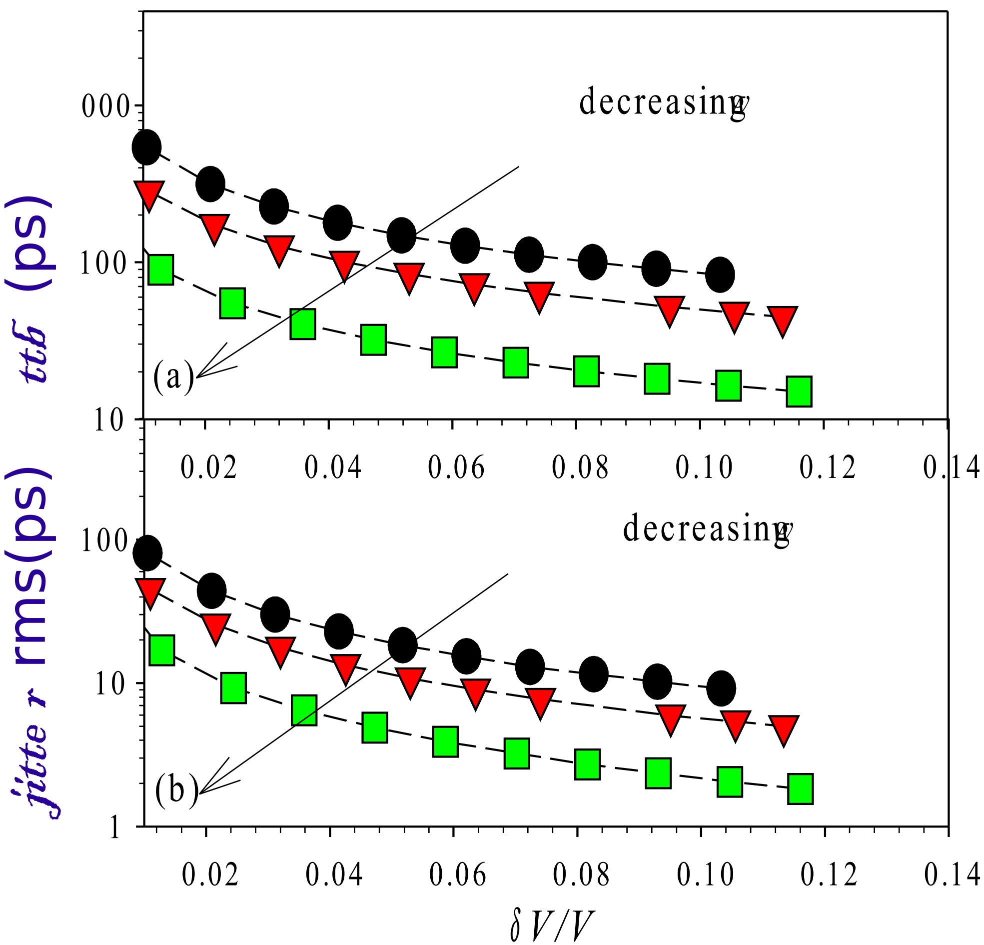

DATA
(DASIPM)

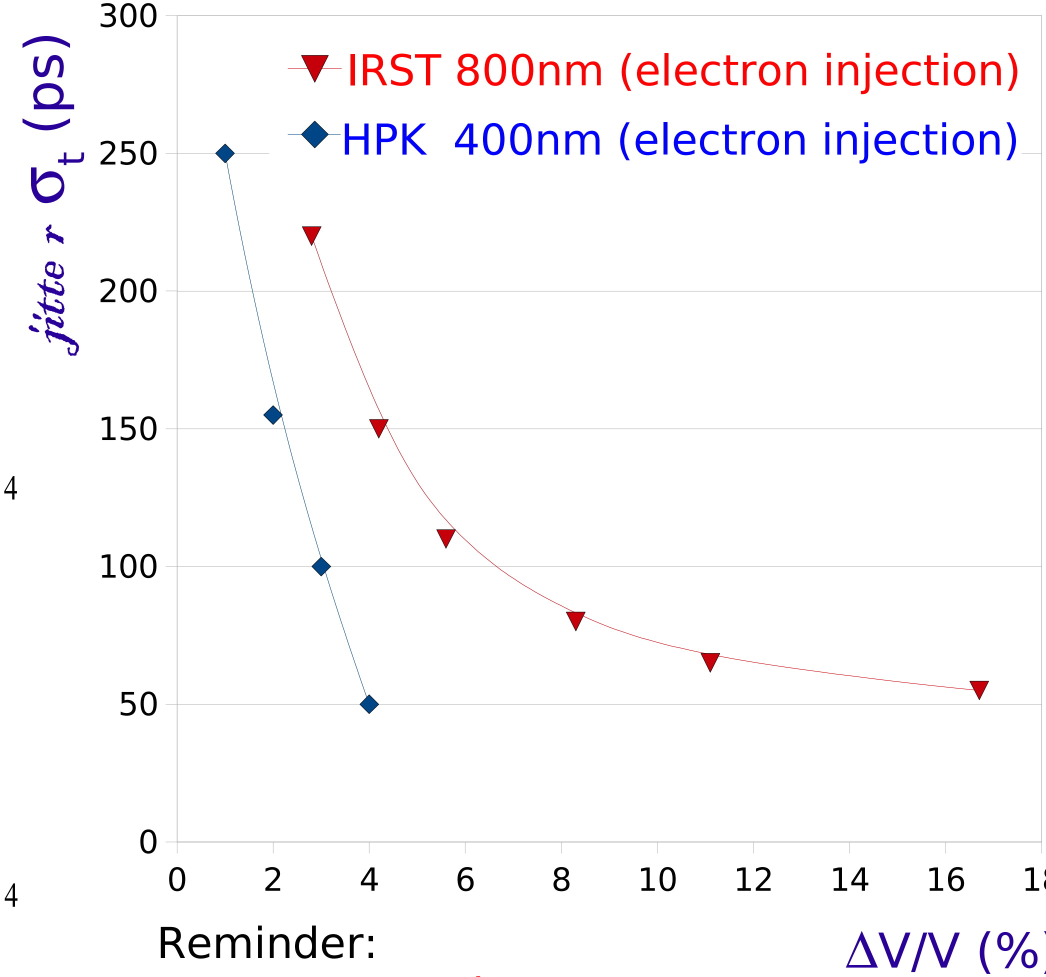

Reminder:
IRST structure is n on p
HPK structure is p on n

Timing vs T (SPAD devices)

Timing: better at low T

Lower jiitter at low T due to higher mobility

(Over-voltage fixed)

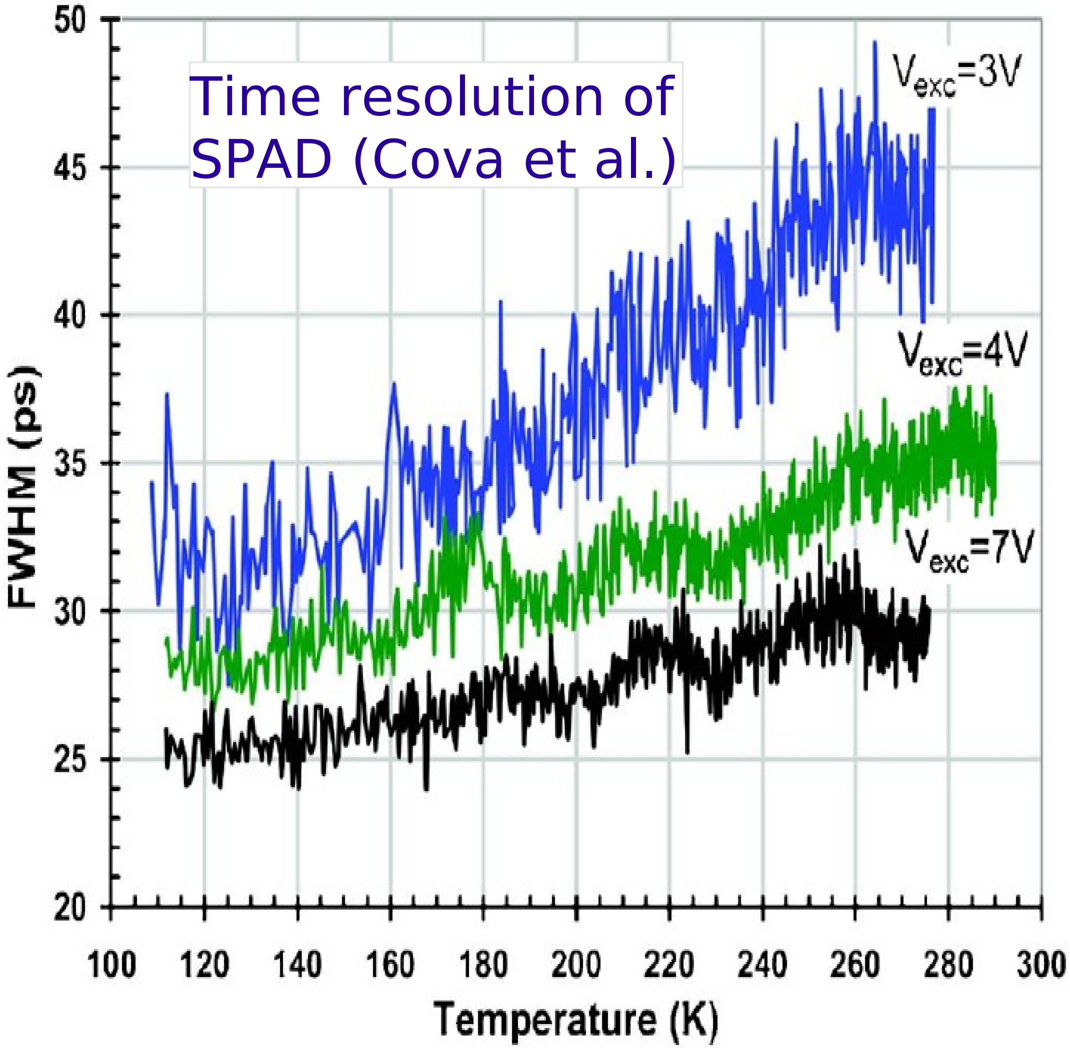

I.Rech el al, Rev.Sci.Instr. 78 (2007)